Adipocyte glucocorticoid receptor deficiency attenuates aging- and HFD-induced obesity, and impairs the feeding-fasting transition

Short title: Adipocyte GR and systemic energy metabolism

Authors

Kristina M. Mueller[1,2]*, Kerstin Hartmann[3*], Doris Kaltenecker[2], Sabine Vettorazzi[3], Mandy Bauer[3], Lea Mauser[3], Sabine Amann[4], Sigrid Jall[5], Katrin Fischer[5], Harald Esterbauer[4], Timo D. Müller[5], Matthias H. Tschöp[5], Christoph Magnes[6], Johannes Haybaeck[7], Thomas Scherer[8], Natalie Bordag[9], Jan P. Tuckermann[3#], Richard Moriggl[1,2,10#]

Affiliations

[1]Institute of Animal Breeding and Genetics, University of Veterinary Medicine Vienna, 1210 Vienna, Austria

[2]Ludwig Boltzmann Institute for Cancer Research, 1090 Vienna, Austria

[3]Institute for Comparative Molecular Endocrinology, University of Ulm, 89081 Ulm, Germany

[4]Department of Laboratory Medicine, Medical University of Vienna, 1090 Vienna, Austria

[5]Institute for Diabetes and Obesity, Helmholtz Diabetes Center, Helmholtz Zentrum München, German Research Center for Environmental Health (GmbH) and German Center for Diabetes Research (DZD), 85764 Neuherberg, Germany; Division of Metabolic Diseases, Department of Medicine, Technische Universität München, 85748 Munich, Germany

[6]HEALTH Institute for Biomedicine and Health Sciences, JOANNEUM RESEARCH Forschungsgesellschaft mbH, Graz, Austria

[7]Institute of Pathology, Medical University of Graz, 8036 Graz, Austria

Diabetes Publish Ahead of Print, published online September 20, 2016

[8]Department of Medicine III, Division of Endocrinology and Metabolism, Medical University of Vienna, 1090 Vienna, Austria

[9]Center for Biomarker Research in Medicine, CBmed GmbH, 8010 Graz, Austria

[10]Medical University of Vienna, 1090 Vienna, Austria

#Corresponding authors

Richard Moriggl; E-mail: richard.moriggl@lbicr.lbg.ac.at, Phone: +43 1 40160 71210; Fax: +43 1 40160 931300

Jan P. Tuckermann; E-mail: jan.tuckermann@uni-ulm.de; Phone: +49 731 50 32600; Fax: +49 731 50 32609

***** These authors contributed equally to this work

[#] These authors contributed equally to this work

Key words: Glucocorticoids, adipose tissue, energy metabolism, fasting, obesity

Word count: 4672

Number of tables and figures: 8

Non-standard abbreviations

AA: Amino acids; **Abhd5**: Comparative gene identification 58 (**CGI58**); **Acaca**: Acyl-CoA carboxylase; **Actb**: β-Actin; **Adipoq**: Adiponectin; **Adra2**: Alpha-2-adrenergic receptor; **Adrb**: β-Adrenergic receptor; **Angptl4**: Angiopoietin-like 4; **BAT**: Brown adipose tissue; **Cd36**: Platelet glycoprotein 4; **Cebpb**: CCAAT/enhancer binding protein beta; **CT**: Computed tomography; **Dgat2**: Diacylglycerol-acyltransferase-3; **EE**: Energy expenditure; **FA**: Fatty acid; **FAO**: Fatty acid oxidation; **Fabp4**: Fatty acid binding protein 4; **Fasn**: Fatty acid synthase; **Fgf21**: Fibroblast growth factor 21; **Gapdh**: Glyceraldehyde 3-phosphate dehydrogenase; **GCs**: Glucocorticoids; **Gnai**: Inhibitory G-protein α-subunit isoforms; **Gnas**: Stimulatory G-protein α-subunit ($G_S\alpha$); **Gpat1**: Glycerol-3-phosphate acyltransferase 1; **Gpat3**: Glycerol-3-phosphate acyltransferase 1; **GR**: Glucocorticoid receptor; **GTT**: Glucose tolerance test; **HFD**: High fat diet; **HGP**: Hepatic glucose production; **ITT**: Insulin tolerance test; **LC-HRMS**: Liquid chromatography–high resolution mass spectrometry; **Lipe**: Hormone sensitive lipase (**HSL**); **MRI**: Magnetic resonance imaging; **NEFA**: Non-esterified fatty acids; **Pck1**: Phosphoenolpyruvate carboxykinase; **Pgc1a**: Peroxisome proliferator-activated receptor gamma coactivator 1-alpha; **PKA**: Protein kinase A; **Pnpla2**: Adipose triglyceride lipase (**ATGL**); **Ppara**: Peroxisome proliferator-activated receptor alpha; **Pparg**: Peroxisome proliferator-activated receptor gamma; **PTT**: pyruvate tolerance test; **RER**: Respiratory exchange ratio; **Slc27a1:** Fatty acid transport protein 1; **Slc27a4**: Long-chain fatty acid transport protein 4; **SNS**: Sympathetic nervous system; **TG**: Triglycerides; **Ucp1**: Uncoupling protein 1; **WAT**: White adipose tissue; **11β-HSD1**: 11β-Hydroxysteroid dehydrogenase 1

Abstract

Glucocorticoids (GCs) are important regulators of systemic energy metabolism, while aberrant GC action is linked to metabolic dysfunctions. Yet, the extent to which normal and pathophysiologic energy metabolism depend on the glucocorticoid receptor (GR) in adipocytes remains unclear. Here, we demonstrate that adipocyte GR-deficiency in mice significantly impacts systemic metabolism in different energetic states. Plasma metabolomics and biochemical analyses revealed a marked global effect of GR-deficiency on systemic metabolite abundance and thus, substrate partitioning in fed and fasted states. This correlated with a decreased lipolytic capacity of GR-deficient adipocytes under post-absorptive and fasting conditions, resulting from impaired signal transduction from β-adrenergic receptors to adenylate cyclase. Upon prolonged fasting, the impaired lipolytic response resulted in abnormal substrate utilization and lean mass wasting. Conversely, GR-deficiency attenuated aging-/diet-associated obesity, adipocyte hypertrophy and liver steatosis. Systemic glucose tolerance was improved in obese GR-deficient mice, which was associated with increased insulin signaling in muscle and adipose tissue.

We conclude that the GR in adipocytes exerts central, but diverging roles in the regulation of metabolic homeostasis depending on the energetic state: The adipocyte GR is indispensable for the feeding-fasting transition, but also promotes adiposity and associated metabolic disorders in fat-fed and aged mice.

Energy homeostasis requires integration of multiple signals between the central nervous system and the periphery to adjust substrate distribution in accordance to metabolic demands. The steroid hormones glucocorticoids (GCs) are important integrators in the body's adaptation to energetic stress by regulating several components of energy homeostasis including glucose and lipid metabolism (1; 2). Consequently, states of chronic GC exposure are associated with metabolic dysfunctions (1; 2). The cellular effects of GCs are mediated in large part through activation of the glucocorticoid receptor (GR). The understanding of how tissue-specific functions of the GC-GR axis contribute to systemic energy metabolism has been substantially extended by mouse models of discrete GR-deficiency in liver and muscle (1; 3; 4).

The most abundant energy reservoir in mammals is white adipose tissue (WAT), which allows non-AT to function normally under conditions of over-nutrition or fasting (5; 6). Thus, an appropriate control in WAT to store and release energy in response to changes in nutrient availability is critical for metabolic homeostasis. GCs were shown to induce lipolysis (7-9), to stimulate lipogenesis in the presence of insulin (10; 11), and to promote lipid storage, uptake, and mobilization (2; 9; 12). An increase of local GC regeneration by the enzyme 11β-hydroxysteroid dehydrogenase 1 (11β-HSD1) within WAT suggests a role of the adipocyte GC-GR axis in common obesity (2; 12-16). These lines of evidence are consistent with a central role of GCs in regulating energy metabolism. However, the exact physiological importance of the adipocyte GR for the maintenance of systemic metabolic homeostasis is yet to be determined.

To delineate this undefined role of the GR, we used an adipocyte-specific gene knockout strategy in mice. We demonstrate that adipocyte GR significantly impacts systemic nutrient partitioning in different energetic states. While GR-deficiency disrupts the feeding-fasting transition, it ameliorates obesity and its associated metabolic disorders, thus, exerting opposing roles in the regulation of metabolic homeostasis.

Research design and methods

Animal experiments

Adipocyte-specific GR-deficient mice (Nr3c1^{tm2Gsc}Tg(Adipoq-cre)1Evdr: **GR$^{\Delta Adip}$**; C57BL/6 x FVB/N) were generated by crossing *Nr3c1 floxed* (17) with *Adipoq-cre* mice (18). *Adipoq-cre* negative littermates served as controls (Nr3c1^{tm2Gs}: **ctrl**). Animals were housed under standardized conditions (12h dark/12h light cycle) and fed a regular diet (Ssniff EF, R/M Kontrolle, Ssniff GmbH, Germany). For high fat diet (HFD) experiments mice received either Ssniff EF acc.D12492 (34.6% crude fat) or Ssniff EF D12450B mod. Animal studies were approved by the Austrian government and the Medical University Vienna (BMWF-66.009/0132-II/3b/2013) and by the regional commission Tuebingen, Germany (TVA1126). Except for HFD and aging-experiments, 8-week-old male mice were used.

Body composition was determined using EchoMRI™-100H (EchoMRI LLC, USA). µ-CT was performed with *in vivo* X-ray microtomograph Skyscan 1176 (RJL Micro+Analytic GmbH, Germany). Fat volume was reconstructed and calculated using NRecon (Version 1.6.9.18) and CTAn (Version 1.14.4.1+).

Glucose and pyruvate tolerance tests (GTT; PTT) were performed in 12-16h-fasted mice; insulin tolerance tests (ITT) were performed on 4h-fasted mice. Glucose (2 g/kg) was administered orally or by intraperitoneal injection (HFD experiments); pyruvate (2 g/kg) and insulin (0.75 U/kg) were given intraperitoneally. Blood glucose levels were determined from tail vein using a glucometer.

Cold tolerance: 4h-fasted mice were housed separately with free access to water at 4°C. Rectal temperature was measured at indicated time points using a BIO-TK9882 thermometer (Biosep, France).

Energy expenditure (EE), locomotor activity, respiratory exchange ratio (RER) and food intake were measured by combined indirect calorimetry over 93.4h (PhenoMaster; TSE Systems, Germany) as described previously (19).

Metabolite and hormone measurements

β-ketones were measured from tail vein blood (Freestyle Precision Xceed, Abbott, USA). Non-esterified fatty acids (NEFA) were determined with the NEFA-HR(2) kit (Wako Chemicals, Germany), glycerol with the Free Glycerol Reagent (Sigma-Aldrich, USA), triglycerides (TG), and cholesterol were measured with a Reflotron Plus analyzer (Roche, Switzerland). Insulin, corticosterone and FGF21 were determined by ELISA (Ultra-Sensitive Mouse Insulin ELISA, Crystal Chem, USA; Corticosterone ELISA, Enzo Life Sciences, USA; Mouse/Rat FGF-21 Quantikine-ELISA, R&D Systems, USA). Liver TG content was determined using a Triglyceride Colorimetric Assay (Cayman Chemical, USA).

Lipolysis Assays

Epididymal WAT was surgically removed and lipolysis was measured as described (20). Stimulations were performed with insulin (30 ng/ml), isoproterenol, forskolin, formoterol or CL-316,243 (all 10 μM) for 120min. NEFA was determined as described, cAMP content in WAT explants by the cAMP complete ELISA (Enzo Life Sciences). Measurements were normalized to tissue weights.

Histology

Tissues were fixed in 4%-buffered formalin, paraffin-embedded, sectioned and stained with hematoxylin-eosin using standard procedures. Adipocyte sizes were quantified from at least 3-5 different fields/mouse and at least 20-60 cells/field using ImageJ (Rasband, W.S., ImageJ,

U.S. NIH, Bethesda, Maryland http://imagej.nih.gov/ij/1997-2011.). Histological evaluation of livers was performed by a board-certified pathologist (JH).

Molecular analyses

RNA was extracted using commercial kits (Qiagen, Germany; Peqlab, Germany). RNA (1µg) was reverse-transcribed using cDNA synthesis kits (Fermentas, Germany; Applied Biosystems, USA). Quantitative real-time PCR was performed on an Eppendorf Realplex system using the Taq DNA polymerase kit (Eppendorf, Germany) or on a ViiA^{TM}7RT-PCR System using the Platinum Sybr Green qPCR Supermix-UDG (Life Technologies; USA). Gene expression was normalized to *Gapdh* or *Actb* mRNA. Primer sequences are provided in Supplementary Table 1.

Western blot analyses (40 µg protein) were performed as described (21). Primary antibodies against HSC70 (sc-7298), GR (sc-1004), AKT (sc-8312), $G_S\alpha$ (sc-823), PPARα (sc-9000; all Santa Cruz Biotechnology, USA), pS473-AKT (#9271), UCP1 (#14670), ATGL (#2439), pSer563-HSL (#4139), pSer660-HSL (#4126), HSL (#4107), pPKA Substrate (RRXS*/T*, #9624; all Cell Signaling, USA) and β-Actin (A1978, Sigma-Aldrich) were used.

Plasma LC-MS metabolomics

Animals were anesthetized with ketamine/xylazin (i.p., 10 mg/kg) or CO_2 inhalation. 500–700 µl blood was drawn via cardiac puncture, filled into lithium-heparin- or EDTA-coated tubes (Greiner Bio-One, Austria) and centrifuged in less than 30 minutes after collection (15 minutes, 7000 rpm, 4°C). Plasma was snap-frozen and stored at -80°C.

Metabolites were analyzed by targeted LC-HRMS metabolomics according to (22) by hydrophilic interaction LC at the HEALTH Institute for Biomedicine and Health Sciences, JOANNEUM RESEARCH (Graz, Austria) as described previously (23): Samples were processed according to (24). Raw data were converted into mzXML by msConvert

(ProteoWizard Toolkit v3.0.5), and metabolites were targeted-searched by the in-house developed tool PeakScout, with a reference list containing accurate mass and retention times in agreement with standards outlined by (25). Pure substances of all analytes, except lipids, were run on the same system to obtain exact reference retention times and fragmentation spectra. The results for 6 samples had to be removed from analysis due to considerable outlier behavior in PCA (two from $GR^{\Delta Adip}$ HFD-cohort, one from each, fasted control-, fasted $GR^{\Delta Adip}$-, fed control- and $GR^{\Delta Adip}$-cohort).

Statistical Analyses

Statistics were performed with GraphPad Prism® or R (26) (v3.2.1, packages *stats*, *missMDA*, *nlme*) using Tibco®Spotfire® (v7.0.0). All data except LC-MS metabolomics are presented as mean ± SEM. Two-tailed Student's t-test or Wilcoxon rank-sum test were used for comparing two groups and one-way ANOVA followed by Tukey's, Dunns' or Bonferroni's post-hoc tests for multiple comparison. Tolerance tests and body growth curves were analyzed with repeated-measures two-way ANOVA followed by Bonferroni's post-hoc tests. $P<0.05$ was considered to be statistically significant. Data for EE were analyzed using ANCOVA with body weight and body composition (fat and lean mass) as covariates as previously suggested (27). For LC-MS metabolomics PCA analysis was performed centered and scaled to unit variance (R function *prcomp*). Missing values were imputed by a regularized expectation-maximization (R function *imputePCA* and *estim_ncpPCA*). Log_{10} transformed data was found to be sufficiently normal distributed according to Kolmogorov-Smirnov (86% of all metabolites were normally distributed) and sufficiently homoscedastic according to Levene (84% of all metabolites were homoscedastic). Differences between independent groups were analyzed by ANOVA (R function *aov*) followed by Benjamini-Hochberg (R function *p.adjust*) post-hoc test.

Results

Abnormal plasma metabolome in $GR^{\Delta Adip}$ mice

Deletion of *Nr3c1* was confirmed by mRNA and protein expression analyses of inguinal WAT (iWAT), epididymal WAT (eWAT), and brown adipose tissue (BAT; Fig. 1A-B). $GR^{\Delta Adip}$ mice displayed no overt alterations in weights or morphology of eWAT, iWAT and BAT compartments (Supplementary Fig. 1A-B). Accordingly, adipogenic markers (*Cebpb, Pparg, Fabp4*) and adipocyte-specific genes (*Adiponectin, Leptin, Ucp1*) were not differentially expressed among genotypes (Supplementary Tab. 2).

To initially illustrate the basal metabolic signature of $GR^{\Delta Adip}$ mice, plasma samples of *ad libtum*-fed mice were analyzed by targeted LC-MS metabolomics (Supplementary Tab. 3, PCA results: Supplementary Fig. 2A). 157 metabolites were of suitable quality for multivariate statistical analysis, 20 metabolites only for univariate statistical analysis. 59 metabolites were significantly decreased ($p<0.05$, ANOVA) and 22 were decreased by trend ($0.05<p<0.1$, ANOVA) in $GR^{\Delta Adip}$ mice compared to controls. The majority of decreased metabolites were related to FA/lipid metabolism (46; most pronounced in long-chain FA), amino acids metabolism (14; mainly proteogenic and branched-chain AA, which have been implicated as independent risk factors for diabetes (28)), and nucleotide metabolism (10; mainly pyrimidine metabolites; Fig. 1C, Supplementary Tab. 3). This demonstrates a considerable impact of adipocyte GR-deficiency on the plasma metabolome and thus, systemic substrate partitioning, which likely affects whole-body glucose and lipid metabolism in $GR^{\Delta Adip}$ mice (6; 29).

Reduced lipolytic and gluconeogenic capacity in $GR^{\Delta Adip}$ mice

First, we analyzed glucose homeostasis in $GR^{\Delta Adip}$ mice. In 4h- and 16h-fasted mice, blood glucose and plasma insulin levels were not significantly altered (Fig. 2A). GTTs revealed no

differences in glucose clearance between the genotypes (Supplementary Fig. 2B). The hypoglycemic response during ITTs was similar in both genotypes (Fig. 2B); whereas blood glucose starting from 30 minutes after insulin administration was lower in $GR^{\Delta Adip}$ mice. This delay in post-hypoglycemic recovery suggests a reduction in counter-regulatory mechanisms such as hepatic glucose production (HGP). Insulin-induced AKT phosphorylation (Ser473) was greater in $GR^{\Delta Adip}$ livers than in controls (Fig. 2C). This was associated with a lower TG content in $GR^{\Delta Adip}$ livers (Fig. 2D). Suppression of WAT lipolysis can indirectly reduce HGP by decreasing the influx of glycerol and NEFA (30). In absence and presence of insulin, NEFA release from eWAT explants of 4h-fasted $GR^{\Delta Adip}$ mice was clearly reduced compared to controls (Fig. 2E). Yet, consistent with a comparable insulin-stimulated AKT phosphorylation in eWAT (Fig. 2C), insulin-mediated suppression of lipolysis was similar between genotypes (49% versus 51%). NEFA release from 16h-fasted $GR^{\Delta Adip}$ eWAT explants was also reduced, which was mirrored in decreased plasma NEFA (indicator for WAT lipolysis) and blood β-ketones (indicator for hepatic FA oxidation (FAO)) in 16h-fasted $GR^{\Delta Adip}$ mice (Fig. 2F). Blood glucose levels of 16h-fasted $GR^{\Delta Adip}$ mice during PTTs were lower compared to controls (Fig. 2G), reflecting reduced glucose production from the carbon precursor pyruvate. Thus, the lipolytic capacity of $GR^{\Delta Adip}$ mice is diminished, which correlates with a decrease in glucose production (Supplementary Fig. 2C).

Reduced thermogenesis in $GR^{\Delta Adip}$ mice

Thermogenesis in BAT requires mobilization of lipid stores, induction of β-oxidation and mitochondrial uncoupling. To evaluate BAT functionality upon adipocyte GR-deficiency, we subjected mice to a brief 4h-fast followed by a 4h exposure to 4°C. Body temperatures of $GR^{\Delta Adip}$ were slightly higher when housed at 23°C (4h-fast; p=0.072), whereas their ability to maintain stable body temperatures at 4°C was mildly reduced (Fig 3A). Despite the impaired cold-adaptation, UCP1 and PPARα levels were similar in BAT of cold-exposed $GR^{\Delta Adip}$ and

ctrl mice (Fig. 3B). While BAT uses FA stores to fuel thermogenesis, WAT provides energy in form of FA for utilization in BAT. Histology of BAT revealed no differences between genotypes when housed at 23°C (Supplementary Fig. 1B). Yet, upon cold exposure the amount of lipid droplets decreased to a higher extent in GR-deficient BAT (Fig 3C), suggesting that BAT lipolysis is not impaired. In contrast, plasma NEFA and β-ketone concentrations, indicators of WAT lipid mobilization and redistribution, were reduced in cold-exposed $GR^{\Delta Adip}$ mice (Fig. 3D). Considering the requirement of external FA supply for BAT-mediated temperature maintenance (31), these data suggest that the reduced cold-induced thermogenesis is related to impaired WAT lipolysis and NEFA flux.

Attenuated aging-associated obesity and hepatic steatosis in $GR^{\Delta Adip}$ mice

Progressing age is linked to abnormalities of carbohydrate and lipid metabolism. Thus, we analyzed whether GR-deficiency would lead to beneficial metabolic effects at older age. Aging-associated weight gain was attenuated in $GR^{\Delta Adip}$ mice (Fig. 4A) and body fat was reduced compared to controls at 52 weeks of age (Fig. ~~3~~4B). Accordingly, $GR^{\Delta Adip}$ mice had smaller WAT compartments (Fig. 4C), in which adipocyte hypertrophy was less frequently observed (Supplementary Fig. 3A). 4h-fasted $GR^{\Delta Adip}$ mice displayed lower blood glucose levels and presented an overall reduction of total TG, cholesterol, NEFA and β-ketones in the circulation, whereas corticosterone level were comparable between genotypes (Supplementary Fig. 3B). Weights of $GR^{\Delta Adip}$ livers were reduced (Fig. 4C) and steatosis scores of >5% were found only in control livers (Fig. 4D).

To further characterize the phenotype of aged GR-deficient mice, we determined their metabolic parameters in a PhenoMaster metabolic cage system. $GR^{\Delta Adip}$ mice had higher RER during light and dark cycles, indicating an overall preference for carbohydrates as metabolic substrate. Locomotor activity, EE, and food intake were not significantly different between genotypes (Fig. 4E, Supplementary Fig. 3C); although $GR^{\Delta Adip}$ mice consumed a slightly

higher amount of food. There was no significant effect of GR-deficiency on EE after ANCOVA with body weight, lean or fat mass as covariate (data not shown). These data indicate that neither increased physical activity/metabolic rates nor decreased food intake are determinants of reduced adiposity in aged $GR^{\Delta Adip}$ mice. Although we cannot fully exclude subtle increases in daily EE and/or locomotor activity over several months that might have contributed to reduced fat mass gain during the aging process.

Reduced HFD-induced obesity, improved glucose tolerance and hepatic steatosis in $GR^{\Delta Adip}$ mice

To investigate whether reduced susceptibility to metabolic dysfunctions also occurs upon diet-induced obesity, mice were subjected to HFD-feeding for 20 weeks. HFD-fed $GR^{\Delta Adip}$ mice gained significantly less weight than HFD-fed controls, despite similar cumulative food intake (Fig. 5A, Supplementary Fig. 4A). Reduced weight gain manifested early in HFD-fed $GR^{\Delta Adip}$ mice (Fig.), accompanied by lower levels of several circulating FA species and a trend towards reduced plasma NEFA (Supplementary Tab. 3, Supplementary Fig. 4B). After 2 weeks of HFD-feeding, mRNA expression of several genes critical for FA storage were either significantly reduced or reduced by trend in $GR^{\Delta Adip}$ eWAT compared to controls (Fig. 5B; Acyl-CoA carboxylase (*Acaca*), glycerol-3-phosphate acyltransferase 3 (*Gpat3*), diacylglycerol-acyltransferase-2 (*Dgat2*), phosphoenolpyruvate carboxykinase (*Pck1*) and fatty acid transport protein 1 (*Slc27a1*)). *Acaca* and *Pck1* mRNA levels showed a similar trend in GR-deficient iWAT, while there was no change in expression of fatty acid synthase (*Fasn*) and the FA transporter *Cd36* in both WAT compartment. At termination, HFD-fed $GR^{\Delta Adip}$ mice displayed lower WAT weights than HFD-fed controls (Supplementary Fig. 4C) and μ-CT analysis confirmed significantly decreased subcutaneous and visceral fat volume of $GR^{\Delta Adip}$ mice (Fig. 5C). Accordingly, adipocyte hypertrophy in $GR^{\Delta Adip}$ eWAT and iWAT was reduced (Fig. 5D, Supplementary Fig. 4D). Consistent with the aging cohort, plasma

corticosterone levels were not significantly different between HFD-fed ctrl and GR-deficient mice (Supplementary Fig. 4E).

Next, we asked whether GR-deficiency improves deteriorated glucose metabolism associated with HFD. Blood glucose levels trended to be lower in HFD-fed $GR^{\Delta Adip}$ mice compared to controls (Fig. 6A), while their fasting plasma insulin levels were significantly lower (Fig. 6B). In agreement, HOMA-IR was decreased in HFD-fed $GR^{\Delta Adip}$ mice, suggesting improved insulin sensitivity (Fig. 6C). Consistent with the lower HOMA-IR, systemic glucose tolerance of HFD-fed $GR^{\Delta Adip}$ mice was improved compared to obese controls (Fig. 6D) and insulin-stimulated AKT phosphorylation (Ser473) in muscle, eWAT and liver of HFD-fed $GR^{\Delta Adip}$ mice was increased (Fig. ~~5~~6E, Supplementary Fig. 4F).

Similar to the aging cohort, adipocyte GR-deficiency attenuated HFD-induced hepatic lipid accumulation and liver weights, which was reflected in lower steatosis scores (Fig. 6F-G). Hepatic mRNA expression of *Fasn* and *Gpat1*, two rate-limiting enzymes of lipogenesis, was reduced in HFD-fed $GR^{\Delta Adip}$ mice, accompanied by diminished expression of *Pparg* and two fatty acid transporters *Cd36* and *Slc27a4* (Fig. 6H). This suggests that decelerated FA uptake and lipogenesis might contribute to lower steatosis scores in GR-deficient mice.

Thus, adipocyte GR-deficiency reduces obesity, diminishes hepatic steatosis and improves glucose tolerance in HFD-fed mice.

Impaired lipolysis disrupts the feeding-fasting transition in $GR^{\Delta Adip}$ mice

Having demonstrated that adipocyte GR promotes metabolic dysfunctions in aged and fat-fed mice, we lastly evaluated the requirement of adipocyte GR for energy homeostasis under prolonged fasting conditions. Upon 48h-fasting, total body weight loss was similar among genotypes (Supplementary Fig. 5A). Notably, all mice survived 48h-fasting and did not present symptoms of a hypoglycemic shock (i.e. trembling, seizures or unconsciousness). Body fat mass was ~2-fold higher in fasted $GR^{\Delta Adip}$ mice compared to controls, while their

lean mass was decreased (Fig. 7A). Accordingly, $GR^{\Delta Adip}$ WAT compartments were enlarged, while their gastrocnemius, heart and liver weights were reduced (Supplementary Fig. 5B). Consistent with their preserved fat mass, $GR^{\Delta Adip}$ mice presented increased adipocyte sizes, lower plasma NEFA and glycerol concentrations, decreased hepatic TG accumulation and reduced circulating TG levels (Fig. 7B-C; Supplementary Fig. 1B, 5C-D). Blood β-ketones were substantially lower (Fig. 7C), indicating reduced FAO and ketogenesis. Hepatic PPARα and FGF21 are key mediators of fasted states, and contribute to lipid utilization by increasing FAO in liver (32). Fasting-induced up-regulation of *Ppara* and *Fgf21* mRNA expression was impaired in $GR^{\Delta Adip}$ livers, accompanied by decreased plasma FGF21 levels (Fig. 7E, Supplementary Fig. 5E). In contrast to shorter fasting periods, 48h-fasting blood glucose was unexpectedly increased in $GR^{\Delta Adip}$ mice compared to controls (Fig. 7D), suggesting that the observed breakdown of lean mass might provide substrates for glucose production. In support of this assumption, circulating corticosterone, which potently induces protein catabolism and HGP (1), increased to a higher extent in 48h- but not in 16h-fasted $GR^{\Delta Adip}$ mice (Fig. 7E). Additionally, fasting-induced up-regulation of gluconeogenic genes *Pgc1a* and *Pck1* was similar in livers of both genotypes (Supplementary Fig. 5F). To characterize the fasting metabolome of $GR^{\Delta Adip}$ mice in more detail, plasma samples were analyzed by targeted LC-MS. From 177 metabolites, 42% were significantly different in 48h-fasted compared to fed $GR^{\Delta Adip}$ mice (Fig. 7F; Supplementary Tab. 3). Strong increases in AA and related metabolites, several FA species and nucleotides were observed. Conversely, in fasted controls, abundance of most AA and nucleotides was either unchanged or lower than in fed controls. 18% of metabolites were significantly different between 48h-fasted $GR^{\Delta Adip}$ mice and controls. These included hexose, pentose, nucleotides, and AA all of which, in contrast to the fed state, displayed a greater quantity in $GR^{\Delta Adip}$ mice (Fig. 1C, 7F, Supplementary Tab. 3).

This reveals that the GR in adipocytes is indispensable for normal substrate mobilization and energy metabolism under prolonged fasting conditions.

Dysregulation of lipolytic signaling in $GR^{\Delta Adip}$ mice

To determine the molecular underpinning of impaired lipolysis, we compared mRNA and protein expression of lipolytic key factors in eWAT of fed and 48h-fasted mice. HSL (*Lipe*; hormone sensitive lipase) mRNA levels were similar among genotypes, while up-regulation of ATGL (*Pnpla2*; adipose triglyceride lipase) and CGI58 (*Abhd5*; comparative gene identification 58) mRNA expression was significantly reduced in fasted $GR^{\Delta Adip}$ eWAT (Fig. 8A). Protein level of ATGL and its co-activator CGI58 displayed a similar expression pattern in eWAT of fasted mice (Fig. 8B). Fasting-induced lipolysis requires cAMP-mediated activation of protein kinase A (PKA), subsequent phosphorylation of HSL and perilipin thereby, indirectly activating ATGL via release of CGI58 (33). Upon fasting, total PKA substrate phosphorylation including HSL (Ser563/660) and perilipin was substantially decreased in $GR^{\Delta Adip}$ eWAT (Fig. 8B-C). Thus, we analyzed mRNA expression of genes critical for β-adrenergic activation of PKA. Expression of the inhibitory α2-adrenergic receptor (AR) and inhibitory G-protein α-subunit isoforms was similar between genotypes (Supplementary Fig. 6A), whereas up-regulation of β2-AR (*Adrb2*) was reduced in $GR^{\Delta Adip}$ eWAT under fasting conditions. Conversely, β3-AR (*Adrb3*) mRNA levels were increased (Fig. 8D). Notably, fasting-induced up-regulation of the stimulatory G-protein α-subunit (*Gnas*; $G_S\alpha$), which couples β-ARs to adenylate cyclase-mediated production of intracellular cAMP (34), was significantly diminished in GR-deficient eWAT (Fig. 8D-E). To functionally identify the GR-dependent signaling step in β-adrenergic signal transduction, we applied pharmacologic agonists on eWAT explants from 16h-fasted mice. GR-deficiency reduced cAMP generation upon treatment with isoproterenol (non-selective β-adrenergic agonist), but not in response to forskolin (direct adenylate cyclase agonist; Fig. 8F). NEFA release from

GR$^{\Delta Adip}$ explants was decreased in response to isoproterenol, CL-316,243 (β3-AR agonist) and formoterol (β2-AR agonist), while forskolin-stimulated lipolysis was similar between both genotypes (Fig. 8G). Similar results were obtained from isoproterenol- or forskolin-treated eWAT explants of fed GR$^{\Delta Adip}$ mice (Supplementary Fig. 6B), albeit the defect in lipolysis was less pronounced than in 16h-fasted mice.

These data demonstrate that the GR is a pivotal permissive factor for β-adrenergic signal transduction to adenylate cyclase and concomitant activation of the lipolytic cascade in WAT.

Discussion

Our study provides the first genetic evidence for the GR in adipocytes as a critical component in normal and pathophysiologic energy metabolism. Initial plasma metabolomics revealed a marked global effect of GR-deficiency on systemic metabolite abundance, including a reduction in various FA species and proteogenic/branched-chain AA (valine, leucine and isoleucine). Albeit steady-state analysis of plasma represents a static net-balance between metabolite production and consumption, the broad changes indicate that systemic fuel partitioning is partly controlled by GR in adipocytes. Along this line, the diminished gluconeogenic capacity of GR$^{\Delta Adip}$ mice during ITT/PTT may be due to increased hepatic responsiveness to insulin, but could also result from a decrease in substrate availability (6). GC exposure at high concentrations is thought to stimulate lipolysis (1; 2). Our data from eWAT explants of 4h-fasted mice show that the GR is a key factor for lipolysis already in the post-absorptive state. Suppression of WAT lipolysis correlates with hepatic insulin sensitivity and reduced HGP (34; 35), and indirectly counter-regulates gluconeogenesis (6; 30; 36) as WAT-derived substrate fluxes provide glycerol as direct substrate, while NEFA oxidation promotes acetyl-CoA-mediated activation of pyruvate carboxylase (37). Therefore, it is conceivable that reduced lipolysis in GR$^{\Delta Adip}$ mice contributes in a similar manner to the observed reduction in gluconeogenic capacity.

GC-stimulated lipolysis has been linked to transcriptional up-regulation of ATGL and HSL (7; 9; 38), elevated adenylate cyclase activity (39), intracellular cAMP production and HSL activation (7; 8). Reduced lipolysis in $GR^{\Delta Adip}$ mice largely resulted from a block in β-adrenergic activation of PKA and lipolytic downstream signaling (33). The sympathetic nervous system (SNS) regulates induction of WAT lipolysis and PKA-mediated phosphorylation of HSL serves as surrogate marker for SNS outflow to WAT (40; 41). In fasting states, systemic GR antagonism with RU486 decreased β-adrenergic signaling in WAT through suppression of angiopoietin-like 4 (*Angptl4*) (8). However, *Angptl4* expression was not affected in $GR^{\Delta Adip}$ eWAT (Supplementary Fig. 6C). GR-deficiency decreased the expression of $G_S\alpha$, which mediates SNS-stimulated lipolysis by transducing signals from β-ARs to adenylate cyclase. Notably, adipocyte-specific deficiency in $G_S\alpha$ blocks WAT lipolysis mimicking the phenotype of the $GR^{\Delta Adip}$ mice (34). In agreement, cAMP generation and NEFA release from $GR^{\Delta Adip}$ eWAT explants was reduced in response to β-AR agonists, but could be normalized by direct adenylate cyclase agonism. GCs were shown to positively regulate $G_S\alpha$ expression in rat brain (42), suggesting that a similar regulatory mechanism might exist in adipocytes to trigger β-adrenergic lipolytic responses. Accordingly, dexamethasone treatment increased $G_S\alpha$ levels in eWAT of ctrl mice but not in liver or GN muscle, suggesting that the GC-mediated induction of $G_S\alpha$ occurs in a tissue-selective manner (Supplementary Fig. 6D). However, sequence analysis of the corresponding *Gnas* promoter region (NM_201616.2, NM_001077510.4, NM_001310083.1; -3000bp of TSS) did not reveal the presence of any sequences likely to act as GRE. Notably, the GR positively regulates transcription through several mechanisms, including DNA-independent means by acting as co-factor for lineage-specific transcription factors (43). At this point, however, we cannot predict which molecular mechanism might account for the reduction in *Gnas* expression in GR-deficient WAT and further molecular studies will be necessary to decipher the underlying

causes. Nevertheless, our current data support a model where the GR is required for signal transduction from β2/3-AR to adenylate cyclase and concomitant induction of lipolysis.

In mice and humans, an increase in GC regeneration by the enzyme 11β-HSD1 within WAT compartments suggests a role of the GC-GR axis in common obesity (2; 12-16). Our findings from aged and HFD-fed $GR^{\Delta Adip}$ mice support that suppressing the adipocyte GC-GR axis restricts obesity and its underlying disease state. We observed no differences in EE and/or food consumption that would explain the attenuated obesity of $GR^{\Delta Adip}$ mice. Recent studies established an interdependence of lipid mobilization and storage in WAT. Chronic stimulation of lipolysis was shown to coincide with an up-regulation of genes critical for FA storage and induction of *de novo* lipogenesis in WAT (44). Conversely, blocking lipolysis in chow- and/or HFD-fed mice resulted in down-regulation of genes critical for FA storage and in decreased lipogenesis/lipid synthesis in WAT (34; 35). Although not functionally proven by our data, the mild, yet collective reduction in several genes related to FA storage in HFD $GR^{\Delta Adip}$ WAT suggests that a decrease in lipid synthesis might contribute to the attenuated obesity-phenotype. However, further studies are required to determine the exact mechanism(s) underlying the anti-obesity effects of adipocyte GR-deficiency.

Dysfunctional hypertrophic adipocytes are thought to be in part causative for metabolic dysfunctions upon progressive adiposity (5; 45). Improved glucose tolerance and reduced hyperinsulinemia indicates enhanced peripheral responsiveness to insulin in HFD-fed $GR^{\Delta Adip}$ mice. Indeed, increased insulin-stimulated AKT phosphorylation was not confined to WAT, but also present in muscle and liver of HFD-fed $GR^{\Delta Adip}$ mice. As NEFA/lipid accumulation can cause deleterious effects on insulin sensitive organs (6), and inhibition of lipolysis improves systemic glucose metabolism (34; 35), the attenuated adiposity and reduced lipolytic capacity are conceivable possibilities for the ameliorated glucose tolerance in $GR^{\Delta Adip}$ mice. Along this line, adipocyte GR-deficiency attenuated HFD-induced steatosis. HFD-feeding promotes hepatic lipid accumulation partly through up-regulation of genes

involved in FA uptake and lipid synthesis (46-48), several of which were down-regulated in livers of HFD-fed $GR^{\Delta Adip}$ mice. Accordingly, reduced FA influx and endogenous lipid production likely contribute to the attenuation of steatosis in HFD-fed $GR^{\Delta Adip}$ mice. Similar to our observations, adipocyte-specific 11β-HSD1 deletion was shown to ameliorate hypercortisolism-induced glucose intolerance and hepatic steatosis (38). Along with the beneficial metabolic state of the aged GR-deficient cohort, these findings indicate that adipocyte GC-GR activity is involved in the development of systemic metabolic dysfunctions. In contrast to HFD-feeding, adipocyte GR-deficiency had adverse consequences when FA became the major energy substrate during prolonged fasting. Fasting induces robust shifts in fuel selection, during which coordinated increases in lipolysis, FA oxidation, and ketogenesis spare glucose and preserve lean mass. Similar to models with impairments in lipolytic enzymes (33; 49-51), GR-deficiency disrupted the transition to lipid-based energy production (i.e. preserved fat, inefficient FA utilization and ketogenesis). The simultaneous impaired up-regulation of *Ppara* and *Fgf21* in 48h-fasted $GR^{\Delta Adip}$ livers is consistent with a proposed necessity of lipolysis for the expression of both genes (51). FGF21 was shown to be required to sustain fasting hypoglycemia by stimulating corticotropin-releasing hormone in hypothalamic neurons and concomitant release of adrenal corticosterone (52). The increased blood glucose levels in 48h-fasted $GR^{\Delta Adip}$ mice combined with elevated corticosterone indicate a uniquely different fasting response upon complete FGF21-deficiency versus its scarcity due to defective lipolysis. GCs stimulate lipolysis, lean mass catabolism, AA utilization and gluconeogenesis (1; 4; 53). Accordingly, fasting metabolism upon muscle-specific GR-deficiency is opposite to $GR^{\Delta Adip}$ mice in that muscle mass is preserved and WAT depleted (3). Conversely, in fasted $GR^{\Delta Adip}$ mice, all tissues except WAT respond to GC, visible as increased circulating AA (proteogenic and urea cycle-related), their metabolites (i.e. 2-ketobutyrate, creatine, creatinine, carnitine) and glucose (4; 53). As gluconeogenesis is intimately connected to the TCA cycle by both substrate supply and energy demand (6; 29),

lean mass-derived AA conceivably provided both sources in 48h-fasted $GR^{\Delta Adip}$ mice. The elevation of purine nucleotide precursor and degradation products (i.e. xanthosine, hypoxanthine, xanthine, urate) additionally suggest that energetic requirements of the disturbed fasting metabolism in $GR^{\Delta Adip}$ mice results in imbalanced ATP synthesis/degradation rates and thus, a reduction in energy state. Thereby, our results determine adipocyte GR as a critical regulator of energy homeostasis during prolonged fasting.

In conclusion, our results demonstrate that the adipocyte GR controls systemic fuel partitioning and energy metabolism. In prolonged fasting states, GR activity is vital to prevent aberrant fuel selection and lean mass wasting by permitting β-adrenergic stimulation of lipolysis and the switch to lipid-based energy production. Conversely, in models of diet- and aging-induced obesity, GR activity is a determinant of systemic metabolic dysfunctions.

Acknowledgement

The authors thank Ute Burret (Institute for Comparative Molecular Endocrinology, University of Ulm) and Safia Zahma (Institute of Animal Breeding and Genetics, University of Veterinary Medicine Vienna) for excellent technical assistance, and the animal facility staff at the University of Ulm; Medical University Vienna and University of Veterinary Medicine Vienna for their support.

Funding: This work was supported by the Austrian Science Fund (FWF) grant SFB F2807-B20 to RM, grants Priority Program Immunobone 1468 (Tu 220/6-1, 6-2), Collaborative Research Centre 1149 (C02/INST 40/492-1), DFG-ANR (TU 220/13-1) from the Deutsche Forschungsgemeinschaft (DFG), and FP7 BRAINAGE from the European Union Research and Innovation funding program to JPT; and grant FWF P26766 to TS. Part of this work has been carried out with the Competence Center CBmed, funded by the Austrian Federal Government within the COMET K1 Centre Program, Land Steiermark and Land Wien. The

funders had no role in study design, data collection and analysis, decision to publish, or preparation of the manuscript.

Author contributions: KMM and KH performed most experiments, supervised experiments and analyzed/interpreted data. DK, SV, MB and LM provided major technical support. SJ, KF, TDM and MT performed metabolic cage experiments, data analyses and interpretation. NB and CM performed LC-MS metabolomics and data analyses. JH conducted histopathologic liver analyses. All other co-authors gave technical and scientific support. TS, HE, NB and JH assisted in data interpretation and contributed to discussion/experimental design. TS and NB contributed to the writing of the manuscript. KMM, KH, JPT and RM designed and coordinated the study, and wrote the manuscript.

JPT and RM are the guarantors of this work and take full responsibility for the work as a whole, including the study design, access to data, and the decision to submit and publish the manuscript.

Duality of Interest

The authors have no potential conflict of interest to report.

References

1. Rose AJ, Herzig S: Metabolic control through glucocorticoid hormones: an update. *Mol Cell Endocrinol* 380:65-78, 2013
2. Geer EB, Islam J, Buettner C: Mechanisms of glucocorticoid-induced insulin resistance: focus on adipose tissue function and lipid metabolism. *Endocrinol Metab Clin North Am* 43:75-102, 2014
3. Shimizu N, Maruyama T, Yoshikawa N, Matsumiya R, Ma Y, Ito N, Tasaka Y, Kuribara-Souta A, Miyata K, Oike Y, Berger S, Schutz G, Takeda S, Tanaka H: A muscle-liver-fat signalling axis is essential for central control of adaptive adipose remodelling. *Nat Commun* 6:6693, 2015
4. Okun JG, Conway S, Schmidt KV, Schumacher J, Wang X, de Guia R, Zota A, Klement J, Seibert O, Peters A, Maida A, Herzig S, Rose AJ: Molecular regulation of urea cycle function by the liver glucocorticoid receptor. *Mol Metab* 4:732-740, 2015
5. Rosen ED, Spiegelman BM: What we talk about when we talk about fat. *Cell* 156:20-44, 2014

6. Samuel VT, Shulman GI: The pathogenesis of insulin resistance: integrating signaling pathways and substrate flux. *J Clin Invest* 126:12-22, 2016
7. Xu C, He J, Jiang H, Zu L, Zhai W, Pu S, Xu G: Direct effect of glucocorticoids on lipolysis in adipocytes. *Mol Endocrinol* 23:1161-1170, 2009
8. Gray NE, Lam LN, Yang K, Zhou AY, Koliwad S, Wang JC: Angiopoietin-like 4 (Angptl4) protein is a physiological mediator of intracellular lipolysis in murine adipocytes. *J Biol Chem* 287:8444-8456, 2012
9. Yu CY, Mayba O, Lee JV, Tran J, Harris C, Speed TP, Wang JC: Genome-wide analysis of glucocorticoid receptor binding regions in adipocytes reveal gene network involved in triglyceride homeostasis. *PLoS One* 5:e15188, 2010
10. Gathercole LL, Morgan SA, Bujalska IJ, Hauton D, Stewart PM, Tomlinson JW: Regulation of lipogenesis by glucocorticoids and insulin in human adipose tissue. *PLoS One* 6:e26223, 2011
11. Chimin P, Farias Tda S, Torres-Leal FL, Bolsoni-Lopes A, Campana AB, Andreotti S, Lima FB: Chronic glucocorticoid treatment enhances lipogenic activity in visceral adipocytes of male Wistar rats. *Acta Physiol (Oxf)* 211:409-420, 2014
12. Lee MJ, Fried SK, Mundt SS, Wang Y, Sullivan S, Stefanni A, Daugherty BL, Hermanowski-Vosatka A: Depot-specific regulation of the conversion of cortisone to cortisol in human adipose tissue. *Obesity (Silver Spring)* 16:1178-1185, 2008
13. Engeli S, Bohnke J, Feldpausch M, Gorzelniak K, Heintze U, Janke J, Luft FC, Sharma AM: Regulation of 11beta-HSD genes in human adipose tissue: influence of central obesity and weight loss. *Obes Res* 12:9-17, 2004
14. Masuzaki H, Paterson J, Shinyama H, Morton NM, Mullins JJ, Seckl JR, Flier JS: A transgenic model of visceral obesity and the metabolic syndrome. *Science* 294:2166-2170, 2001
15. Morton NM, Paterson JM, Masuzaki H, Holmes MC, Staels B, Fievet C, Walker BR, Flier JS, Mullins JJ, Seckl JR: Novel adipose tissue-mediated resistance to diet-induced visceral obesity in 11 beta-hydroxysteroid dehydrogenase type 1-deficient mice. *Diabetes* 53:931-938, 2004
16. Kershaw EE, Morton NM, Dhillon H, Ramage L, Seckl JR, Flier JS: Adipocyte-specific glucocorticoid inactivation protects against diet-induced obesity. *Diabetes* 54:1023-1031, 2005
17. Tronche F, Kellendonk C, Kretz O, Gass P, Anlag K, Orban PC, Bock R, Klein R, Schutz G: Disruption of the glucocorticoid receptor gene in the nervous system results in reduced anxiety. *Nat Genet* 23:99-103., 1999
18. Eguchi J, Wang X, Yu S, Kershaw EE, Chiu PC, Dushay J, Estall JL, Klein U, Maratos-Flier E, Rosen ED: Transcriptional control of adipose lipid handling by IRF4. *Cell Metab* 13:249-259, 2011
19. Muller TD, Muller A, Yi CX, Habegger KM, Meyer CW, Gaylinn BD, Finan B, Heppner K, Trivedi C, Bielohuby M, Abplanalp W, Meyer F, Piechowski CL, Pratzka J, Stemmer K, Holland J, Hembree J, Bhardwaj N, Raver C, Ottaway N, Krishna R, Sah R, Sallee FR, Woods SC, Perez-Tilve D, Bidlingmaier M, Thorner MO, Krude H, Smiley D, DiMarchi R, Hofmann S, Pfluger PT, Kleinau G, Biebermann H, Tschop MH: The orphan receptor Gpr83 regulates systemic energy metabolism via ghrelin-dependent and ghrelin-independent mechanisms. *Nat Commun* 4:1968, 2013
20. Schweiger M, Eichmann TO, Taschler U, Zimmermann R, Zechner R, Lass A: Measurement of lipolysis. *Methods Enzymol* 538:171-193, 2014
21. Engblom D, Kornfeld JW, Schwake L, Tronche F, Reimann A, Beug H, Hennighausen L, Moriggl R, Schutz G: Direct glucocorticoid receptor-Stat5 interaction in hepatocytes controls body size and maturation-related gene expression. *Genes Dev* 21:1157-1162, 2007

22. Bajad SU, Lu W, Kimball EH, Yuan J, Peterson C, Rabinowitz JD: Separation and quantitation of water soluble cellular metabolites by hydrophilic interaction chromatography-tandem mass spectrometry. *J Chromatogr A* 1125:76-88, 2006
23. Frohlich EE, Farzi A, Mayerhofer R, Reichmann F, Jacan A, Wagner B, Zinser E, Bordag N, Magnes C, Frohlich E, Kashofer K, Gorkiewicz G, Holzer P: Cognitive impairment by antibiotic-induced gut dysbiosis: Analysis of gut microbiota-brain communication. *Brain Behav Immun*, 2016
24. Yuan M, Breitkopf SB, Yang X, Asara JM: A positive/negative ion-switching, targeted mass spectrometry-based metabolomics platform for bodily fluids, cells, and fresh and fixed tissue. *Nat Protoc* 7:872-881, 2012
25. Sumner LW, Amberg A, Barrett D, Beale MH, Beger R, Daykin CA, Fan TW, Fiehn O, Goodacre R, Griffin JL, Hankemeier T, Hardy N, Harnly J, Higashi R, Kopka J, Lane AN, Lindon JC, Marriott P, Nicholls AW, Reily MD, Thaden JJ, Viant MR: Proposed minimum reporting standards for chemical analysis Chemical Analysis Working Group (CAWG) Metabolomics Standards Initiative (MSI). *Metabolomics* 3:211-221, 2007
26. Team: RC: R: A Language and Environment for Statistical Computing. . 2015
27. Tschop MH, Speakman JR, Arch JR, Auwerx J, Bruning JC, Chan L, Eckel RH, Farese RV, Jr., Galgani JE, Hambly C, Herman MA, Horvath TL, Kahn BB, Kozma SC, Maratos-Flier E, Muller TD, Munzberg H, Pfluger PT, Plum L, Reitman ML, Rahmouni K, Shulman GI, Thomas G, Kahn CR, Ravussin E: A guide to analysis of mouse energy metabolism. *Nat Methods* 9:57-63, 2011
28. Wang TJ, Larson MG, Vasan RS, Cheng S, Rhee EP, McCabe E, Lewis GD, Fox CS, Jacques PF, Fernandez C, O'Donnell CJ, Carr SA, Mootha VK, Florez JC, Souza A, Melander O, Clish CB, Gerszten RE: Metabolite profiles and the risk of developing diabetes. *Nat Med* 17:448-453, 2011
29. Satapati S, Sunny NE, Kucejova B, Fu X, He TT, Mendez-Lucas A, Shelton JM, Perales JC, Browning JD, Burgess SC: Elevated TCA cycle function in the pathology of diet-induced hepatic insulin resistance and fatty liver. *J Lipid Res* 53:1080-1092, 2012
30. Rebrin K, Steil GM, Getty L, Bergman RN: Free fatty acid as a link in the regulation of hepatic glucose output by peripheral insulin. *Diabetes* 44:1038-1045, 1995
31. Wu Q, Kazantzis M, Doege H, Ortegon AM, Tsang B, Falcon A, Stahl A: Fatty acid transport protein 1 is required for nonshivering thermogenesis in brown adipose tissue. *Diabetes* 55:3229-3237, 2006
32. Badman MK, Pissios P, Kennedy AR, Koukos G, Flier JS, Maratos-Flier E: Hepatic fibroblast growth factor 21 is regulated by PPARalpha and is a key mediator of hepatic lipid metabolism in ketotic states. *Cell Metab* 5:426-437, 2007
33. Zechner R, Zimmermann R, Eichmann TO, Kohlwein SD, Haemmerle G, Lass A, Madeo F: FAT SIGNALS--lipases and lipolysis in lipid metabolism and signaling. *Cell Metab* 15:279-291, 2012
34. Li YQ, Shrestha YB, Chen M, Chanturiya T, Gavrilova O, Weinstein LS: Gsalpha deficiency in adipose tissue improves glucose metabolism and insulin sensitivity without an effect on body weight. *Proc Natl Acad Sci U S A* 113:446-451, 2016
35. Schreiber R, Hofer P, Taschler U, Voshol PJ, Rechberger GN, Kotzbeck P, Jaeger D, Preiss-Landl K, Lord CC, Brown JM, Haemmerle G, Zimmermann R, Vidal-Puig A, Zechner R: Hypophagia and metabolic adaptations in mice with defective ATGL-mediated lipolysis cause resistance to HFD-induced obesity. *Proc Natl Acad Sci U S A* 112:13850-13855, 2015
36. Perry RJ, Zhang XM, Zhang D, Kumashiro N, Camporez JP, Cline GW, Rothman DL, Shulman GI: Leptin reverses diabetes by suppression of the hypothalamic-pituitary-adrenal axis. *Nat Med* 20:759-763, 2014
37. Kumashiro N, Beddow SA, Vatner DF, Majumdar SK, Cantley JL, Guebre-Egziabher F, Fat I, Guigni B, Jurczak MJ, Birkenfeld AL, Kahn M, Perler BK, Puchowicz MA, Manchem

VP, Bhanot S, Still CD, Gerhard GS, Petersen KF, Cline GW, Shulman GI, Samuel VT: Targeting pyruvate carboxylase reduces gluconeogenesis and adiposity and improves insulin resistance. *Diabetes* 62:2183-2194, 2013
38. Morgan SA, McCabe EL, Gathercole LL, Hassan-Smith ZK, Larner DP, Bujalska IJ, Stewart PM, Tomlinson JW, Lavery GG: 11beta-HSD1 is the major regulator of the tissue-specific effects of circulating glucocorticoid excess. *Proc Natl Acad Sci U S A* 111:E2482-2491, 2014
39. Lacasa D, Agli B, Giudicelli Y: Permissive action of glucocorticoids on catecholamine-induced lipolysis: direct "in vitro" effects on the fat cell beta-adrenoreceptor-coupled-adenylate cyclase system. *Biochem Biophys Res Commun* 153:489-497, 1988
40. Bartness TJ, Shrestha YB, Vaughan CH, Schwartz GJ, Song CK: Sensory and sympathetic nervous system control of white adipose tissue lipolysis. *Mol Cell Endocrinol* 318:34-43, 2009
41. Scherer T, O'Hare J, Diggs-Andrews K, Schweiger M, Cheng B, Lindtner C, Zielinski E, Vempati P, Su K, Dighe S, Milsom T, Puchowicz M, Scheja L, Zechner R, Fisher SJ, Previs SF, Buettner C: Brain insulin controls adipose tissue lipolysis and lipogenesis. *Cell Metab* 13:183-194, 2011
42. Saito N, Guitart X, Hayward M, Tallman JF, Duman RS, Nestler EJ: Corticosterone differentially regulates the expression of Gs alpha and Gi alpha messenger RNA and protein in rat cerebral cortex. *Proc Natl Acad Sci U S A* 86:3906-3910, 1989
43. Lim HW, Uhlenhaut NH, Rauch A, Weiner J, Hubner S, Hubner N, Won KJ, Lazar MA, Tuckermann J, Steger DJ: Genomic redistribution of GR monomers and dimers mediates transcriptional response to exogenous glucocorticoid in vivo. *Genome Res* 25:836-844, 2015
44. Mottillo EP, Balasubramanian P, Lee YH, Weng C, Kershaw EE, Granneman JG: Coupling of lipolysis and de novo lipogenesis in brown, beige, and white adipose tissues during chronic beta3-adrenergic receptor activation. *J Lipid Res* 55:2276-2286, 2014
45. Goossens GH: The role of adipose tissue dysfunction in the pathogenesis of obesity-related insulin resistance. *Physiol Behav* 94:206-218, 2008
46. Moran-Salvador E, Lopez-Parra M, Garcia-Alonso V, Titos E, Martinez-Clemente M, Gonzalez-Periz A, Lopez-Vicario C, Barak Y, Arroyo V, Claria J: Role for PPARgamma in obesity-induced hepatic steatosis as determined by hepatocyte- and macrophage-specific conditional knockouts. *FASEB J* 25:2538-2550, 2011
47. Koonen DP, Jacobs RL, Febbraio M, Young ME, Soltys CL, Ong H, Vance DE, Dyck JR: Increased hepatic CD36 expression contributes to dyslipidemia associated with diet-induced obesity. *Diabetes* 56:2863-2871, 2007
48. Wilson CG, Tran JL, Erion DM, Vera NB, Febbraio M, Weiss EJ: Hepatocyte-Specific Disruption of CD36 Attenuates Fatty Liver and Improves Insulin Sensitivity in HFD-Fed Mice. *Endocrinology* 157:570-585, 2016
49. Wu JW, Wang SP, Casavant S, Moreau A, Yang GS, Mitchell GA: Fasting energy homeostasis in mice with adipose deficiency of desnutrin/adipose triglyceride lipase. *Endocrinology* 153:2198-2207, 2012
50. Heckmann BL, Zhang X, Xie X, Saarinen A, Lu X, Yang X, Liu J: Defective adipose lipolysis and altered global energy metabolism in mice with adipose overexpression of the lipolytic inhibitor G0/G1 switch gene 2 (G0S2). *J Biol Chem* 289:1905-1916, 2014
51. Jaeger D, Schoiswohl G, Hofer P, Schreiber R, Schweiger M, Eichmann TO, Pollak NM, Poecher N, Grabner GF, Zierler KA, Eder S, Kolb D, Radner FP, Preiss-Landl K, Lass A, Zechner R, Kershaw EE, Haemmerle G: Fasting-induced G0/G1 switch gene 2 and FGF21 expression in the liver are under regulation of adipose tissue derived fatty acids. *J Hepatol*, 2015

52. Liang Q, Zhong L, Zhang J, Wang Y, Bornstein SR, Triggle CR, Ding H, Lam KS, Xu A: FGF21 maintains glucose homeostasis by mediating the cross talk between liver and brain during prolonged fasting. *Diabetes* 63:4064-4075, 2014
53. Bordag N, Klie S, Jurchott K, Vierheller J, Schiewe H, Albrecht V, Tonn JC, Schwartz C, Schichor C, Selbig J: Glucocorticoid (dexamethasone)-induced metabolome changes in healthy males suggest prediction of response and side effects. *Sci Rep* 5:15954, 2015

Figure Legends

Figure 1: Basal metabolic signature in plasma of GR$^{\Delta Adip}$ mice.

A Relative mRNA expression of *GR* as determined by qRT-PCR in total inguinal white adipose tissue (iWAT), epididymal WAT (eWAT), brown adipose tissue (BAT) of 10-12 week old *ad libitum*-fed ctrl and GR$^{\Delta Adip}$ mice. Ct values were normalized to *Actb* (n= 4-7/genotype). **B** Representative Western Blot of GR expression in total iWAT, eWAT, BAT and liver protein extracts of *ad libitum*-fed ctrl and GR$^{\Delta Adip}$ mice. **C** Volcano plots of relative abundance ratios of metabolites in plasma of *ad libitum*-fed GR$^{\Delta Adip}$ compared to ctrl mice as detected by LC-MS (n=5-6/genotype). Each arrow represents an individual metabolite within the indicated metabolite classes, while the direction of the arrow indicates, if the metabolite is increased or decreased. Respective p-values are plotted on the y-axis. For all analyses: 8-week-old male mice; standard diet. Data are shown as the mean ±SEM; **P*<0.05; ***P*<0.01; ****P*<0.001. For all analyses: 8-week-old male mice; standard diet *ad libitum*.

Figure 2: Reduced lipolytic and gluconeogenic capacity in GR$^{\Delta Adip}$ mice.

A Fasting blood glucose and plasma insulin level at indicated time points. Insulin concentrations were determined by ELISA (n≥6/genotype). **B** Insulin tolerance test. Following a 4h fast, insulin was administered through intraperitoneal injection (0.75 U/kg body weight; n=9/genotype). Blood glucose levels were determined at indicated time points. **C** Representative Western blot analysis and quantification of insulin-stimulated phosphorylation of AKT in liver and eWAT (0.75 U/kg body weight). HSC70 was used as a

loading control. Protein bands were quantified by densitometry and total protein expression was corrected for the respective loading control (n=3/genotype,). **D** Total liver TG content in *ad libitum*-fed mice as determined by a colorimetric assay (n≥6/genotype). **E** NEFA release from eWAT explants of 4h-fasted mice in absence or presence of insulin (30 ng/ml; n≥2 mice/genotype/treatment; n=10 explants/genotype). **F** NEFA release from eWAT explants of 16h-fasted mice (n≥2 mice/genotype/treatment; n=10 explants/genotype). Plasma NEFA and blood β-ketone level of 16h-fasted mice. Parameters were determined by colorimetric assays (n≥6/genotype). **G** Pyruvate tolerance test through intraperitoneal injection of pyruvate (2 g/kg body weight) following a 16h fast (n≥7/genotype). Blood glucose levels were determined at indicated time points. For **B** and **G**: results from 2-3 independent experiments. Data are shown as the mean ±SEM; **P*<0.05; ***P*<0.01; ****P*<0.001. For all analyses: 8-week-old male mice; standard diet *ad libitum*.

Figure 3: Reduced thermogenesis in GR$^{\Delta Adip}$ mice.

A Body temperatures of GR$^{\Delta Adip}$ and ctrl mice upon acute exposure to 4°C for the indicated time (n≥6/genotype). **B** Western blot analysis and quantification of UCP1 and PPARα protein levels in BAT of 4h cold exposed mice. HSC70 was used as a loading control. Protein bands were quantified by densitometry and total protein expression was corrected for the respective loading control (n=4/genotype,). **C** Representative H&E staining of BAT sections from GR$^{\Delta Adip}$ and ctrl mice after 4h of cold exposure. Scale bar indicates 200 µm. **D** Plasma NEFA, corticosterone and blood β-ketone level of 4h cold exposed mice. NEFA was determined by colorimetric assays and corticosterone was measured by ELISA (n≥6/genotype). Data are shown as the mean ±SEM; *P<0.05; **P<0.01. UCP1: Uncoupling protein 1; PPARα: Peroxisome proliferator-activated receptor alpha

Figure 4: Attenuated aging-associated obesity and hepatic steatosis in adipocyte GR-deficient mice.

A Postnatal body weight gain of $GR^{\Delta Adip}$ mice and ctrl littermates (n=12/genotype; 4 independent litter). **B** Non-invasive monitoring of body compositions of 52-week-old $GR^{\Delta Adip}$ and ctrl mice using EchoMRI. Total body fat and lean mass are depicted in relation to body weight (n=10). **C** Wet weight of eWAT, iWAT and liver in relation to body weight of 52-week-old mice (n≥7/genotype). **D** Representative hematoxylin-eosin stainings of livers and quantification of steatosis scores at 52 weeks of age (n≥7/genotype)**.** Score 1: < 5%, score 2: 5-20%, score 3: > 20% and score 4: > 50%. Scale bar indicates 200 µm. **E** Cumulative food intake, daily locomotor activity, energy expenditure and respiratory exchange ratios (RER) of aged mice (n≥6/genotype). For all analyses mice were fed a standard diet *ad libitum*; data are shown as the mean ±SEM; **P*<0.05; ***P*<0.01; ****P*<0.001.

Figure 5: Adipocyte-specific GR-deficient mice gain less weight under HFD conditions.

Mice from each genotype received either a chow or a high fat diet (HFD) starting at week 3-5 after birth. **A** Weight gain of ctrl and $GR^{\Delta Adip}$ mice littermates over a time period of 16 weeks (n=5-10/genotype). **B**-Relative mRNA expression of genes critical for lipid storage in eWAT and iWAT as determined by qRT-PCR of HFD-fed ctrl and $GR^{\Delta Adip}$ mice. Ct values were normalized to *Actb* (n≥5/genotype). **C** Three-dimensional models of subcutaneous (pink) and visceral (grey) fat in the abdominal region of HFD-fed mice. Quantification of subcutaneous and visceral fat volume after high fat or chow diet of the indicated genotypes (n=5-10/genotype). **D** Representative hematoxylin-eosin staining of eWAT and quantification of adipocyte cell size from eWAT of ctrl and $GR^{\Delta Adip}$ mice after HFD (n=5/genotype). Scale bar indicates 25 µm. Data are shown as the mean ±SEM; **P*<0.05; ***P*<0.01; ****P*<0.001. *Fasn*: Fatty acid synthase; *Acaca*: Acyl-CoA carboxylase; *Gpat3*: Glycerol-3-phosphate acyltransferase 3; *Dgat2*: Diglyceride acyltransferase-2; *Pck1*: Phosphoenolpyruvate

carboxykinase; *Cd36*: Platelet glycoprotein 4; *Slc27a1*: Fatty acid transport protein 1; *Actb*: β-Actin

Figure 6: Adipocyte-specific GR loss improves glucose tolerance and hepatic steatosis under HFD conditions.

A Blood glucose levels of 12h-fasted ctrl and $GR^{\Delta Adip}$ mice (n=5-10 mice/genotype). Plasma insulin levels (**B**) and HOMA-IR (**C**) of 12h-fasted ctrl and $GR^{\Delta Adip}$ mice (n=5-10 mice/genotype). Insulin concentrations were determined by ELISA. **D** Glucose tolerance test 18 weeks after chow/HFD. Glucose was administered by intraperitoneal injection (2 g/kg body weight) following a 16h fast. Blood glucose levels were determined at indicated time points (n=5-10/genotype). **E** Western blot analysis of insulin-stimulated phosphorylation of AKT in muscle (1 U/kg body weight) from ctrl and $GR^{\Delta Adip}$ mice after chow or HFD. **F** Representative hematoxylin-eosin staining of liver sections from ctrl and $GR^{\Delta Adip}$ mice after chow or HFD and histopathological characterization of liver phenotypes from HFD mice (n≥9/genotype)**.** Steatosis score 1: < 5%, score 2: 5-20%, score 3: > 20% and score 4: > 50%. Scale bar indicates 25 µm. **G** Comparison of wet weight of liver after chow and HFD of the indicated genotypes (n=5-10 mice/genotype). **H** Relative mRNA expression of *Fasn, Gpat1*, *Pparg, Cd36* and *Scl27a4* in liver as determined by qRT-PCR of HFD-fed ctrl and $GR^{\Delta Adip}$ mice. Ct values were normalized to *Actb* (n=8-10/genotype). For all analyses, ctrl and $GR^{\Delta Adip}$ mice received either a chow or a high fat diet (HFD) for 18-20 weeks starting at week 3-5 after birth; data are shown as the mean ±SEM; **P*<0.05; ***P*<0.01; ****P*<0.001. *Fasn*: Fatty acid synthase; *Gpat1*: Glycerol-3-phosphate acyltransferase 1; *Pparg*: peroxisome proliferator-activated receptor gamma; *Cd36*: Platelet glycoprotein 4; *Slc27a4*: Long-chain fatty acid transport protein 4; *Actb*: β-Actin

Figure 7: Impaired lipolysis in white adipose tissue of $GR^{\Delta Adip}$ mice results in aberrant substrate metabolism and lean mass wasting under prolonged fasting conditions.

A Non-invasive monitoring of body compositions in fed and 48h fasted mice using EchoMRI. Total body fat and lean mass are depicted in relation to body weight (n=6/genotype). **B** Representative hematoxylin-eosin staining of eWAT from 48h-fasted mice. Scale bar indicates 50 μm. **C** Plasma NEFA, glycerol and TG level, liver TG content, blood β-ketone level and blood glucose of fed and 48h-fasted mice. Plasma parameters and liver TG were determined by colorimetric assays (n≥6/genotype). **D** Plasma FGF21 level of *ad libitum* fed and 48h-fasted $GR^{\Delta Adip}$ and ctrl mice as determined by ELISA **E** Plasma corticosterone level of *ad libitum* fed, 16h- and 48h-fasted $GR^{\Delta Adip}$ and ctrl mice as determined by ELISA. **F** Volcano plots depicting relative abundance ratios of metabolites as detected by LC-MS metabolomics in plasma of following groups: 48h-fasted compared to fed $GR^{\Delta Adip}$ mice, 48h-fasted compared to fed ctrl mice and 48h-fasted $GR^{\Delta Adip}$ compared to ctrl mice (n=5-6/genotype). Each arrow represents an individual metabolite within the indicated metabolite classes, while the direction of the arrow indicates, if the metabolite is increased or decreased. Respective p-values are plotted on the y-axis. For **A**, **C, D** and **E**: Data are shown as the mean ±SEM; **P*<0.05; ***P*<0.01; ****P*<0.001. For all analyses: 8-week-old male mice; standard diet.

Figure 8: Adipocyte GR-deficiency impairs the lipolytic response of white adipocytes through impairment of β-adrenergic signal transduction.

A Relative mRNA expression levels of genes with key functions in lipolysis were quantified by qRT-PCR in eWAT under *ad libitum* feeding and 48h-fasting conditions. Ct values were normalized to *Gapdh* (n≥8/genotype). **B** Representative Western blots displaying the activation status and/or total expression levels of lipolytic key proteins eWAT under fed or fasted conditions. HSC70 served as loading control. Quantification of CGI58, ATGL

expression and HSL activation status upon fasting (n=5/genotype). Protein bands were quantified by densitometry; total protein expression was corrected for the respective loading control. **C** Western blot of eWAT from *ad libitum* fed and 48h-fasted mice using an antibody raised against phosphorylated PKA substrates containing a RRX(S*/T*) epitope motif. Quantification of PKA activity upon fasting (n=3/genotype). Total phosphorylated PKA substrates were quantified by densitometry and corrected for the respective loading control. **D** Relative mRNA expression levels of in eWAT under *ad libitum* feeding and 48h fasting conditions. Ct values were normalized to *Gapdh* (n≥8/genotype). **E** Representative Western blot of $G_S\alpha$ in eWAT under fed or fasted conditions. HSC70 served as loading control. Quantification of $G_S\alpha$ levels (n=5/genotype). Protein bands were quantified by densitometry; total protein expression was corrected for the respective loading control. **F** cAMP level in eWAT explants of 16h-fasted mice in response to treatment with indicated agonists (10 μM; n≥2 mice/genotype/treatment; n=10 explants/genotype). **G** NEFA release from eWAT explants of 16h-fasted mice in absence or presence of indicated agonists (10 μM; n≥2 mice/genotype/treatment; n=10 explants/genotype). Data are shown as the mean ±SEM; **P*<0.05; ***P*<0.01; ****P*<0.001. For all analyses: 8-week-old male mice; standard diet. *Lipe*: Hormone sensitive lipase (HSL); *Pnpla2*: Adipose triglyceride lipase (ATGL); *Abhd5*: Comparative gene identification 58 (CGI58); *Gapdh:* Glyceraldehyde 3-phosphate dehydrogenase; PKA: protein kinase A; *Adrb*: β-adrenergic receptor; *Gnas*: stimulatory G protein α-subunit ($G_S\alpha$). Iso: Isoproterenol; FK: Forskolin; CL: CL-316,243; For: Formoterol.

Figure 1

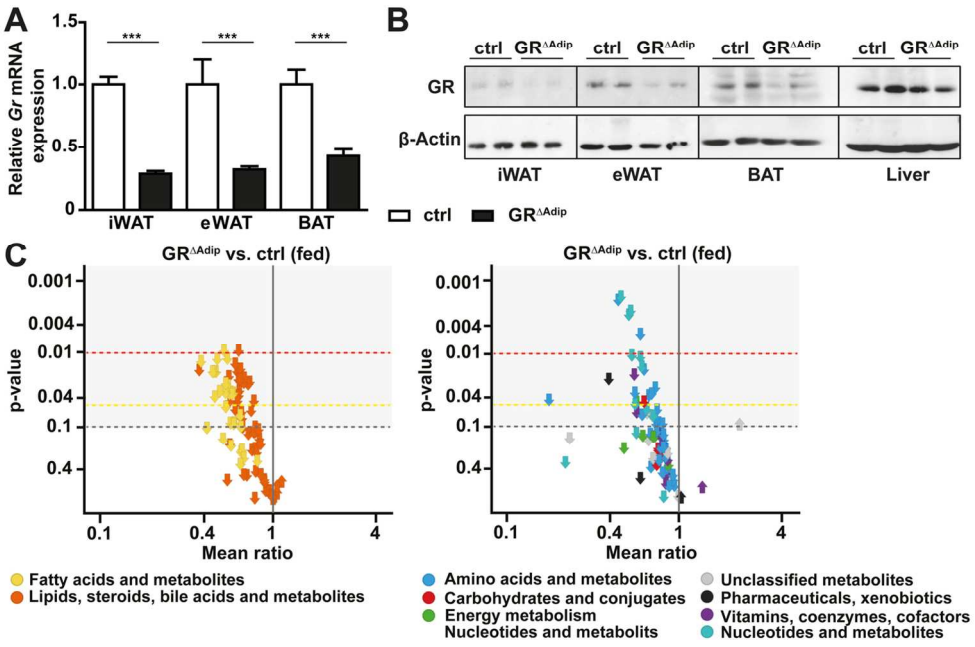

Figure 1: Basal metabolic signature in plasma of $GR^{\Delta Adip}$ mice.
A Relative mRNA expression of GR as determined by qRT-PCR in total inguinal white adipose tissue (iWAT), epididymal WAT (eWAT), brown adipose tissue (BAT) of 10-12 week old ad libitum-fed ctrl and $GR^{\Delta Adip}$ mice. Ct values were normalized to *Actb* (n= 4-7/genotype). B Representative Western Blot of GR expression in total iWAT, eWAT, BAT and liver protein extracts of ad libitum-fed ctrl and $GR^{\Delta Adip}$ mice. C Volcano plots of relative abundance ratios of metabolites in plasma of ad libitum-fed $GR^{\Delta Adip}$ compared to ctrl mice as detected by LC-MS (n=5-6/genotype). Each arrow represents an individual metabolite within the indicated metabolite classes, while the direction of the arrow indicates, if the metabolite is increased or decreased. Respective p-values are plotted on the y-axis. For all analyses: 8-week-old male mice; standard diet. Data are shown as the mean ±SEM; *P<0.05; **P<0.01; ***P<0.001. For all analyses: 8-week-old male mice; standard diet ad libitum.

Fig. 1
133x91mm (300 x 300 DPI)

Figure 2

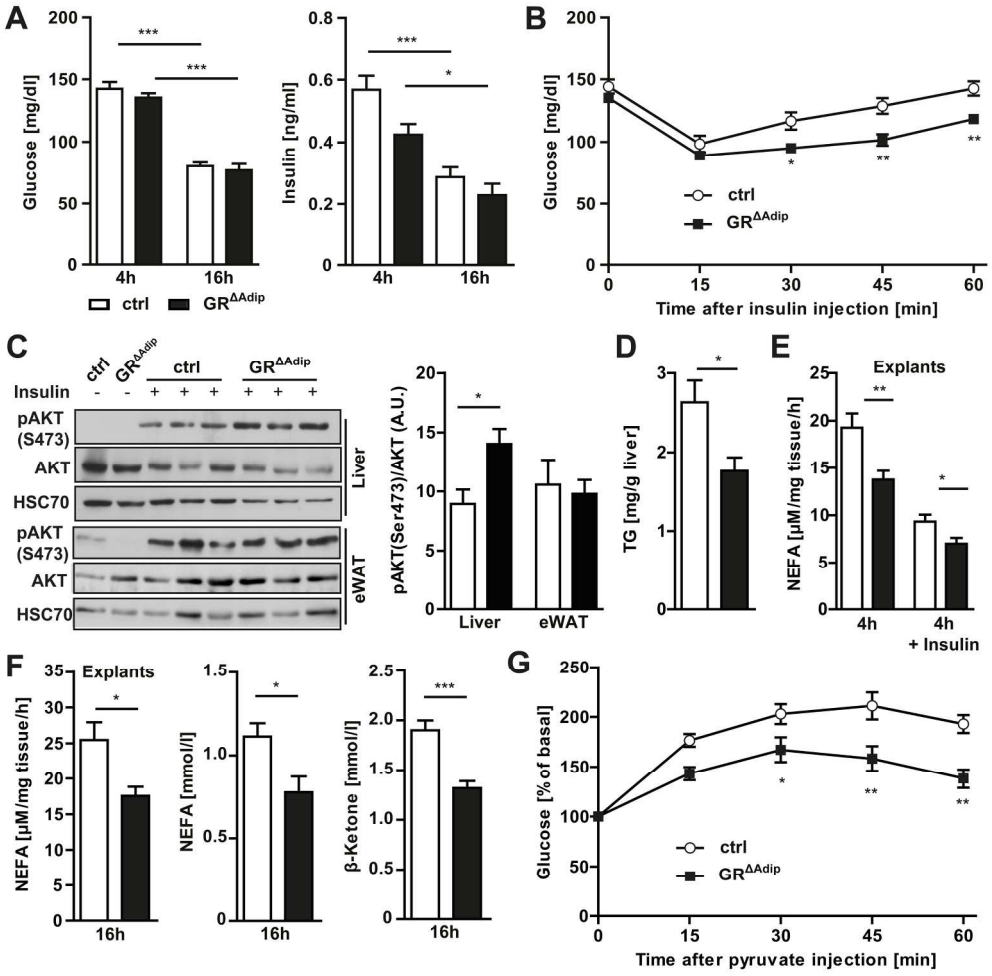

Figure 2: Reduced lipolytic and gluconeogenic capacity in $GR^{\Delta Adip}$ mice. A Fasting blood glucose and plasma insulin level at indicated time points. Insulin concentrations were determined by ELISA (n≥6/genotype). B Insulin tolerance test. Following a 4h fast, insulin was administered through intraperitoneal injection (0.75 U/kg body weight; n=9/genotype). Blood glucose levels were determined at indicated time points. C Representative Western blot analysis and quantification of insulin-stimulated phosphorylation of AKT in liver and eWAT (0.75 U/kg body weight). HSC70 was used as a loading control. Protein bands were quantified by densitometry and total protein expression was corrected for the respective loading control (n=3/genotype,). D Total liver TG content in ad libitum-fed mice as determined by a colorimetric assay (n≥6/genotype). E NEFA release from eWAT explants of 4h-fasted mice in absence or presence of insulin (30 ng/ml; n≥2 mice/genotype/treatment; n=10 explants/genotype). F NEFA release from eWAT explants of 16h-fasted mice (n≥2 mice/genotype/treatment; n=10 explants/genotype). Plasma NEFA and blood β-ketone level of 16h-fasted mice. Parameters were determined by colorimetric assays (n≥6/genotype). G Pyruvate tolerance test through intraperitoneal injection of pyruvate (2 g/kg body weight) following a 16h fast (n≥7/genotype). Blood glucose levels were determined at indicated time points. For B and G: results from 2-3 independent experiments. Data are shown as the mean ±SEM; *P<0.05; **P<0.01; ***P<0.001. For all analyses: 8-week-old male mice; standard diet ad libitum.

Fig. 2
207x212mm (300 x 300 DPI)

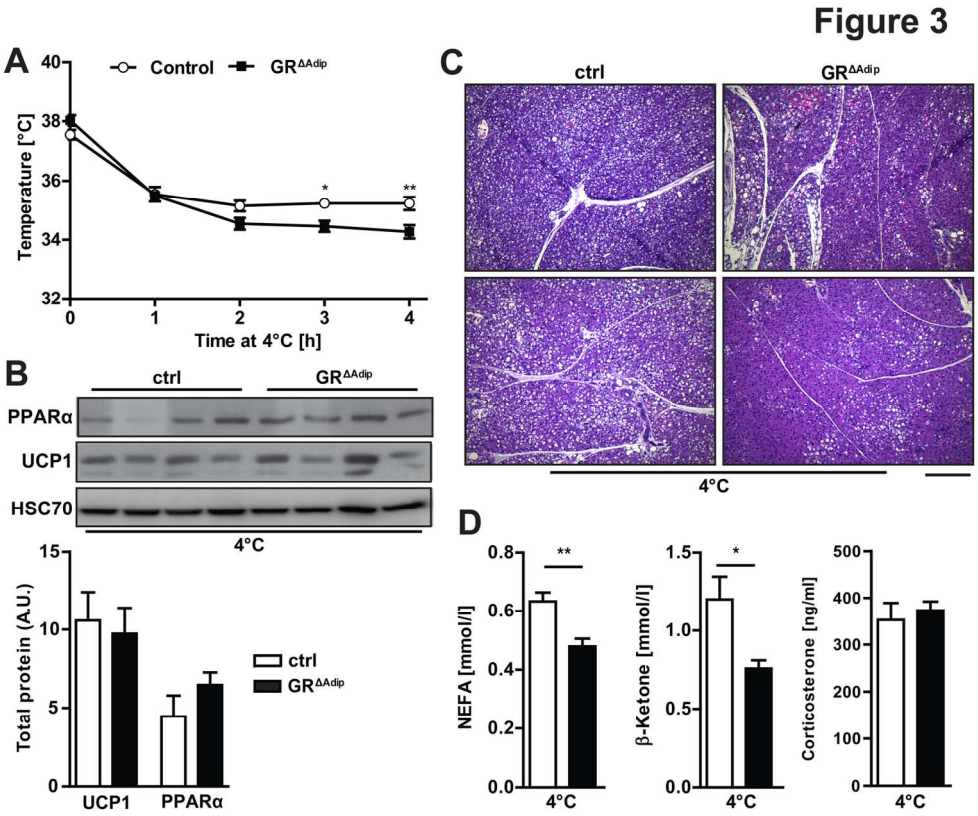

Figure 3: Reduced thermogenesis in $GR^{\Delta Adip}$ mice.
A Body temperatures of $GR^{\Delta Adip}$ and ctrl mice upon acute exposure to 4°C for the indicated time (n≥6/genotype). B Western blot analysis and quantification of UCP1 and PPARα protein levels in BAT of 4h cold exposed mice. HSC70 was used as a loading control. Protein bands were quantified by densitometry and total protein expression was corrected for the respective loading control (n=4/genotype,). C Representative H&E staining of BAT sections from $GR^{\Delta Adip}$ and ctrl mice after 4h of cold exposure. Scale bar indicates 200 µm. D Plasma NEFA, corticosterone and blood β-ketone level of 4h cold exposed mice. NEFA was determined by colorimetric assays and corticosterone was measured by ELISA (n≥6/genotype). Data are shown as the mean ±SEM; *P<0.05; **P<0.01. UCP1: Uncoupling protein 1; PPARα: Peroxisome proliferator-activated receptor alpha

Fig. 3
151x125mm (300 x 300 DPI)

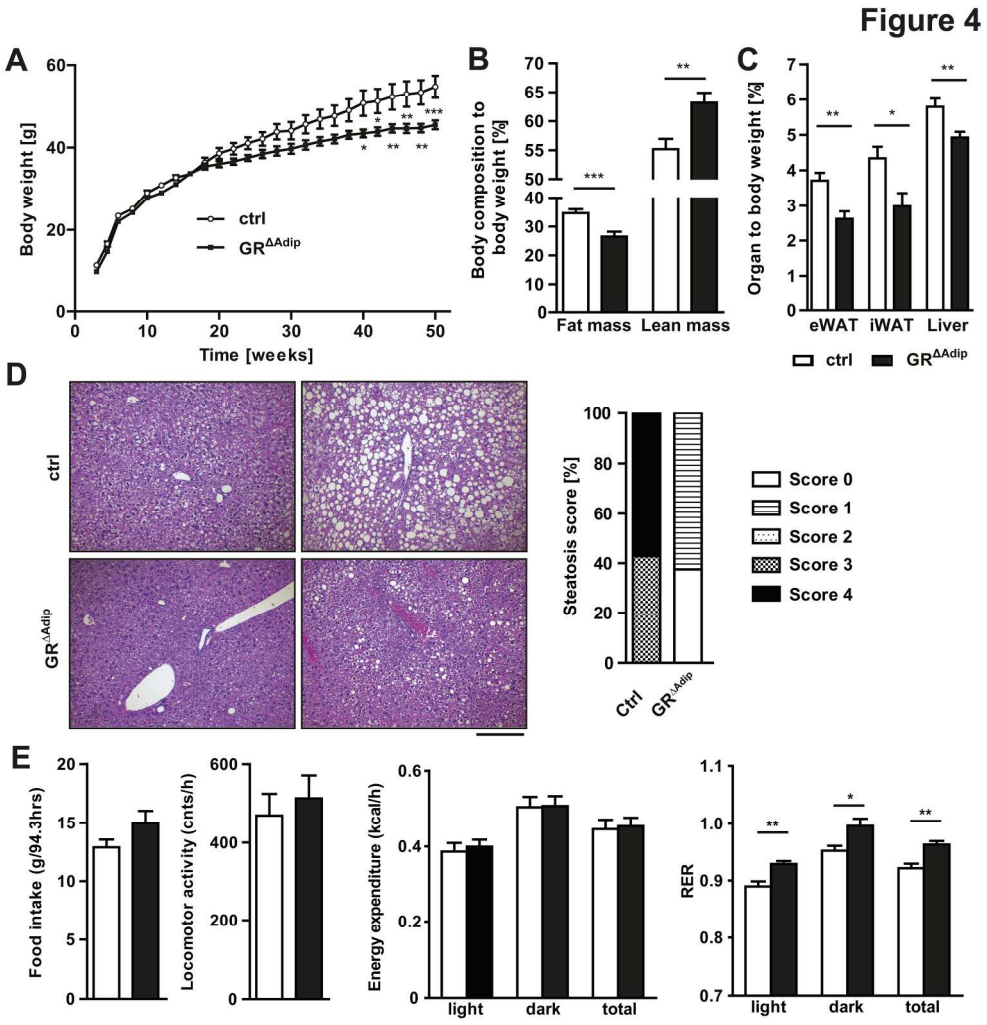

Figure 4: Attenuated aging-associated obesity and hepatic steatosis in adipocyte GR-deficient mice. A Postnatal body weight gain of $GR^{\Delta Adip}$ mice and ctrl littermates (n=12/genotype; 4 independent litter). B Non-invasive monitoring of body compositions of 52-week-old $GR^{\Delta Adip}$ and ctrl mice using EchoMRI. Total body fat and lean mass are depicted in relation to body weight (n=10). C Wet weight of eWAT, iWAT and liver in relation to body weight of 52-week-old mice (n≥7/genotype). D Representative H&E stainings of livers and quantification of steatosis scores at 52 weeks of age (n≥7/genotype). Score 1: < 5%, score 2: 5-20%, score 3: > 20% and score 4: > 50%. Scale bar indicates 200 µm. E Cumulative food intake, daily locomotor activity, energy expenditure and respiratory exchange ratios (RER) of aged mice (n≥6/genotype). For all analyses mice were fed a standard diet ad libitum; data are shown as the mean ±SEM; *P<0.05; **P<0.01; ***P<0.001.

Fig. 4
210x217mm (300 x 300 DPI)

Figure 5

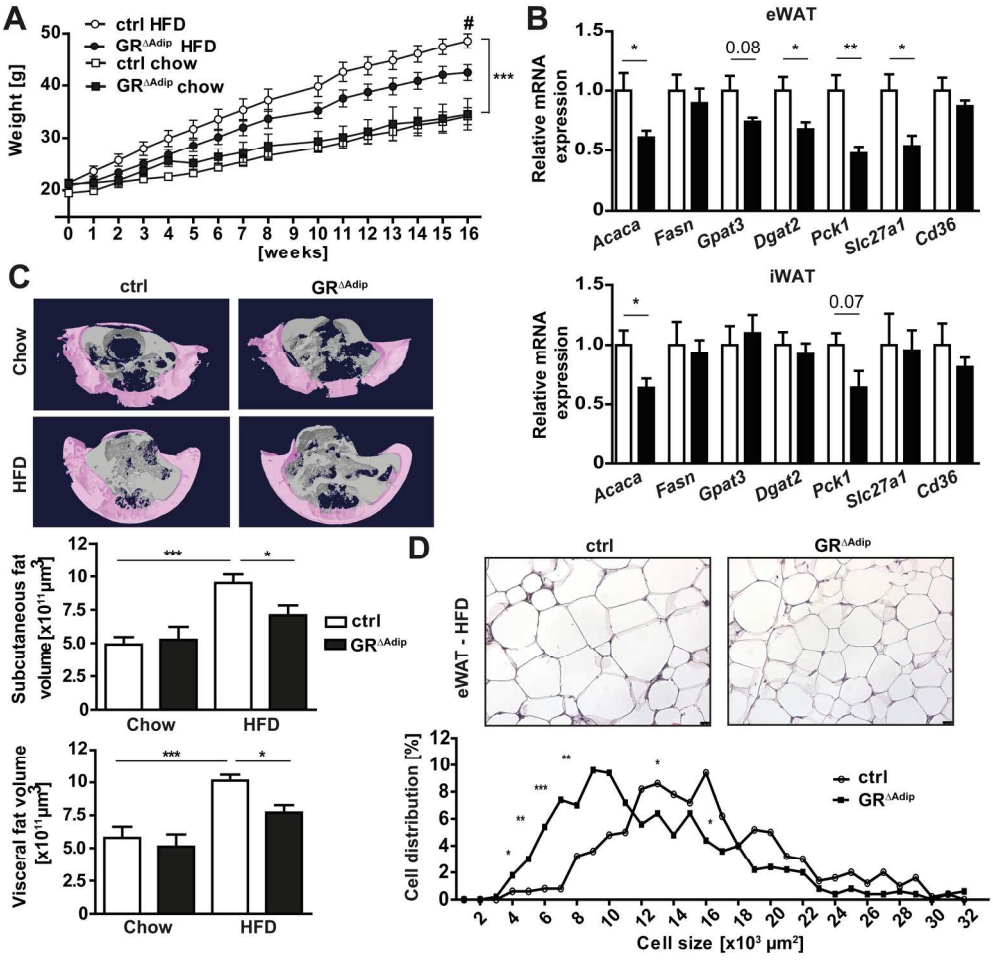

Figure 5: Adipocyte-specific GR-deficient mice gain less weight under HFD conditions.
Mice from each genotype received either a chow or a high fat diet (HFD) starting at week 3-5 after birth. A Weight gain of ctrl and $GR^{\Delta Adip}$ mice littermates over a time period of 16 weeks (n=5-10/genotype). B Relative mRNA expression of genes critical for lipid storage in eWAT and iWAT as determined by qRT-PCR of HFD-fed ctrl and $GR^{\Delta Adip}$ mice. Ct values were normalized to Actb (n≥5/genotype). C Three-dimensional models of subcutaneous (pink) and visceral (grey) fat in the abdominal region of HFD-fed mice. Quantification of subcutaneous and visceral fat volume after high fat or chow diet of the indicated genotypes (n=5-10/genotype). D Representative hematoxylin-eosin staining of eWAT and quantification of adipocyte cell size from eWAT of ctrl and $GR^{\Delta Adip}$ mice after HFD (n=5/genotype). Scale bar indicates 25 µm. Data are shown as the mean ±SEM; *P<0.05; **P<0.01; ***P<0.001. Fasn: Fatty acid synthase; Acaca: Acyl-CoA carboxylase; Gpat3: Glycerol-3-phosphate acyltransferase 3; Dgat2: Diglyceride acyltransferase-2; Pck1: Phosphoenolpyruvate carboxykinase; Cd36: Platelet glycoprotein 4; Slc27a1: Fatty acid transport protein 1; Actb: β-Actin

Fig. 5
199x201mm (300 x 300 DPI)

Figure 6

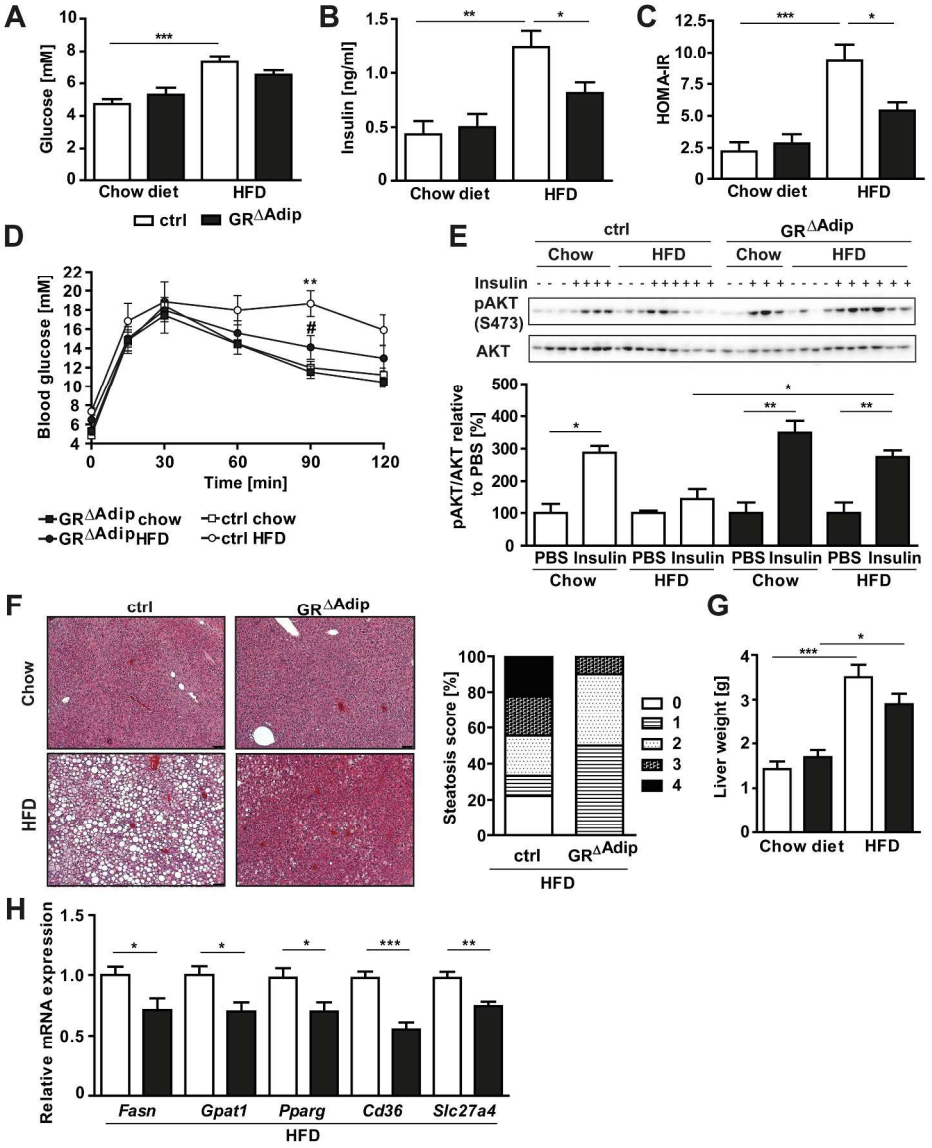

Figure 6: Adipocyte-specific GR loss improves glucose tolerance and hepatic steatosis under HFD conditions. A Blood glucose levels of 12h-fasted ctrl and $GR^{\Delta Adip}$ mice (n=5-10 mice/genotype). Plasma insulin levels (B) and HOMA-IR (C) of 12h-fasted ctrl and $GR^{\Delta Adip}$ mice (n=5-10 mice/genotype). Insulin concentrations were determined by ELISA. D Glucose tolerance test 18 weeks after chow/HFD. Glucose was administered by intraperitoneal injection (2 g/kg body weight) following a 16h fast. Blood glucose levels were determined at indicated time points (n=5-10/genotype). E Western blot analysis of insulin-stimulated phosphorylation of AKT in muscle (1 U/kg body weight) from ctrl and $GR^{\Delta Adip}$ mice after chow or HFD. F Comparison of wet weight of liver after chow and HFD of the indicated genotypes (n=5-10 mice/genotype). G Representative H&E staining of liver sections from ctrl and $GR^{\Delta Adip}$ mice after chow or HFD and histopathological characterization of liver phenotypes from HFD mice (n≥9/genotype). Steatosis score 1: < 5%, score 2: 5-20%, score 3: > 20% and score 4: > 50%. Scale bar indicates 25 µm. H Relative mRNA expression of Fasn, Gpat1, Pparg, Cd36 and Scl27a4 in liver as determined by qRT-PCR of HFD-fed ctrl and $GR^{\Delta Adip}$ mice. Ct values were normalized to Actb (n=8-10/genotype). For all analyses, ctrl and $GR^{\Delta Adip}$ mice

received either a chow or a high fat diet (HFD) for 18-20 weeks starting at week 3-5 after birth; data are shown as the mean ±SEM; *P<0.05; **P<0.01; ***P<0.001. Fasn: Fatty acid synthase; Gpat1: Glycerol-3-phosphate acyltransferase 1; Pparg: peroxisome proliferator-activated receptor gamma; Cd36: Platelet glycoprotein 4; Slc27a4: Long-chain fatty acid transport protein 4; Actb: β-Actin

Fig. 6

254x323mm (300 x 300 DPI)

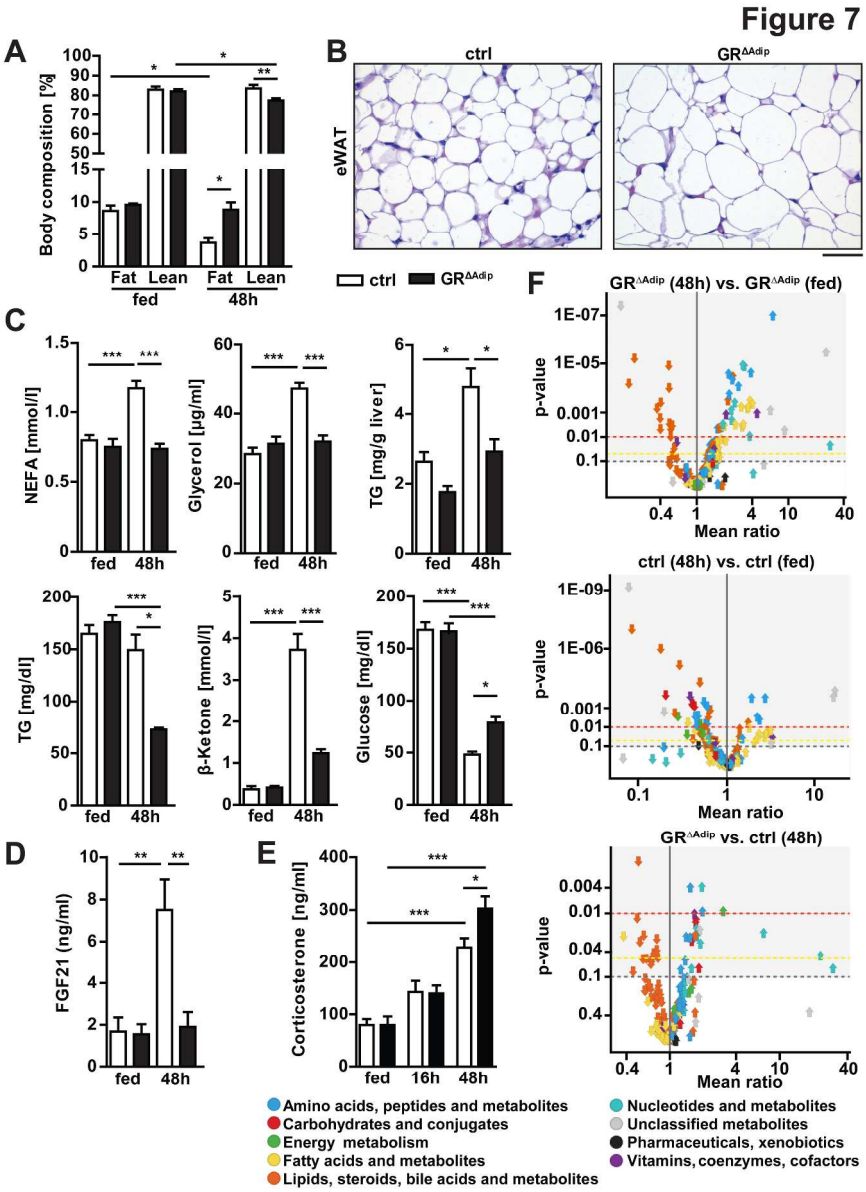

Figure 7: Impaired lipolysis in white adipose tissue of $GR^{\Delta Adip}$ mice results in aberrant substrate metabolism and lean mass wasting under prolonged fasting conditions. ├ ┬ A Non-invasive monitoring of body compositions in 48h fasted mice using EchoMRI. Total body fat and lean mass are depicted in relation to body weight (n=6/genotype). B Representative H&E staining of eWAT from 48h-fasted mice. Scale bar indicates 50 µm. C Plasma NEFA, glycerol and TG level, liver TG content, blood β-ketone level and blood glucose of 48h-fasted mice. Plasma parameters and liver TG were determined by colorimetric assays (n≥6/genotype). D Plasma FGF21 level of ad libitum fed and 48h-fasted $GR^{\Delta Adip}$ and ctrl mice as determined by ELISA E Plasma corticosterone level of ad libitum fed, 16h- and 48h-fasted $GR^{\Delta Adip}$ and ctrl mice as determined by ELISA. F Volcano plots depicting relative abundance ratios of metabolites as detected by LC-MS metabolomics in plasma of following groups: 48h-fasted compared to fed $GR^{\Delta Adip}$ mice, 48h-fasted compared to fed ctrl mice and 48h-fasted $GR^{\Delta Adip}$ compared to ctrl mice (n=5-6/genotype). Each arrow represents an individual metabolite within the indicated metabolite classes, while the direction of the arrow indicates, if the metabolite is increased or decreased. Respective p-values are plotted on the y-axis. For A,

C, D and E: Data are shown as the mean ±SEM; *P<0.05; **P<0.01; ***P<0.001. For all analyses: 8-week-old male mice; standard diet.

Fig. 7
246x332mm (300 x 300 DPI)

Figure 8

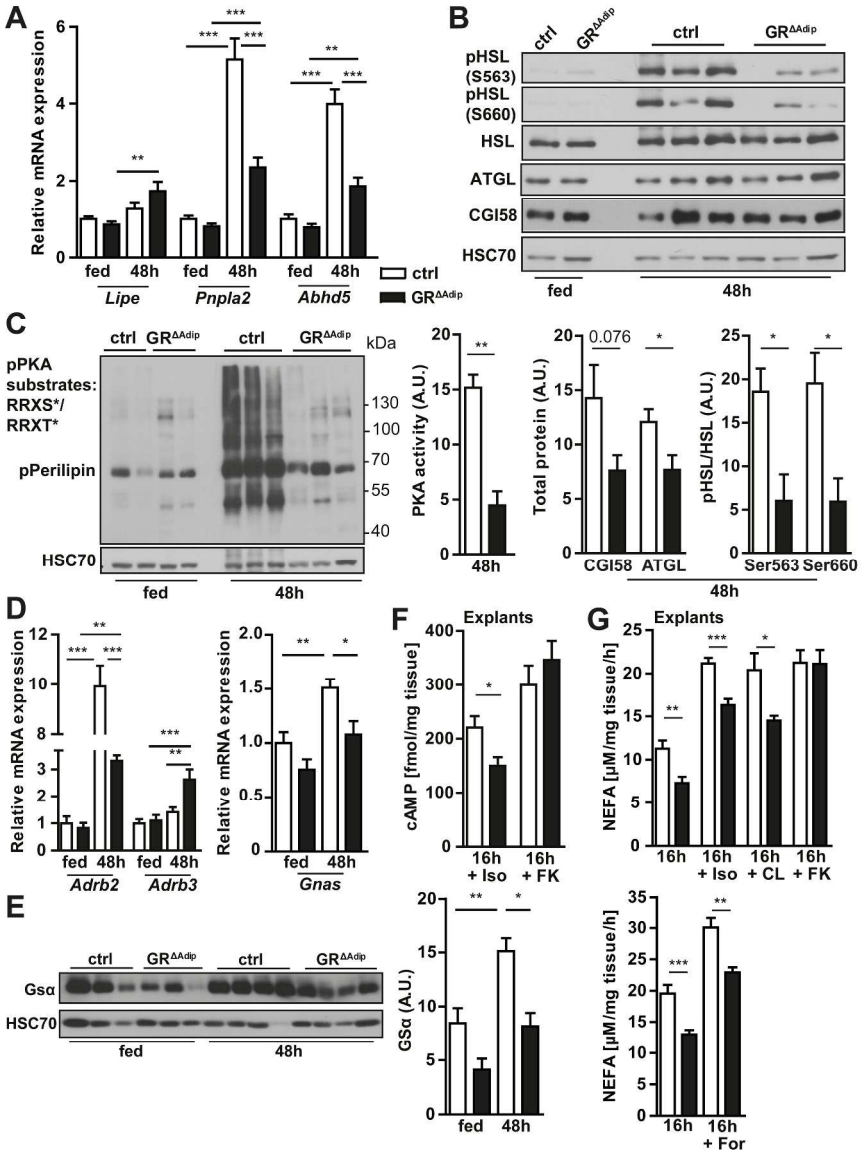

Figure 8: Adipocyte GR-deficiency impairs the lipolytic response of white adipocytes through impairment of β-adrenergic signal transduction.%"A Relative mRNA expression levels of genes with key functions in lipolysis were quantified by qRT-PCR in eWAT under ad libitum feeding and 48h-fasting conditions. Ct values were normalized to Gapdh (n≥8/genotype). B Representative Western blots displaying the activation status and/or total expression levels of lipolytic key proteins in eWAT under fed or fasted conditions. HSC70 served as loading control. Quantification of CGI58, ATGL expression and HSL activation status upon fasting (n=5/genotype). Protein bands were quantified by densitometry; total protein expression was corrected for the respective loading control. C Western blot of eWAT from ad libitum fed and 48h-fasted mice using an antibody raised against phosphorylated PKA substrates containing a RRX(S*/T*) epitope motif. Quantification of PKA activity upon fasting (n=3/genotype). Total phosphorylated PKA substrates were quantified by densitometry and corrected for the respective loading control. D Relative mRNA expression levels of in eWAT under ad libitum feeding and 48h fasting conditions. Ct values were normalized to Gapdh (n≥8/genotype). E Representative Western blot of $G_S\alpha$ in eWAT under fed or fasted conditions.

HSC70 served as loading control. Quantification of $G_S\alpha$ levels (n=5/genotype). Protein bands were quantified by densitometry; total protein expression was corrected for the respective loading control. F cAMP level in eWAT explants of 16h-fasted mice in response to treatment with indicated agonists (10 µM; n≥2 mice/genotype/treatment; n=10 explants/genotype). G NEFA release from eWAT explants of 16h-fasted mice in absence or presence of indicated agonists (10 µM; n≥2 mice/genotype/treatment; n=10 explants/genotype). Data are shown as the mean ±SEM; *P<0.05; **P<0.01; ***P<0.001. For all analyses: 8-week-old male mice; standard diet. Lipe: Hormone sensitive lipase (HSL); Pnpla2: Adipose triglyceride lipase (ATGL); Abhd5: Comparative gene identification 58 (CGI58); Gapdh: Glyceraldehyde 3-phosphate dehydrogenase; PKA: protein kinase A; Adrb: β-adrenergic receptor; Gnas: stimulatory G protein α-subunit. Iso: Isoproterenol; FK: Forskolin; CL: CL-316,243; For: Formoterol.

Fig. 8

250x349mm (300 x 300 DPI)

Online Supplemental Materials

Adipocyte glucocorticoid receptor deficiency attenuates aging- and HFD-induced obesity, and impairs the feeding-fasting transition

Kristina M. Mueller, Kerstin Hartmann, Doris Kaltenecker, Sabine Vettorazzi, Mandy Bauer, Lea Mauser, Sabine Amann, Sigrid Jall, Katrin Fischer, Harald Esterbauer, Timo D. Müller, Matthias H. Tschöp, Christoph Magnes, Johannes Haybaeck, Thomas Scherer, Natalie Bordag, Jan P. Tuckermann, Richard Moriggl

Supplementary figures and tables

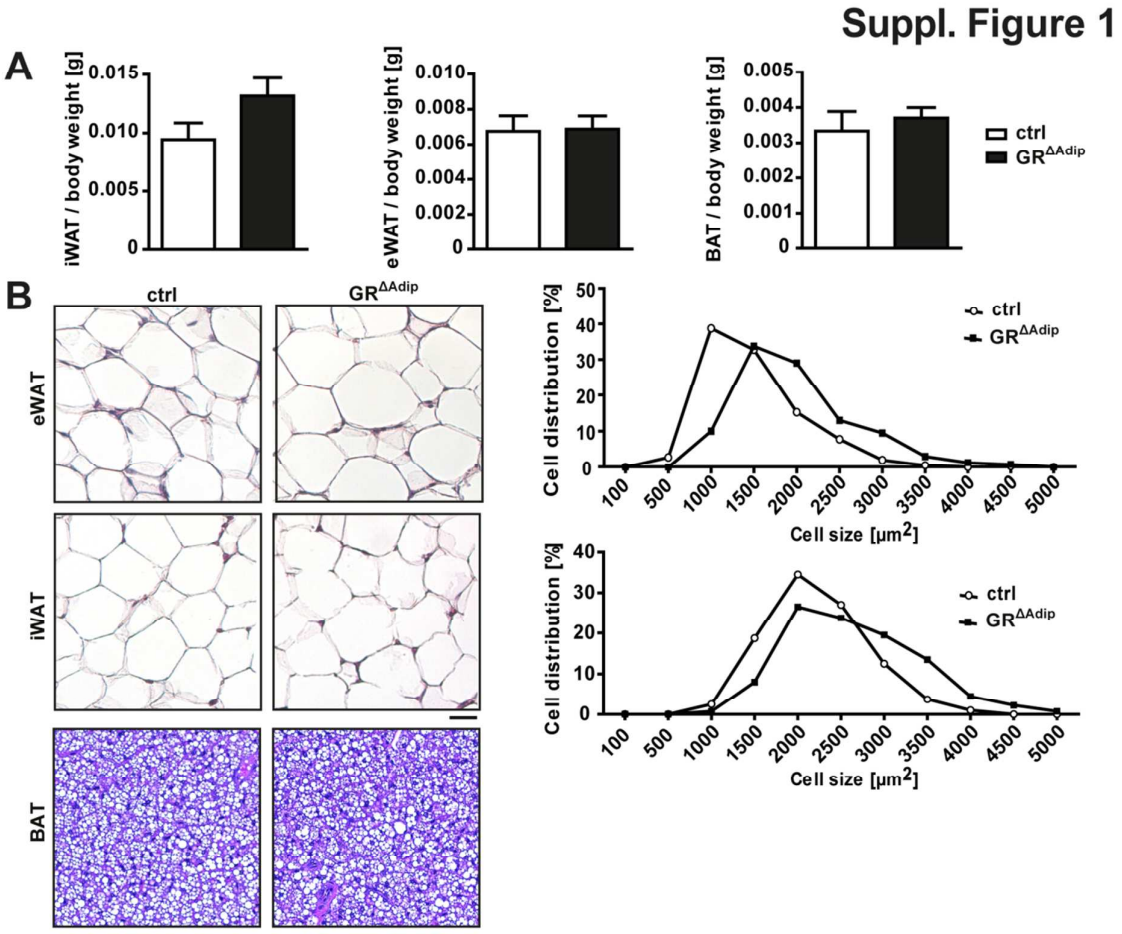

Supplementary Figure 1: Adipocyte-specific GR deficiency has no impact on adipose tissue size and morphology in 8-week-old mice. A Wet weight of eWAT, iWAT and BAT in relation to body weight (n=4-8/genotype). **B** Representative H&E staining of eWAT, iWAT and BAT from *ad libitum*-fed ctrl and $GR^{\Delta Adip}$ mice, and quantification of adipocyte cell size of eWAT and iWAT (n=5/genotype). Scale bar indicates 25 µm.

Suppl. Figure 2

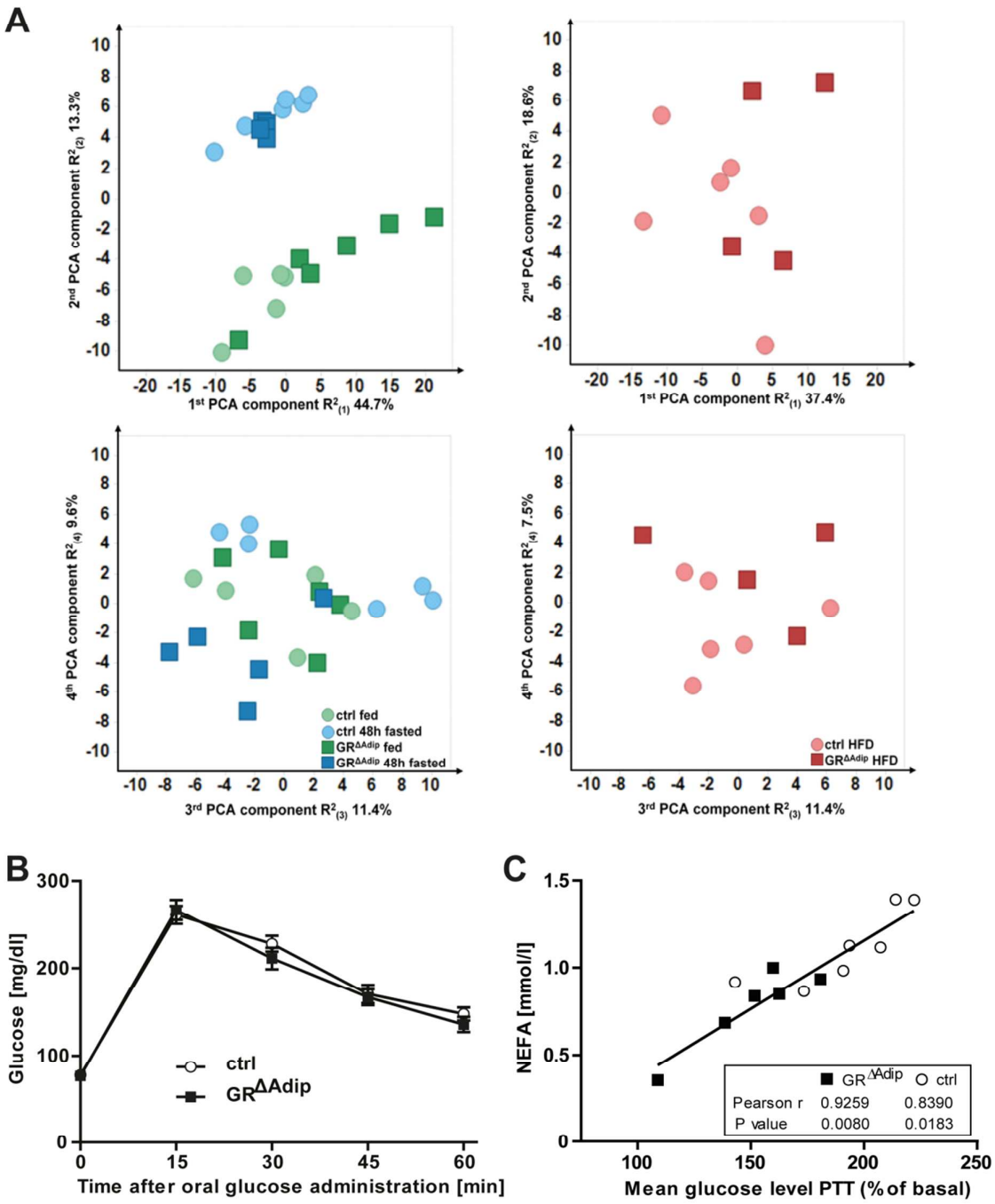

Supplementary Figure 2: Plasma metabolomics and glucose metabolism in 8-week-old GR$^{\Delta Adip}$ mice. A Scores plot of the principal component analysis (PCA) with 157 metabolites analyzed by LC-MS. Strong group separation was observed between genotypes in the first two components and a weak group separation between fasted and fed state in the third and

fourth component. A tendency for group separation between genotypes under HFD conditions was visible in the first four components. **B** Oral glucose tolerance test. Glucose was administered through oral gavage (2 g/kg body weight) following a 16h fast (n=10/genotype). **C** Correlation between plasma NEFA and mean of plasma glucose increase during pyruvate tolerance tests in 16h-fasted ctrl and $GR^{\Delta Adip}$ mice.

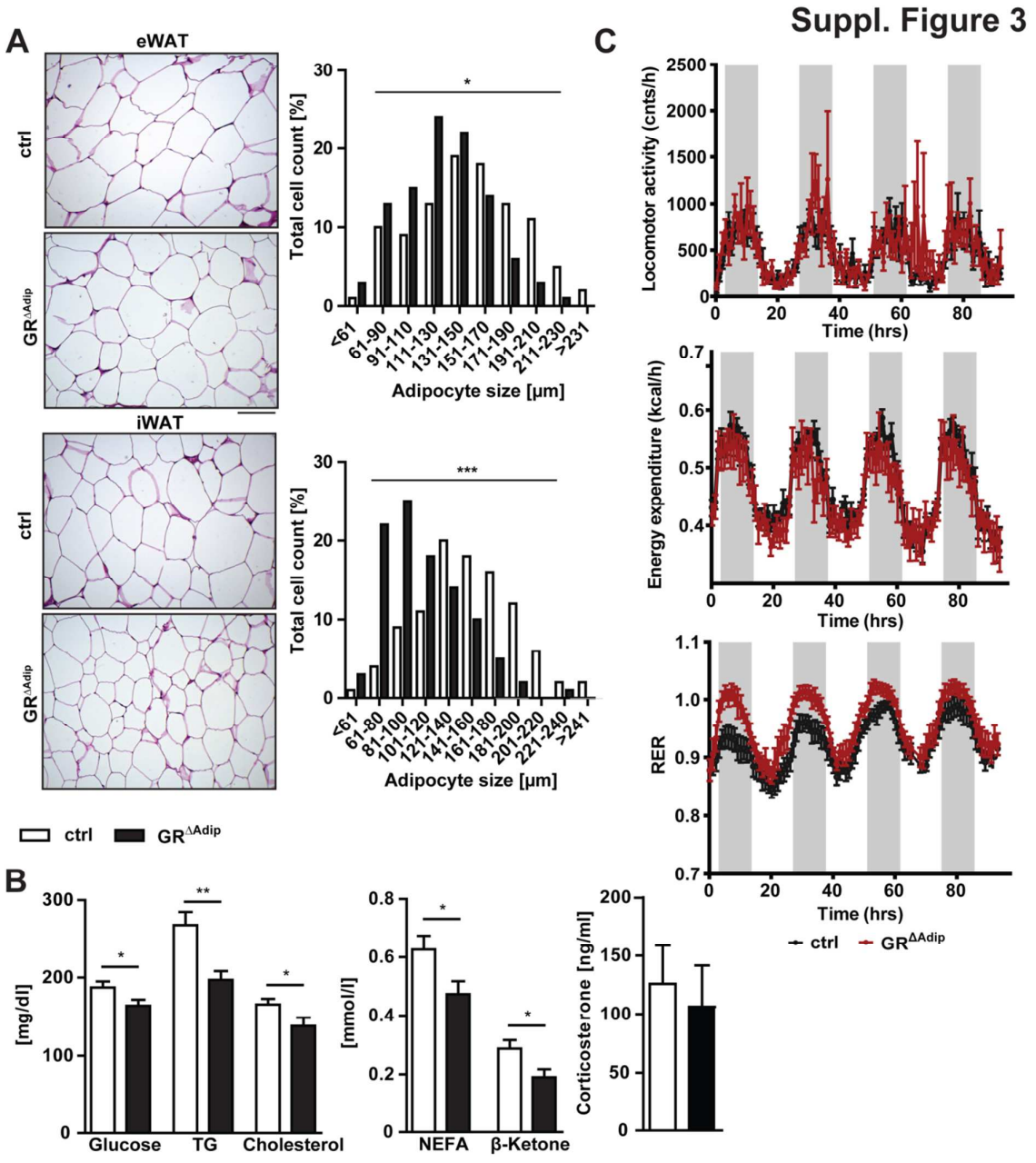

Supplementary Figure 3: Aging-associated metabolic phenotype 52-week-old $GR^{\Delta Adip}$ mice. A Representative H&E staining of eWAT and iWAT, and quantification of adipocyte

sizes (n≥5/genotype). Scale bar indicates 100 μm. **B** Plasma TG, cholesterol, NEFA, blood β-ketone level and plasma corticosterone level. Plasma metabolites were determined by colorimetric assays (n≥8/genotype); corticosterone was determined by ELISA (n≥7/genotype). **C** Patterns of locomotor activity, energy expenditure and respiratory exchange ratios (RER) during light and dark cycles (93.4h; n≥6/genotype). Data are shown as the mean ±SEM. **P*<0.05; ***P*<0.01; ****P*<0.001.

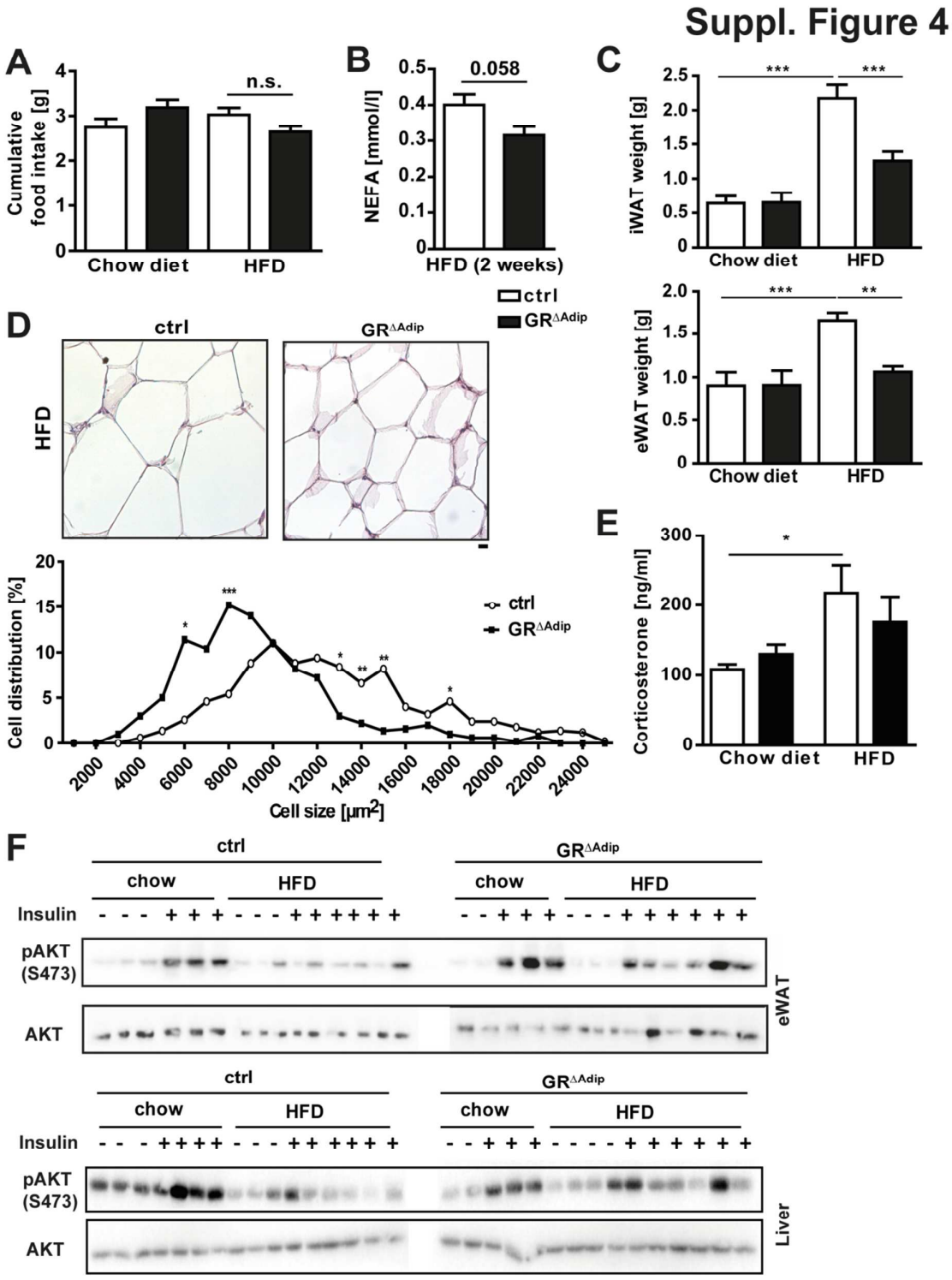

Supplementary Figure 4: Reduced weight gain of HFD-fed GR$^{\Delta Adip}$ mice is associated with diminished adipocyte hypertrophy and improved insulin signaling. A Measurement of cumulative food intake over a time period of 3 days from ctrl and GR$^{\Delta Adip}$ mice that either

received a chow or a high fat diet (HFD) (n=5-10/genotype). **B** Plasma NEFA levels of ctrl and $GR^{\Delta Adip}$ mice after 2 weeks of HFD feeding. Parameters were determined by colorimetric assays (n≥5/genotype). **C** Wet weight of iWAT and eWAT after chow and HFD of the indicated genotypes (n≥5/genotype). **D** Representative H&E staining of iWAT and quantification of adipocyte cell sizes in iWAT from ctrl and $GR^{\Delta Adip}$ mice after 20 weeks of HFD (n=5/genotype). Scale bar indicates 25 µm. **E** Plasma corticosterone levels of chow- and HFD-fed mice as determined by ELISA (n≥5/genotype). **F** Western blot analysis of insulin-stimulated phosphorylation of AKT in eWAT and liver (1 U/kg body weight) of chow- or HFD-fed ctrl and $GR^{\Delta Adip}$ mice. Data are shown as the mean ±SEM; **P*<0.05; ***P*<0.01; ****P*<0.001.

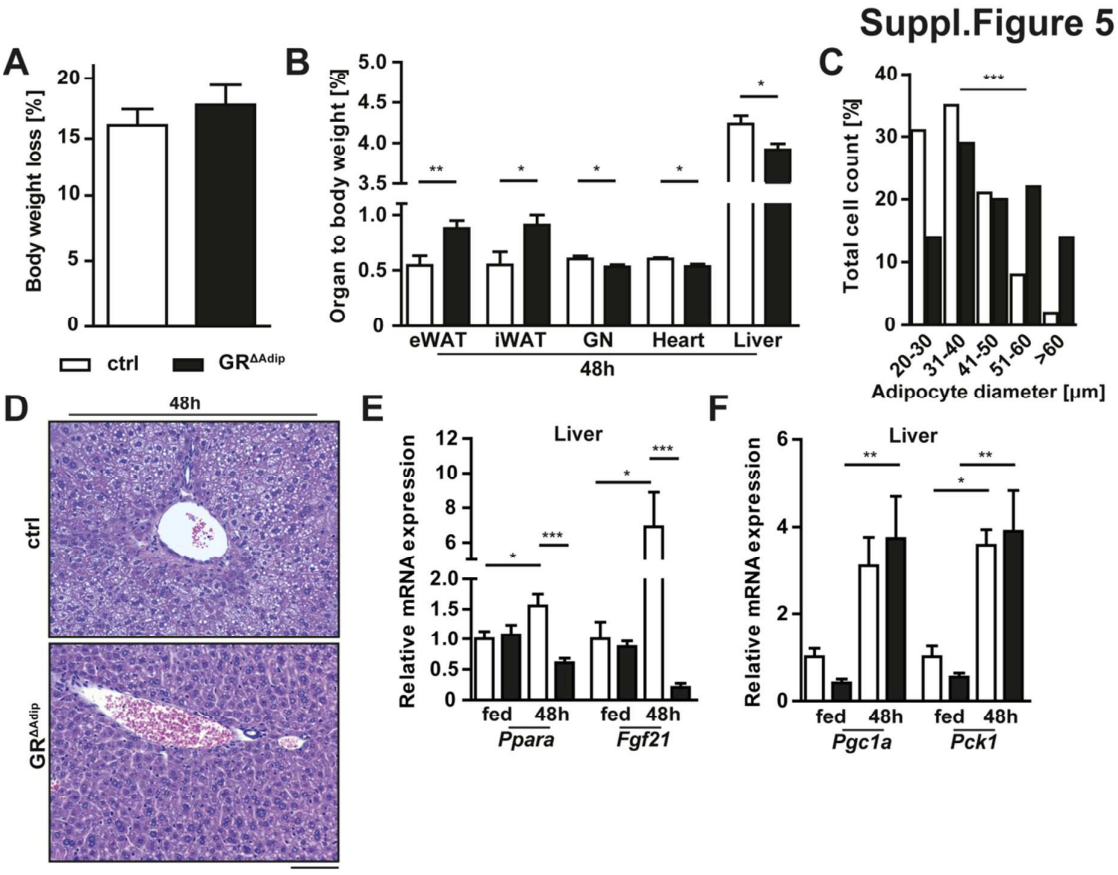

Supplementary Figure 5: Adipocyte-specific GR-deficiency reduces fasting-induced lipolysis in white adipose tissues and impairs energy metabolism. A Percent body weight

loss of 48h-fasted GR$^{\Delta Adip}$ and ctrl mice (n≥8/genotype). **B** Wet weight of eWAT, iWAT, gastrocnemius muscle (GN), heart and liver in relation to body weight (48h-fasted; n≥6/genotype). **C** Quantification of adipocyte cell size of eWAT of 48h-fasted mice (n≥4/genotype). **D** Representative H&E staining of livers of 48h-fasted GR$^{\Delta Adip}$ and ctrl mice. Scale bar indicates 100 µm. **E** Relative mRNA expression of *Ppara* and *Fgf21* as determined by qRT-PCR in livers of *ad libitum*-fed and 48h-fasted mice. Ct values were normalized to *Gapdh* (n≥5/genotype). **F** Relative mRNA expression of *Pgc1a* and *Pck1* as determined by qRT-PCR in livers of *ad libitum*-fed and 48h-fasted mice. Ct values were normalized to *Gapdh* (n≥5/genotype). Data are shown as the mean ±SEM; **P*<0.05; ***P*<0.01; ****P*<0.001. *Ppara*: Peroxisome proliferator-activated receptor alpha; *Fgf21*: Fibroblast growth factor 21; *Pgc1a*: Peroxisome proliferator-activated receptor gamma coactivator 1-alpha; *Pck1*: Phosphoenolpyruvate carboxykinase; *Gapdh:* Glyceraldehyde 3-phosphate dehydrogenase.

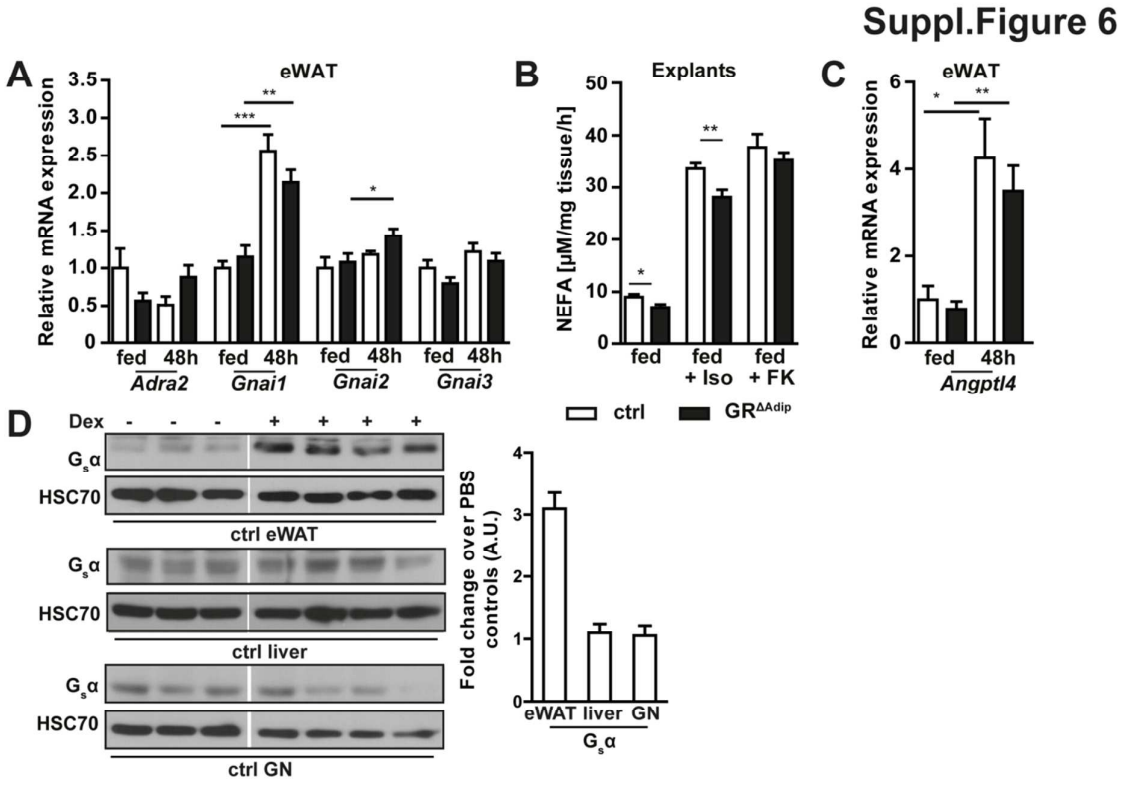

Supplementary Figure 6: Adipocyte-specific GR-deficiency reduces fasting-induced lipolysis in white adipose tissue. A Relative mRNA expression of *Adra2* and *Gnai1-3* as determined by qRT-PCR in eWAT of ad libitum-fed and 48h-fasted mice. Ct values were normalized to *Gapdh* (n≥8/genotype). **B** NEFA release from eWAT explants of *ad libitum*-fed mice in absence or presence of indicated agonists (10 µM; n≥2 mice/genotype/treatment; n=10 explants/genotype). **C** Relative mRNA expression of *Angptl4* as determined by qRT-PCR in eWAT of *ad libitum*-fed and 48h-fasted mice. Ct values were normalized to *Gapdh* (n≥8/genotype). **D** Western blot of $G_S\alpha$ in eWAT, liver and gastrocnemius muscle (GN) of dexamethasone-treated control mice (10 days; 5 mg/kg i.p.). HSC70 served as loading control. Quantification of $G_S\alpha$ levels (n≥3/genotype). Protein bands were quantified by densitometry; total protein expression was corrected for the respective loading control. Data are shown as the mean ±SEM; *P<0.05; **P<0.01; ***P<0.001. *Adra2:* Alpha-2-adrenergic receptor; *Gnai:* Inhibitory G-protein α-subunit isoform; *Angptl4*: Angiopoietin-like 4; *Gapdh:* Glyceraldehyde 3-phosphate dehydrogenase; Iso: Isoproterenol; FK: Forskolin.

Supplementary Table 1: qRT-PCR primer sequences for specific amplification of cDNA.

Gene symbol	**Sequence (5´ - 3´)**
Cebpb	ATCGACTTCAGCCCCTACCT
	TAGTCGTCGGCGAAGAGG
Pparg	GAAAGACAACGGACAAATCACC
	GGGGGTGATATGTTTGAACTTG
Fabp4	GGATGGAAAGTCGACCACAA
	TGGAAGTCACGCCTTTCATA
Ucp1	GACGTCCCCTGCCATTTAC
	CGCAGAAAAGAAGCCACAA
Adipoq	GGAGAGAAAGGAGATGCAGGT
	CTTTCCTGCCAGGGGTTC
Leptin	CAGGGAGGAAAATGTGCTGGAG
	CCGACTGCGTGTGTGAAATGT
Nr3c1	GGCCGCTCAGTGTTTTCTAA
	GCAGAGTTTGGGAGGTGGT
Fasn	GCTGCTGTTGGAAGTCAGC
	AGTGTTCGTTCCTCGGAGTG
Gpat1	GGAAGGTGCTGCTATTCCTG
	TGGGATACTGGGGTTGAAAA

Cd36	TTGTACCTATACTGTGGCTAATGAGA
	CTTGTGTTTTGAACATTTCTGCTT
Slc27a4	CTTGCCTGAGCTGCACAA
	GCGGGTCTTTCACAACAGT
Actb	GCACCAGGGTGTGATGGTG
	CCAGATCTTCTCCATGTCGTCC
Pnpla2	GTTGAAGGAGGGATGCAGAG
	GCCACTCACATCTACGGAGC
Lipe	GGAGAGAGTCTGCAGGAACG
	CCTGCAAGAGTATGTCACGC
Abhd5	GATGTGGGACACCAGGTAGG
	CGGTGATGAAAGCGATGG
Ppara	ATCGCGTACGGCAATGGCTTTA
	GCCTCGGAGGTCCCTGAACAG
Fgf21	GTCCTCCAGCAGCAGTTCTC
	CCTGGGTGTCAAAGCCTCTA
Angptl4	GGAAAAGTCCACTGTGCCTC
	TTTCCAAGATGACCCAGCTC
Pck1	CGTTTTCTGGGTTGATAGCC
	CCTAGTGCCTGTGGGAAGAC
Pgc1a	TGAGGACCGCTAGCAAGTTT
	TGAAGTGGTGTAGCGACCAA
Adrb2	TGACTAGATCAGCACACGCC
	GCCATCCTCATGTCGGTTAT
Adrb3	TCGAGCATAGACGAAGAGCA
	ACAGGAATGCCACTCCAATC
Adra2	CAGCGCCCTTCTTCTCTATG
	CAGGCCATCGAGTACAACCT
Gnas	TCTGTGGGAGGATGAGGGAG
	TGGTCACTTGGCACGTAGTC
Gnai1	CAAGATGATCGACCGCAACC
	ACCTCCCCATGGCTCTAATG
Gnai2	GGTGTTGCTGTAGACCACGG
	GGGAGGTGAAGTTGCTTCTG
Gnai3	TCGTCCTCTGAATAGCCGTC
	GAGAAAGCGGCCAAAGAAGT
Gapdh	TTGAGGTCAATGAAGGGGTC
	TCGTCCCGTAGACAAAATGG
Acaca	GAAGCCACAGTGAAATCTCG
	GATGGTTTGGCCTTTCACAT
Gpat3	GTGCTGGGTGTCCTAGTGC
	AAGCTGATCCCAATGAAAGC
Dgat2	GGCGCTACTTCCGAGACTAC
	TGGTCAGCAGGTTGTGTGTC
Slc27a1	CGGCGTTCTGTGTGTACG
	CCGAACACGAATCAGAACAG

Supplementary Table 2: Relative gene expression of adipogenic and adipocyte-specific markers. Relative mRNA expression of *Cebpb*, *Pparg*, *Fabp4*, *Adiponectin*, *Leptin* and *Ucp1* as determined by qRT-PCR in iWAT, eWAT and BAT of ctrl and $GR^{\Delta Adip}$ mice. Ct values were normalized to Actb (n≥8/genotype). Data are shown as the mean ±SEM. Cebpb: CCAAT/enhancer binding protein beta; Pparg: peroxisome proliferator-activated receptor gamma; Fabp4: fatty acid binding protein 4; Ucp1: uncoupling protein 1; Actb: β-Actin.

Gene	Tissue	ctrl	$GR^{\Delta Adip}$
Cebpb	iWAT	1.000 ± 0.1384	0.7921 ± 0.05627
	eWAT	0.6018 ± 0.1329	0.6798 ± 0.09286
	BAT	2.847 ± 0.6499	2.523 ± 0.3279
Pparg	iWAT	1.000 ± 0.1810	0.9196 ± 0.09747
	eWAT	0.8784 ± 0.1901	1.007 ± 0.1297
	BAT	2.958 ± 0.6028	2.961 ± 0.1977
Fabp4	iWAT	1.000 ± 0.1541	0.8510 ± 0.09064
	eWAT	0.3600 ± 0.07333	0.3523 ± 0.03811
	BAT	0.5616 ± 0.1018	0.4811 ± 0.03504
Adiponectin	iWAT	1.0 ± 0.1102	0.8592 ± 0.07639
	eWAT	0.4778 ± 0.09838	0.4613 ± 0.04948
	BAT	0.5216 ± 0.05834	0.4826 ± 0.02067
Leptin	iWAT	1.000 ± 0.03984	0.9988 ± 0.03957
	eWAT	0.9005 ± 0.02766	0.8336 ± 0.02457
	BAT	0.6903 ± 0.03423	0.7355 ± 0.01381
Ucp1	iWAT	0.003017 ± 0.002504	0.01176 ± 0.01135
	eWAT	0.0001496 ± 0.00006723	0.02537 ± 0.02471
	BAT	1.000 ± 0.1248	1.156 ± 0.09576

Sample_name	group	mouse_ID	Genotype	Feeding	BW_terminal_g	age_weeks	sex	Seq_Pos	PC1_Cfed_GRfed_C48_GR48_15 7metabolites	PC2_Cfed_GRfed_C48_GR48_15 7metabolites	PC3_Cfed_GRfed_C48_GR48_15 7metabolites	PC4_Cfed_GRfed_C48_GR48_15 7metabolites	PC5_Cfed_GRfed_C48_GR48_15 7metabolites	PC6_Cfed_GRfed_C48_GR48_15 7metabolites	PC1_CHFD ites
03_M1_pE_5552_Cfed	Cfed	5552	CTRL	fed	30.63	8	male	3	-6.06	-5.04	2.09	1.90	4.09	3.77	
14_M1_pE_9618_Cfed	Cfed	9618	CTRL	fed	29.03	8	male	14	-0.19	-5.16	-6.16	1.66	1.16	2.01	
25_M1_pE_5583_Cfed	Cfed	5583	CTRL	fed	24.58	8	male	25	-9.10	-10.05	4.58	-0.50	-1.14	0.28	
34_M1_pE_3188_Cfed	Cfed	3188	CTRL	fed	28.8	8	male	34	-0.70	-4.97	-3.98	0.88	1.22	-1.85	
45_M1_pE_5587_Cfed	Cfed	5587	CTRL	fed	28.32	8	male	45	-1.30	-7.14	0.90	-3.61	-5.82	0.34	
05_M1_pE_5558_C48	C48	5558	CTRL	48h fast	22.26	8	male	5	-10.16	3.08	6.24	-0.35	2.23	2.19	
13_M1_pE_3186_C48	C48	3186	CTRL	48h fast	25.3	8	male	13	2.51	6.21	-2.45	4.02	0.87	1.94	
23_M1_pE_5559_C48	C48	5559	CTRL	48h fast	24.26	8	male	23	3.19	6.81	10.05	0.19	1.84	1.73	
35_M1_pE_9114_C48	C48	9114	CTRL	48h fast	25.8	8	male	35	-5.84	4.77	-2.37	5.34	-3.52	-0.73	
44_M1_pE_5563_C48	C48	5563	CTRL	48h fast	21.48	8	male	44	-0.50	5.84	9.38	1.15	-2.01	-2.40	
64_M1_pE_9110_C48	C48	9110	CTRL	48h fast	22.5	8	male	64	0.03	6.54	-4.39	4.81	-4.23	2.77	
04_M1_pE_5553_GRfed	GRfed	5553	GR KO	fed	31.02	8	male	4	1.90	-3.96	-2.43	-1.86	0.71	0.11	
15_M1_pE_3189_GRfed	GRfed	3189	GR KO	fed	30.3	8	male	15	3.55	-4.89	-4.21	3.04	2.96	-2.38	
24_M1_pE_5579_GRfed	GRfed	5579	GR KO	fed	26.52	8	male	24	8.63	-3.12	3.81	-0.10	1.24	-1.15	
33_M1_pE_3187_GRfed	GRfed	3187	GR KO	fed	33.3	8	male	33	14.82	-1.66	-0.42	3.63	3.22	-1.98	
43_M1_pE_5584_GRfed	GRfed	5584	GR KO	fed	26.76	8	male	43	-6.66	-9.28	2.39	0.78	-1.96	-0.86	
65_M1_pE_5585_GRfed	GRfed	5585	GR KO	fed	27.68	8	male	65	21.22	-1.18	2.25	-4.03	-3.42	2.47	
08_M1_pE_5564_GR48	GR48	5564	GR KO	48h fast	20.08	8	male	8	-3.34	5.05	-2.49	-7.32	4.00	1.11	
19_M1_pE_3185_GR48	GR48	3185	GR KO	48h fast	25.5	8	male	19	-2.76	4.92	-7.78	-3.28	0.68	-0.46	
29_M1_pE_5589_GR48	GR48	5589	GR KO	48h fast	19.53	8	male	29	-2.80	4.73	-1.72	-4.46	-0.21	-2.77	
38_M1_pE_3184_GR48	GR48	3184	GR KO	48h fast	22.48	8	male	38	-2.77	3.94	-5.93	-2.26	-2.20	0.24	
50_M1_pE_5591_GR48	GR48	5591	GR KO	48h fast	20.93	8	male	50	-3.66	4.57	2.66	0.36	0.28	-4.38	
09_M1_pE_1_CHFD	CHFD	1	CTRL	HFD	21.18	6	male	9							-10.78
20_M1_pE_6_CHFD	CHFD	6	CTRL	HFD	21.03	6	male	20							4.02
28_M1_pE_2_CHFD	CHFD	2	CTRL	HFD	26.03	6	male	28							-0.88
40_M1_pE_5_CHFD	CHFD	5	CTRL	HFD	20.8	6	male	40							3.02
49_M1_pE_3_CHFD	CHFD	3	CTRL	HFD	27.36	6	male	49							-2.37
58_M1_pE_4_CHFD	CHFD	4	CTRL	HFD	21.75	6	male	58							-13.35
10_M1_pE_7_GRHFD	GRHFD	7	GR KO	HFD	23.63	6	male	10							-0.75
30_M1_pE_8_GRHFD	GRHFD	8	GR KO	HFD	20.94	6	male	30							6.53
39_M1_pE_11_GRHFD	GRHFD	11	GR KO	HFD	21.42	6	male	39							2.08
48_M1_pE_9_GRHFD	GRHFD	9	GR KO	HFD	23.75	6	male	48							12.47

_GRHFD_157metabol	PC2_CHFD_GRHFD_157metabol ites	PC3_CHFD_GRHFD_157metabol ites	PC4_CHFD_GRHFD_157metabol ites	PC5_CHFD_GRHFD_157metabol ites	PC6_CHFD_GRHFD_157metabol ites	MVA_UVA.1.1,5-Anhydrosorbitol.LOG_Peakarea	MVA_UVA.108.Hexose.LOG_Pe akarea	MVA_UVA.111.Hippuric acid.LOG_Peakarea	MVA_UVA.113.Histidine.LOG_P eakarea	MVA_UVA.117.Hypoxanthine.L OG_Peakarea	MVA_UVA.118.Indoxyl sulphate.LOG_Peakarea	MVA_UVA.123.Kynurenine.LOG _Peakarea	MVA_UVA.125.L-Cystathionine.LOG_Peakarea	MVA_UVA.126.Isoleucine, Leucine.LOG_Peakarea	MVA_UVA.129.Lysine.LOG_Pea karea	MVA_UVA.130.Malic acid.LOG_Peakarea	MVA_UVA.135.Mannitol, Sorbitol.LOG_Peaka	MVA_UVA _Pe
					9.21	10.31	7.45	8.83	5.89	8.89	7.30	6.21	10.22	8.96	9.00	7.81	8.41	
					9.38	10.46	7.78	8.88	5.39	9.44	7.50	6.85	10.17	9.15	9.21	7.27	8.42	
					9.25	10.34	7.78	8.96	5.95	9.07	7.51	6.63	10.35	9.17	9.06	7.96	8.47	
					9.31	10.40	7.61	8.88	7.63	9.46	7.69	6.57	10.21	9.06	8.96	7.57	8.56	
					9.30	10.38	7.99	8.91	7.19	8.99	7.64	6.52	10.23	8.98	9.10	7.79	8.27	
					8.48	9.57	6.85	8.94	6.00	9.17	7.47	6.26	10.38	8.94	8.86	7.18	8.46	
					9.00	10.08	7.12	8.78		9.50	7.99	6.72	10.01	8.78	8.88	6.57	8.48	
					8.50	9.58	6.69	8.54		8.85	7.25	5.78	10.06	8.68	8.51	7.05	8.38	
					9.07	10.15	7.29	9.00	6.09	9.46	7.66	6.47	10.34	8.89	8.82	7.00	8.59	
					8.75	9.83	6.98	8.54	6.87	8.90	7.51	5.87	10.15	8.64	8.59	7.25	8.31	
					9.17	10.23	7.08	8.91	5.41	9.08	7.90	6.40	10.22	8.88	8.84	6.94	8.55	
					9.28	10.38	7.68	8.85	7.07	9.28	7.41	6.55	10.27	9.03	9.10	7.66	8.40	
					9.30	10.38	7.04	8.88	5.84	9.55	7.79	6.47	10.21	9.04	9.01	7.42	8.46	
					9.05	10.14	7.24	8.64	5.48	9.05	7.48	6.19	10.07	8.87	8.73	7.61	8.32	
					9.04	10.12	6.64	8.51	4.90	9.09	7.43	6.55	9.87	8.87	8.85	7.10	8.33	
					9.31	10.39	8.08	8.96	6.42	9.04	7.63	6.49	10.27	9.08	9.07	7.94	8.40	
					8.89	9.95	7.34	8.51	5.49	8.50	7.10	6.27	9.85	8.85	8.67	7.49	8.18	
					9.07	10.17	7.57	8.91	5.77	9.41	7.78	6.31	10.37	9.03	8.78	7.49	8.43	
					9.17	10.26	7.37	8.93	8.40	9.49	7.85	6.65	10.24	8.95	9.16	7.28	8.53	
					9.13	10.22	6.97	8.94	7.74	9.37	7.55	6.33	10.40	9.00	8.82	7.33	8.55	
					9.22	10.30	7.25	8.95	6.41	9.37	7.78	6.58	10.27	8.99	9.10	7.31	8.51	
					9.07	10.16	7.11	8.74	7.86	9.47	7.65	6.24	10.27	8.81	8.62	7.00	8.44	
5.07	-2.03	1.49	6.42	1.79	9.29	10.36	6.11	8.59	7.63	8.46	6.95		10.22	8.76	9.05	7.25	8.32	
-9.97	0.37	-2.83	2.33	-0.32	9.27	10.35	6.77	8.71	6.62	8.45	7.18	6.05	10.24	8.83	9.18	7.30	8.27	
1.62	-1.89	-3.17	2.20	-3.06	9.30	10.37	6.28	8.52	7.38	8.20	6.98	5.53	10.13	8.76	8.98	7.22	8.24	
-1.47	-3.05	-5.65	-1.21	3.24	9.24	10.33	6.46	8.62	7.56	8.54	7.12	5.38	10.20	8.74	9.04	7.33	8.26	
0.72	-3.63	2.03	-3.87	4.39	9.23	10.31	6.48	8.57	7.60	8.26	6.91	5.59	10.21	8.91	9.00	7.19	8.34	
-1.85	6.24	-0.35	-3.89	0.37	9.27	10.35	6.67	8.71	7.28	8.52	7.12	5.97	10.16	8.88	8.89	7.21	8.29	
-3.52	-6.45	4.52	-2.21	-4.85	9.27	10.37	6.73	8.73	7.48	8.30	6.94	5.21	10.23	8.86	8.99	7.15	8.32	
-4.49	5.89	4.71	2.50	1.15	9.23	10.31	6.75	8.61	7.04	8.52	7.22	5.82	10.28	8.81	8.87	7.23	8.31	
6.63	3.97	-2.28	-1.41	-4.43	9.26	10.34	5.44	8.50	7.86	8.07	7.12	5.52	10.07	8.65	8.96	7.32	8.24	
7.26	0.58	1.54	-0.86	1.72	9.19	10.27	5.59	8.43	7.75	7.92	6.98	5.84	10.14	8.62	8.75	7.21	8.24	

...akarea	...136.Methionine.LOG	MVA_UVA.154.Niacinamide.LO G_Peakarea	MVA_UVA.157.Ornithine.LOG_ Peakarea	MVA_UVA.158.Orotic acid.LOG_Peakarea	MVA_UVA.162.Oxoglutaric acid.LOG_Peakarea	MVA_UVA.167.Palmitoylcarniti ne.LOG_Peakarea	MVA_UVA.171.Pantothenic acid.LOG_Peakarea	MVA_UVA.172.p-Cresyl glucuronide.LOG_Peakarea	MVA_UVA.173.p-Cresyl sulphate.LOG_Peakarea	MVA_UVA.174.Pentose.LOG_Pe akarea	MVA_UVA.176.Phenylalanin.LO G_Peakarea	MVA_UVA.177.Phosphocholine. LOG_Peakarea	MVA_UVA.178.Phosphocreatin e.LOG_Peakarea	MVA_UVA.182.Phytanic acid.LOG_Peakarea	MVA_UVA.183.Proline.LOG_Pe akarea	MVA_UVA.186.Pyridoxine.LOG_ Peakarea	MVA_UVA.187.Pyroglutamic acid.LOG_Peakarea	MVA_UVA.19.Acetylglycin G_Peakarea	MVA_UVA Peak
8.86	8.21	6.78	8.05	7.69	8.12	5.85	8.55	8.41	9.65	7.42	6.91	7.96	8.11	5.94	8.05	8.15	7.07		
8.85	8.22	6.93	8.02	7.36	8.09	5.76	8.29	8.57	9.63	7.64	7.15	7.81	8.05	7.38	8.00	7.81	7.39		
9.01	8.38	6.62	7.98	7.77	8.06	5.09	8.75	8.46	9.75	7.85	6.60	8.19	8.18	6.23	8.48	7.86	7.12		
8.77	8.20	6.77	8.11	7.22	8.01	6.52	8.75	8.55	9.66	7.47	6.63	7.82	8.13	7.15	8.00	7.68	7.09		
8.86	8.16	6.69	8.18	7.44	7.82		8.15	8.48	9.64	8.19	6.16	7.78	8.11	6.13	8.43	8.01	7.27		
8.76	8.18	6.75	7.98	8.23	8.33	7.03	9.85	7.73	9.66	7.22	6.22	7.72	8.05	5.20	8.11	8.49	7.09		
8.40	7.98	6.67	7.90	7.92	8.13	7.59	9.95	8.19	9.60	7.23	6.62	7.35	7.97	7.20	7.86	8.42	6.74		
8.37	7.87	6.58	7.72	8.07	7.96	7.15	9.32	7.79	9.38	7.44	5.52	7.46	7.75	4.49	8.08	8.30	6.73		
8.28	8.04	6.87	7.93	7.86	8.22	7.54	10.08	8.30	9.76	7.64	6.50	7.87	7.80	7.00	8.03	8.39	7.06		
8.27	7.69	6.83	7.82	8.21	8.01	6.45	8.87	7.96	9.49	7.59	6.00	7.60	7.65	4.58	8.10	8.18	6.83		
8.48	8.09	6.74	8.01	7.89	8.04	7.26	9.67	8.40	9.73	7.22	6.52	7.45	8.01	7.13	8.11	8.36	7.17		
8.82	8.23	6.83	8.23	7.34	8.08	6.65	8.85	8.49	9.65	7.49	6.39	7.81	8.09	5.78	7.97	7.81	7.03		
8.87	8.24	6.89	8.09	5.76	8.05	6.05	8.39	8.52	9.65	7.56	6.70	7.67	8.16	7.37	7.91	7.67	7.10		
8.87	8.06	6.50	7.77	7.28	7.79		7.61	8.27	9.51	7.04	6.39	7.51	7.80	5.94	7.92	7.36	6.83		
8.55	8.04	6.38	7.86	6.90	7.65	6.38	8.49	8.29	9.33	6.97	6.58	7.58	7.92	7.21	7.79	7.41	6.87		
8.89	8.32	6.88	8.11	7.73	8.04		8.12	8.54	9.66	7.59	6.54	8.04	8.18	5.72	8.23	7.72	7.05		
8.79	8.09	5.78	7.80	7.20	7.63		7.34	8.10	9.28	7.32	6.04	7.27	7.93	5.65	8.20	7.22	6.64		
8.44	8.35	7.04	7.91	7.97	8.33	7.34	9.76	8.27	9.75	7.01	6.43	7.69	8.22	5.65	8.14	8.46	7.25		
8.65	8.03	6.82	8.19	8.01	8.32	7.62	9.90	8.38	9.78	7.26	6.39	7.63	8.02	7.18	8.01	8.55	7.17		
8.87	8.30	6.74	7.75	7.89	8.20	7.26	9.89	8.31	9.80	7.14	6.25	7.65	8.11	5.50	8.15	8.32	6.94		
8.32	8.27	6.43	8.12	7.82	8.11	7.49	9.82	8.44	9.80	7.43	6.55	7.68	8.09	7.09	8.28	8.27	7.01		
8.40	7.99	6.77	7.77	8.04	8.15	6.99	9.53	8.23	9.65	7.04	6.50	7.71	7.90	5.18	8.06	8.39	6.81		
9.08	7.80		8.15	6.79	7.24		8.91	8.47	9.64	7.44	6.12	7.38	7.56		7.06	6.43	6.95		
9.04	7.99	5.84	8.21	6.75	7.70	5.68	8.80	8.49	9.64	7.67	6.60	7.12	7.75		7.66	7.34	7.15		
9.10	7.75	5.81	8.17	6.77	7.40	5.77	8.97	8.52	9.53	7.92	6.16	7.09	7.48	4.59	7.09	6.76	7.04		
8.97	7.84		8.09	6.68	7.58	5.79	9.23	8.47	9.58	7.19	6.25	7.20	7.65		7.05	7.28	7.05		
9.09	7.95	5.29	8.04	6.74	7.52	5.79	9.01	8.47	9.61	7.51	6.28	7.31	7.76		7.19	6.58	7.02		
9.05	7.93	5.75	7.99	7.07	7.75	5.69	8.94	8.50	9.57	7.92	6.42	7.44	7.81		7.42	7.20	7.04		
9.02	7.94	5.53	8.23	6.65	7.63	6.25	9.19	8.48	9.59	8.03	6.38	7.20	7.74		7.67	7.33	7.03		
9.04	7.84		8.00	6.84	7.53	6.37	9.17	8.44	9.65	7.56	6.31	7.09	7.57	5.01	7.26	7.12	7.21		
9.11	7.73		8.16	6.95	6.80	5.50	8.88	8.46	9.54	7.65	6.01	7.08	7.50		7.12	6.11	7.10		
9.14	7.61		7.80	6.79	6.73	4.99	8.83	8.42	9.57	7.40	5.85	7.03	7.20		6.96	5.84	6.95		

.LO karea	.190.Riboflavin.LOG_ MVA_UVA.192.Serine.LOG_Pea karea	MVA_UVA.199.Succinic acid.LOG_Peakarea	MVA_UVA.20.Adenine.LOG_Pe akarea	MVA_UVA.201.Tartaric acid.LOG_Peakarea	MVA_UVA.202.Taurine.LOG_Pe akarea	MVA_UVA.203.Taurodeoxychol ate,	Taurochenodeoxycholate.LOG_ Peakarea	MVA_UVA.204.Taurocholic acid.LOG_Peakarea	MVA_UVA.208.Threonine.LOG_ Peakarea	MVA_UVA.209.Thymidine.LOG_ Peakarea	MVA_UVA.21.Adenosine.LOG_P eakarea	MVA_UVA.210.Thymine.LOG_P eakarea	MVA_UVA.211.Thymol.LOG_Pe akarea	MVA_UVA.214.Trimethylamin-n-oxid.LOG_Peakarea	MVA_UVA.215.Tryptophan.LOG _Peakarea	MVA_UVA.216.Tyrosine.LOG_P eakarea	MVA_UVA.219.Uric acid.LOG_Peakarea	MVA_UVA aka
7.86	9.01	7.57	6.57	9.30	5.47	6.83	7.83	7.89	7.12	7.88	6.83	8.49	9.19	8.34	8.95	9.02		
7.90	9.13	7.80	6.26	9.24	6.60	7.84	7.96	7.56	7.03	7.62	6.80	8.79	9.09	8.34	9.07	9.15		
7.86	9.01	7.85	6.84	9.24	6.76	7.28	7.94	7.70	6.89	7.81	7.03	8.57	9.11	8.25	8.83	8.95		
7.91	8.77	7.89	6.37	9.10	6.70	7.00	7.98	7.67	9.26	7.72	6.86	8.62	9.25	8.27	8.90	9.04		
7.83	9.24	7.46	7.05	9.11	6.23	7.33	7.94	7.88	8.11	7.91	7.12	8.49	9.13	8.11	8.90	9.18		
7.89	8.78	7.45	6.33	9.37	6.67	6.37	7.95	7.85	7.09	7.86	6.65	7.47	9.10	8.15	8.82	9.08		
7.81	8.12	7.65	6.27	9.16	6.67	7.24	7.97	7.71	7.51	7.73	6.69	7.61	9.26	8.01	8.56	8.74		
7.69	8.26	7.21	6.62	8.98	4.95	5.97	7.78	7.55	6.76	7.54	6.55	7.26	9.00	7.85	8.43	8.62		
7.99	8.49	7.76	6.22	9.23	6.59	6.83	8.14	7.81	7.88	7.79	6.89	7.59	9.13	8.22	8.78	9.01		
7.59	8.53	7.43	6.52	8.97	6.52	7.78	7.74	7.71	6.64	7.64	6.65	7.56	9.07	7.89	8.54	8.84		
7.92	8.54	7.70	6.26	9.06	6.21	6.74	8.05	7.75	7.46	7.73	6.98	7.35	9.30	8.08	8.73	8.94		
7.80	8.99	7.42	6.29	9.09	6.57	7.35	7.91	7.60	8.72	7.60	7.02	8.67	9.15	8.17	8.92	9.05		
7.93	8.42	7.59	6.10	8.97	6.41	6.75	8.01	7.48	6.52	7.59	6.72	8.70	9.31	8.26	8.88	8.73		
7.72	8.82	7.38	6.22	9.02	6.72	7.34	7.82	7.40	6.79	7.43	6.65	8.75	9.08	7.97	8.60	8.76		
7.77	8.12	7.42	6.09	8.79	6.28	6.73	7.90	7.24	6.03	7.28	6.59	8.54	9.06	8.00	8.54	8.39		
7.83	9.19	7.72	6.45	9.14	6.10	7.16	7.91	7.67	6.98	7.75	6.88	8.44	9.20	8.21	9.03	9.03		
7.61	8.49	7.21	6.51	8.90	6.08	7.12	7.80	7.16	6.34	7.21	6.74	8.40	8.80	7.74	8.43	8.39		
7.89	8.87	7.79	6.46	9.36	5.47	6.24	8.00	8.15	7.28	8.15	6.65	8.02	9.36	8.19	8.90	9.00		
7.97	9.22	7.97	6.29	9.37	6.21	6.99	8.10	7.89	9.38	7.98	6.79	7.71	9.31	8.26	9.04	9.38		
7.97	8.87	7.43	6.28	9.31	6.26	7.08	8.11	7.95	7.25	8.00	6.68	7.46	9.03	8.17	8.87	9.23		
7.99	9.10	7.50	6.76	9.06	7.09	7.95	8.11	8.03	7.18	8.05	6.66	7.60	9.29	8.22	8.98	9.13		
7.75	8.65	7.58	6.16	9.15	6.94	7.28	7.95	7.80	7.53	7.85	6.75	7.83	9.21	7.95	8.70	9.04		
7.32	9.85	7.85		8.31			7.32	7.55	6.40	7.52	6.94	6.05	9.13	8.02	8.80	9.13		
7.49	9.73	6.84	5.96	8.66	7.10	7.94	7.49	7.63	6.61	7.57	6.85	6.30	9.07	8.07	8.78	9.10		
7.33	9.71	6.39		8.58		5.79	7.36	7.58	6.54	7.58	6.60	6.20	9.05	7.96	8.75	9.04		
7.39	9.76	7.52		8.45	5.99	6.58	7.36	7.56	6.31	7.57	6.67	6.06	9.08	7.96	8.75	9.08		
7.45	9.67	6.52	4.77	8.50		6.14	7.54	7.59	5.91	7.62	6.87	6.41	9.14	8.05	8.66	9.04		
7.69	9.47	6.85	5.49	8.63		6.72	7.71	7.69	5.90	7.71	6.54	6.23	9.08	8.02	8.68	8.92		
7.63	9.75	6.21		8.43			7.61	7.55	6.00	7.56	6.69	6.20	9.05	8.06	8.85	9.07		
7.52	9.56	6.46		8.48	8.26	9.16	7.50	7.80	6.46	7.71	6.96	5.85	9.21	8.00	8.71	8.96		
7.25	9.71	6.38	5.16	8.42	5.56	5.53	7.11	7.77	5.94	7.70	6.57	5.95	9.13	7.88	8.67	8.91		
7.11	9.51	6.40		8.40	6.10	6.02	7.09	7.73	5.93	7.66	6.90	5.82	9.09	7.87	8.63	8.87		

.220.Uridine.LOG_Pe rea	MVA_UVA.225.Valine.LOG_Pea karea	MVA_UVA.227.Xanthine.LOG_Pea eakarea	MVA_UVA.228.Xanthosine.LOG _Peakarea	MVA_UVA.230.PC 32:0.LOG_Peakarea	MVA_UVA.231.PC 32:1.LOG_Peakarea	MVA_UVA.232.PC 32:2.LOG_Peakarea	MVA_UVA.233.PC 34:1.LOG_Peakarea	MVA_UVA.234.PC 34:3.LOG_Peakarea	MVA_UVA.236.PC 36:2.LOG_Peakarea	MVA_UVA.237.PC 36:3.LOG_Peakarea	MVA_UVA.238.PC 36:4.LOG_Peakarea	MVA_UVA.239.PC 36:5.LOG_Peakarea	MVA_UVA.24.ADMA.LOG_Peak area	MVA_UVA.240.PC 38:3.LOG_Peakarea	MVA_UVA.241.PC 38:4.LOG_Peakarea	MVA_UVA.242.PC 38:5.LOG_Peakarea	MVA_UVA.243.PC 38:6.LOG_Peakarea	MVA_UVA 38:7
10.29	4.61	6.77	8.13	7.68	7.12	9.26	8.45	9.74	9.16	9.53	8.15	7.34	8.44	9.35	8.75	9.40	7.76	
10.23		6.76	7.91	7.50	6.85	9.21	8.40	9.66	9.01	9.46	8.22	7.59	8.40	9.25	8.63	9.25	7.56	
10.38		5.51	8.17	7.93	6.92	9.65	8.27	9.66	9.21	9.38	8.03	7.55	8.55	9.07	8.76	9.24	7.58	
10.36	8.30	6.82	8.02	7.95	7.09	9.41	8.31	9.61	9.11	9.45	8.11	7.43	8.43	9.20	8.77	9.22	7.61	
10.37	8.09	6.62	8.11	8.03	7.04	9.54	8.28	9.54	9.09	9.34	8.02	7.42	8.40	9.00	8.67	9.08	7.52	
10.32	4.58	6.35	8.38	7.67	6.86	9.39	8.36	9.47	8.85	9.61	7.90	7.63	7.81	9.29	8.79	9.61	7.78	
10.27	7.26		8.03	7.50	6.51	9.10	8.35	9.47	8.83	9.46	8.09	6.77	7.37	9.19	8.58	9.40	7.68	
10.05		5.99	8.14	7.63	6.83	9.17	8.25	9.29	8.70	9.42	8.07	7.25	7.41	9.07	8.64	9.37	7.78	
10.33	6.29	6.12	7.90	7.60	7.21	9.13	8.54	9.50	8.93	9.61	8.16	7.46	7.14	9.24	8.66	9.60	7.88	
10.18	7.75	6.25	8.21	7.73	7.01	9.22	8.34	9.43	8.78	9.51	8.07	7.25	6.78	9.27	8.67	9.38	7.74	
10.32	4.50	5.68	7.80	7.43	6.98	8.97	8.41	9.42	8.77	9.53	7.96	7.29	6.80	9.19	8.54	9.50	7.65	
10.21	8.24	6.41	7.99	7.71	7.18	9.29	8.34	9.61	8.99	9.36	8.06	7.42	8.36	9.14	8.58	9.16	7.65	
10.25		6.03	7.98	8.10	6.91	9.39	8.23	9.56	9.13	9.37	8.20	7.35	8.47	9.09	8.76	9.10	7.65	
10.14		6.10	7.90	7.96	6.97	9.44	8.17	9.39	9.01	9.22	8.05	7.22	8.31	8.91	8.60	9.02	7.57	
9.98		5.23	7.73	7.93	6.97	9.35	8.08	9.41	9.01	9.17	8.14	7.05	8.25	8.85	8.56	8.93	7.69	
10.39	5.64	7.01	8.09	8.01	7.11	9.62	8.44	9.70	9.23	9.48	8.23	7.49	8.52	9.12	8.76	9.24	7.74	
10.08		5.20	7.84	7.56	6.70	9.24	7.88	9.28	8.82	9.02	7.95	7.18	8.05	8.60	8.32	8.75	7.38	
10.15		6.95	8.23	7.52	6.88	9.13	7.99	9.33	8.66	9.34	7.92	7.59	7.70	9.09	8.53	9.42	7.61	
10.33	8.90	7.24	7.97	7.36		8.91	8.10	9.41	8.69	9.37	8.16	7.40	7.54	9.13	8.42	9.37	7.73	
10.35	8.55	7.01	7.96	7.44	6.69	9.12	8.06	9.44	8.78	9.40	8.11	7.54	7.51	9.15	8.59	9.44	7.77	
10.34	7.54	6.99	8.01	7.35	6.51	9.09	8.10	9.46	8.75	9.42	8.01	7.34	7.75	9.18	8.54	9.52	7.58	
10.29	8.39	6.33	8.11	7.63	6.90	9.26	8.21	9.50	8.82	9.56	8.17	7.41	7.40	9.33	8.73	9.51	7.83	
10.32	8.44	6.86	7.80	7.62	6.59	9.25	8.13	9.49	9.04	9.39	7.99	6.71	8.29	9.17	8.76	9.13	7.74	
10.28	8.12	6.45	7.52	7.35	6.16	9.13	7.87	9.33	8.86	9.05	7.87	7.22	8.32	8.91	8.42	8.76	7.47	
10.36	8.34	6.58	7.62	7.43	6.49	9.17	8.01	9.35	8.93	9.19	7.98	6.93	8.21	8.91	8.54	8.95	7.64	
10.31	8.38	6.79	7.44	7.23	6.03	9.02	7.86	9.27	8.71	9.06	7.90	7.02	8.15	8.91	8.44	8.78	7.64	
10.30	8.42	6.66	7.70	7.56	6.39	9.14	8.00	9.30	8.94	9.27	8.06	7.02	8.26	9.03	8.63	8.96	7.79	
10.40	8.19	6.57	7.81	7.61	6.49	9.29	8.12	9.44	9.02	9.35	8.04	7.12	8.35	9.13	8.74	9.02	7.77	
10.34	8.42	6.93	7.81	7.50	6.39	9.17	8.04	9.34	8.89	9.27	8.00	7.22	8.21	9.05	8.62	8.99	7.81	
10.36	8.23	6.35	7.64	7.32	6.21	9.11	7.89	9.32	8.78	9.10	7.86	7.18	8.14	8.84	8.46	8.86	7.48	
10.35	8.44	6.78	7.66	7.51	6.56	9.11	7.98	9.14	8.83	9.22	7.88	6.96	8.14	8.92	8.63	8.95	7.70	
10.23	8.38	6.81	7.48	7.36	6.41	9.02	7.90	9.15	8.75	9.05	7.93	6.90	8.06	8.76	8.40	8.80	7.57	

.244.PC .1LOG_Peakarea	MVA_UVA.245.PC 40:4.LOG_Peakarea	MVA_UVA.246.PC 40:5.LOG_Peakarea	MVA_UVA.247.PC 40:6.LOG_Peakarea	MVA_UVA.248.PC 40:7.LOG_Peakarea	MVA_UVA.249.PC 40:8.LOG_Peakarea	MVA_UVA.250.PE 34:2.LOG_Peakarea	MVA_UVA.253.PE 36:3.LOG_Peakarea	MVA_UVA.254.PE 36:4.LOG_Peakarea	MVA_UVA.255.PE 38:2.LOG_Peakarea	MVA_UVA.256.LPE 16:0.LOG_Peakarea	MVA_UVA.257.LPE 18:0.LOG_Peakarea	MVA_UVA.258.LPE 18:1.LOG_Peakarea	MVA_UVA.259.LPE 18:2.LOG_Peakarea	MVA_UVA.260.LPE 20:4.LOG_Peakarea	MVA_UVA.261.LPE 20:5.LOG_Peakarea	MVA_UVA.262.LPE 22:5.LOG_Peakarea	MVA_UVA.263.LPE 22:6.LOG_Peakarea	MVA_UVA 16:0
7.75	8.07	8.95	8.31	7.78	7.37	7.00	7.45	8.06	8.57	8.69	8.10	8.85	9.00	8.01	7.77	9.03	10.32	
7.37	7.93	8.79	8.18	7.48	7.55	7.21	7.66	8.10	8.46	8.57	8.05	8.62	8.73	7.68	7.48	8.77	10.11	
7.64	8.09	8.72	8.24	7.57	7.59	7.06	7.70	8.15	8.75	8.65	8.53	9.12	9.30	7.97	8.33	9.19	10.41	
7.46	7.98	8.70	8.28	7.48	7.49	7.02	7.59	8.14	8.40	8.33	8.13	8.69	8.91	7.55	7.71	8.78	10.10	
7.48	7.88	8.51	8.08	7.38	7.82	7.33	7.87	8.02	8.51	8.47	8.23	8.75	8.87	7.70	7.88	8.70	10.21	
7.28	8.10	8.99	8.47	7.59	7.61	6.97	7.78	8.02	8.79	8.75	8.27	8.72	9.09	7.70	8.07	9.40	10.36	
5.80	7.77	8.81	8.29	7.30	7.51	7.08	7.60	8.02	8.48	8.43	7.97	8.49	8.68	7.61	7.42	8.84	10.10	
7.14	7.78	8.73	8.22	7.37	7.42	6.79	7.63	7.87	8.49	8.42	7.94	8.50	8.85	7.73	7.87	9.06	10.19	
6.57	7.68	8.93	8.45	7.75	7.83	7.43	7.96	8.00	8.78	8.75	8.16	8.49	8.74	7.40	7.51	9.00	10.21	
7.21	7.85	8.85	8.27	7.51	7.62	7.21	7.64	7.96	8.44	8.41	7.95	8.54	8.75	7.66	7.64	8.87	10.13	
6.33	6.10	8.88	8.33	7.65	7.67	7.21	7.84	7.98	8.62	8.56	7.97	8.43	8.68	6.96	7.39	8.91	10.15	
7.53	7.85	8.67	8.12	7.50	7.47	7.01	7.58	8.04	8.29	8.42	7.94	8.62	8.77	7.77	7.53	8.76	10.07	
7.25	7.90	8.60	8.33	7.50	7.40	7.19	7.67	8.07	8.31	8.29	8.03	8.52	8.72	7.61	7.48	8.67	10.03	
7.37	7.79	8.52	8.06	7.35	7.38	7.00	7.65	7.80	8.28	8.22	8.03	8.53	8.78	7.58	7.73	8.64	10.04	
7.32	7.76	8.42	8.11	7.40	7.33	7.05	7.44	7.95	8.06	8.05	7.82	8.42	8.55	7.64	7.43	8.43	9.89	
7.67	8.01	8.67	8.20	7.64	7.83	7.40	7.90	8.16	8.75	8.73	8.45	9.04	9.16	8.17	8.09	9.01	10.36	
7.13	7.54	8.20	7.74	7.09	7.63	7.20	7.55	7.78	8.05	8.04	7.75	8.32	8.32	7.37	7.36	8.16	9.91	
7.29	7.93	8.86	8.24	7.50	7.26	6.65	7.64	7.92	8.40	8.37	7.79	8.11	8.54	7.27	7.47	8.90	10.09	
6.68	7.65	8.78	8.24	7.33	7.36	6.76	7.65	8.05	8.34	8.23	7.62	8.14	8.52	7.45	7.08	8.71	10.08	
7.28	7.42	8.84	8.25	7.61	7.51	6.99	7.76	8.05	8.35	8.33	7.75	8.21	8.56	7.46	7.38	8.77	10.02	
6.81	7.79	8.94	8.38	7.57	7.53	7.09	7.77	8.07	8.52	8.43	7.85	8.21	8.56	7.30	7.18	8.86	10.08	
7.45	8.01	8.94	8.34	7.69	7.74	6.94	7.88	8.13	8.59	8.52	7.90	8.45	8.76	7.68	7.62	8.87	10.15	
7.05	7.78	8.53	8.20	7.79	5.80	6.11	6.47	8.06	7.75	8.03	7.77	8.19	8.43	7.38	7.11	8.16	9.94	
7.09	7.64	8.33	7.84	7.33	6.16	6.26	6.78	7.79	7.52	7.75	7.46	7.91	8.12	7.08	6.82	7.94	9.68	
7.06	7.49	8.35	8.03	7.58	6.03	6.23	6.72	7.89	7.68	7.90	7.55	7.90	8.23	7.15	6.76	8.03	9.81	
7.05	7.59	8.26	7.84	7.39	5.82	5.59	6.40	7.80	7.54	7.80	7.42	7.77	8.19	7.13	6.98	7.95	9.71	
7.05	7.63	8.35	8.06	7.64	5.39	5.87	6.47	7.84	7.54	7.78	7.52	7.91	8.17	7.20	6.85	7.90	9.78	
7.45	7.85	8.47	8.12	7.74	5.81	6.01	6.85	7.95	7.82	8.04	7.73	8.02	8.38	7.16	7.19	8.15	9.90	
7.22	7.69	8.32	8.05	7.63	5.76	6.10	6.60	7.86	7.65	7.80	7.44	7.75	8.09	7.10	6.77	7.90	9.76	
6.95	7.63	8.31	7.84	7.36	6.40	5.32	6.97	7.83	7.68	7.80	7.44	7.89	8.22	7.05	6.99	7.99	9.70	
7.12	7.71	8.29	8.06	7.58	5.55	5.28	6.75	7.73	7.79	7.92	7.55	7.79	8.37	6.96	7.09	8.22	9.81	
7.04	7.45	8.16	7.80	7.28	5.91	5.54	6.74	7.73	7.57	7.71	7.36	7.82	8.18	7.05	6.87	7.94	9.69	

.264.LPC .LOG_Peakarea	MVA_UVA.265.LPC 16:1.LOG_Peakarea	MVA_UVA.266.LPC 18:1.LOG_Peakarea	MVA_UVA.267.LPC 18:2.LOG_Peakarea	MVA_UVA.268.LPC 18:3.LOG_Peakarea	MVA_UVA.269.LPC 20:2.LOG_Peakarea	MVA_UVA.270.LPC 20:3.LOG_Peakarea	MVA_UVA.271.LPC 20:4.LOG_Peakarea	MVA_UVA.273.LPC 22:5.LOG_Peakarea	MVA_UVA.274.LPC 22:6.LOG_Peakarea	MVA_UVA.275.SM 34:1.LOG_Peakarea	MVA_UVA.276.SM 34:2.LOG_Peakarea	MVA_UVA.28.Allantoin.LOG_Pe akarea	MVA_UVA.285.SM 42:3.LOG_Peakarea	MVA_UVA.286.PS 38:0.LOG_Peakarea	MVA_UVA.287.PS 38:1.LOG_Peakarea	MVA_UVA.288.PS 40:2.LOG_Peakarea	MVA_UVA.289.PS 40:3.LOG_Peakarea	MVA_UVA Ami
8.60	9.56	10.22	8.96	7.91	8.85	9.67	8.32	9.41	8.69	7.96	9.10	8.03	7.37	8.19	7.33	7.72	7.71	
8.33	9.36	10.03	8.69	7.69	8.76	9.46	8.06	9.10	8.47	7.61	9.50	7.76	7.45	8.24	7.30	7.74	7.84	
8.89	9.80	10.17	8.77	7.96	8.95	9.54	8.43	9.27	8.54	7.84	9.24	7.88	7.78	8.14	7.42	7.61	7.62	
8.56	9.50	9.93	8.52	7.61	8.64	9.39	8.10	8.99	8.41	7.67	9.31	7.78	7.61	8.09	7.36	7.66	7.83	
8.72	9.58	9.94	8.77	7.71	8.69	9.29	8.12	8.90	8.34	7.69	9.23	7.65	7.71	8.14	7.38	7.59	7.59	
8.53	9.50	10.01	8.92	7.32	8.37	9.60	8.18	9.45	8.66	7.92	9.41	8.00	7.50	8.16	7.10	7.81	7.97	
8.33	9.30	9.92	8.79	6.85	8.24	9.40	8.01	9.10	8.48	7.73	9.55	7.84	7.32	8.19	7.19	7.76	7.77	
8.45	9.34	9.82	8.99	7.14	8.38	9.41	8.07	9.19	8.57	7.85	9.14	7.95	7.43	8.10	7.03	7.73	7.98	
8.35	9.30	9.92	8.70	6.85	8.18	9.35	7.87	9.15	8.47	7.73	9.54	7.80	7.46	8.35	7.32	7.89	8.12	
8.44	9.35	9.89	8.87	7.05	8.27	9.46	7.97	9.15	8.64	7.88	9.22	7.98	7.45	8.14	7.13	7.79	8.04	
8.23	9.24	9.89	8.31	6.81	7.98	9.38	7.80	9.13	8.45	7.72	9.45	7.75	7.38	8.25	7.18	7.88	8.11	
8.43	9.31	9.87	8.77	7.52	8.57	9.27	7.91	8.93	8.34	7.67	9.20	7.61	7.36	8.07	7.23	7.56	7.78	
8.67	9.57	9.93	8.65	7.63	8.80	9.42	8.10	9.00	8.33	7.60	9.27	7.63	7.63	8.07	7.43	7.67	7.60	
8.70	9.53	9.84	8.64	7.64	8.73	9.31	8.14	8.98	8.38	7.67	8.99	7.75	7.72	8.01	7.36	7.55	7.68	
8.43	9.40	9.74	8.67	7.60	8.67	9.16	7.97	8.81	8.25	7.52	9.06	7.61	7.65	8.04	7.40	7.56	7.54	
8.83	9.70	10.11	9.04	7.87	8.89	9.48	8.26	9.08	8.47	7.87	9.19	7.77	7.79	8.26	7.43	7.70	7.69	
8.23	9.22	9.62	8.59	7.29	8.37	8.91	7.73	8.52	8.22	7.58	8.77	7.46	7.57	8.08	7.27	7.43	7.54	
8.22	9.17	9.68	8.82	6.98	8.28	9.23	7.85	9.14	8.55	7.69	9.64	8.03	7.24	7.93	6.87	7.51	8.07	
8.17	9.12	9.77	8.93	6.75	8.32	9.24	7.61	9.04	8.40	7.64	9.52	7.71	7.24	8.12	7.08	7.69	7.96	
8.14	9.12	9.72	8.91	6.86	8.27	9.22	7.68	9.02	8.36	7.63	9.34	7.80	7.30	8.08	7.05	7.68	7.99	
8.12	9.18	9.78	8.73	6.86	8.19	9.24	7.67	9.12	8.45	7.62	9.50	7.89	7.43	8.11	7.13	7.74	7.96	
8.26	9.29	9.85	9.01	7.13	8.42	9.39	7.92	9.11	8.54	7.74	9.36	7.96	7.54	8.21	7.08	7.80	7.96	
8.41	9.56	9.86	8.65	7.67	8.87	9.59	8.12	9.01	8.50	7.70	8.85	7.72	7.40	7.83	7.09	7.55	7.19	
8.16	9.38	9.65	8.52	7.42	8.76	9.29	7.84	8.70	8.16	7.35	9.10	7.31	7.39	7.73	7.20	7.33	7.26	
8.32	9.43	9.72	8.66	7.52	8.80	9.38	7.85	8.83	8.29	7.58	9.01	7.46	7.44	7.77	7.20	7.42	7.22	
8.18	9.35	9.60	8.71	7.22	8.68	9.35	7.85	8.69	8.16	7.45	8.98	7.30	7.40	7.59	7.04	7.33	7.20	
8.38	9.41	9.67	8.74	7.48	8.83	9.43	7.86	8.80	8.24	7.44	8.83	7.46	7.45	7.74	7.21	7.54	7.06	
8.46	9.57	9.82	8.70	7.63	8.91	9.56	8.10	8.93	8.39	7.63	9.06	7.61	7.52	7.79	7.21	7.55	7.29	
8.27	9.37	9.58	8.72	7.36	8.74	9.40	7.81	8.78	8.32	7.51	9.08	7.50	7.43	7.65	7.07	7.49	7.29	
8.07	9.33	9.66	8.50	7.25	8.59	9.28	7.92	8.75	8.34	7.61	9.11	7.47	7.36	7.71	7.14	7.37	7.40	
8.40	9.45	9.58	8.61	7.44	8.74	9.45	7.91	8.86	8.24	7.49	9.15	7.63	7.39	7.57	7.08	7.52	7.29	
8.19	9.28	9.54	8.61	7.20	8.61	9.21	7.73	8.66	8.17	7.44	9.03	7.42	7.41	7.71	7.07	7.39	7.14	

.29.Alpha-hobutyric acid.LOG_Peakarea	MVA_UVA.3.1_ Methylhistidine.LOG_Peakarea	MVA_UVA.302.FA 12:0.LOG_Peakarea	MVA_UVA.303.FA 14:0.LOG_Peakarea	MVA_UVA.304.FA 15:0.LOG_Peakarea	MVA_UVA.305.FA 16:0.LOG_Peakarea	MVA_UVA.306.FA 17:0.LOG_Peakarea	MVA_UVA.307.FA 18:0.LOG_Peakarea	MVA_UVA.308.FA 19:0.LOG_Peakarea	MVA_UVA.309.FA 20:0.LOG_Peakarea	MVA_UVA.31.Alpha-Tocopherol.LOG_Peakarea	MVA_UVA.310.FA 12:1.LOG_Peakarea	MVA_UVA.311.FA 14:1.LOG_Peakarea	MVA_UVA.312.FA 15:1.LOG_Peakarea	MVA_UVA.313.FA 16:1.LOG_Peakarea	MVA_UVA.314.FA 17:1.LOG_Peakarea	MVA_UVA.315.FA 18:1.LOG_Peakarea	MVA_UVA.316.FA 19:1.LOG_Peakarea	MVA_UVA 20:1
7.47	8.14	8.91	8.26	10.25	8.23	9.73	7.59	7.96	6.45	7.67	8.09	7.22	9.49	8.03	10.05	7.27	8.45	
7.48	8.01	8.57	8.02	9.95	8.03	9.44	7.39	7.81	6.21	7.20	7.80	6.91	9.01	7.70	9.77	7.15	8.29	
7.34	8.44	9.28	8.71	10.49	8.52	9.75	7.91	8.19	6.47	7.87	8.65	7.96	9.93	8.63	10.48	8.01	8.97	
7.47	8.07	8.84	8.12	10.04	8.06	9.41	7.62	7.82	6.33	7.36	8.06	7.18	9.45	8.02	9.94	7.46	8.48	
7.16	8.50	9.08	8.20	10.14	8.10	9.40	7.44	7.78	6.37	8.07	8.60	7.30	9.69	8.05	10.04	7.45	8.48	
8.01	8.77	9.39	8.46	10.44	8.42	9.73	7.77	7.72	6.47	8.48	9.06	7.48	9.94	8.31	10.38	7.76	8.56	
7.83	8.16	8.68	8.06	9.93	8.14	9.42	7.43	7.35	6.14	7.73	8.29	6.86	9.15	7.73	9.81	7.31	8.09	
7.62	8.46	9.12	8.21	10.13	8.17	9.44	7.61	7.46	6.24	8.01	8.79	7.27	9.72	7.96	10.04	7.46	8.27	
7.68	8.39	8.97	8.30	10.14	8.31	9.66	7.46	7.87	6.34	8.23	8.84	7.28	9.40	7.98	10.07	7.47	8.47	
7.61	8.66	9.37	8.29	10.26	8.28	9.51	7.60	7.60	6.45	8.29	8.98	7.49	9.91	8.27	10.29	7.80	8.51	
7.71	8.16	8.67	8.08	9.92	8.11	9.42	7.37	7.45	6.40	7.88	8.57	6.94	9.09	7.65	9.82	7.29	8.23	
7.36	8.01	8.77	8.04	9.95	8.01	9.36	7.36	7.81	6.32	7.47	7.95	7.04	9.28	7.81	9.78	7.13	8.21	
7.55	7.90	8.72	8.00	9.93	7.99	9.45	7.44	7.67	6.47	7.21	7.97	7.08	9.39	7.88	9.79	7.30	8.27	
7.08	8.07	8.89	7.96	9.95	7.88	9.26	7.22	7.51	6.23	7.65	8.37	7.12	9.50	7.92	9.88	7.28	8.31	
7.26	7.52	8.45	7.81	9.73	7.82	9.14	7.34	7.58	6.22	6.86	7.65	6.78	9.13	7.73	9.65	7.26	8.27	
7.35	8.44	9.18	8.30	10.29	8.17	9.52	7.67	8.04	6.45	8.05	8.64	7.45	9.80	8.29	10.28	7.74	8.80	
6.83	7.89	8.39	7.71	9.60	7.64	8.94	6.89	7.27	6.00	7.02	7.54	6.66	8.85	7.40	9.44	6.83	7.89	
8.11	8.49	9.04	8.24	10.05	8.16	9.47	7.61	7.69	6.27	8.00	8.65	7.31	9.47	7.90	9.95	7.46	8.34	
7.82	8.35	8.95	8.13	10.06	8.18	9.52	7.60	7.63	6.44	7.95	8.65	7.06	9.36	7.80	9.91	7.42	8.22	
7.82	8.59	9.09	8.33	10.13	8.27	9.49	7.67	7.65	6.36	8.26	8.81	7.30	9.51	8.04	10.04	7.59	8.43	
7.79	8.33	8.90	8.20	10.06	8.24	9.63	7.53	7.68	6.33	7.89	8.56	7.06	9.25	7.87	9.98	7.53	8.37	
7.76	8.57	9.24	8.31	10.21	8.31	9.58	7.77	7.71	6.39	8.10	8.79	7.36	9.71	8.10	10.16	7.69	8.52	
7.21	8.25	8.75	8.03	9.64	8.07	9.37	7.20	7.38	6.22	8.04	8.39	7.11	8.96	7.82	9.64	7.27	7.95	
7.28	8.15	8.49	7.82	9.29	7.77	9.04	6.85	7.12	5.90	8.05	8.30	6.93	8.69	7.49	9.28	6.91	7.67	
7.15	8.27	8.61	7.79	9.44	7.79	9.09	6.90	7.09	6.19	8.00	8.32	6.96	8.89	7.61	9.46	7.03	7.66	
7.23	8.29	8.68	7.85	9.43	7.78	9.10	6.95	7.20	6.06	8.07	8.56	7.00	8.94	7.63	9.46	7.05	7.75	
7.14	8.17	8.62	7.83	9.43	7.85	9.14	7.04	7.31	6.22	8.02	8.42	7.03	8.84	7.62	9.44	7.09	7.84	
7.28	8.30	8.88	8.05	9.68	8.12	9.36	7.21	7.44	6.25	8.22	8.66	7.19	9.17	7.95	9.76	7.40	8.08	
7.39	8.24	8.63	7.91	9.41	7.86	9.15	6.87	7.20	5.93	7.95	8.23	6.94	8.70	7.52	9.35	6.92	7.66	
7.29	8.14	8.48	7.75	9.30	7.70	8.99	6.84	7.09	6.07	7.97	8.18	6.75	8.64	7.44	9.29	6.86	7.57	
7.23	8.37	8.58	7.81	9.40	7.76	9.03	6.87	7.08	5.93	8.03	8.23	6.89	8.77	7.56	9.40	7.01	7.73	
7.05	8.01	8.39	7.64	9.20	7.65	8.93	6.82	7.03	5.77	7.88	8.17	6.78	8.55	7.36	9.16	6.81	7.54	

.317.FA .LOG_Peakarea	MVA_UVA.318.FA 12:2.LOG_Peakarea	MVA_UVA.319.FA 14:2.LOG_Peakarea	MVA_UVA.320.FA 16:2.LOG_Peakarea	MVA_UVA.321.FA 18:2.LOG_Peakarea	MVA_UVA.322.FA 20:2.LOG_Peakarea	MVA_UVA.324.FA 16:3.LOG_Peakarea	MVA_UVA.325.FA 18:3.LOG_Peakarea	MVA_UVA.326.FA 20:3.LOG_Peakarea	MVA_UVA.327.FA 18:4.LOG_Peakarea	MVA_UVA.328.FA 20:4.LOG_Peakarea	MVA_UVA.329.FA 22:6.LOG_Peakarea	MVA_UVA.33.Anserine.LOG_Pe akarea	MVA_UVA.330.Xylazine.LOG_P eakarea	MVA_UVA.331.Ketamine.LOG_ Peakarea	MVA_UVA.332.Alanine.LOG_ akarea	MVA_UVA.35.Arginine.LOG_Pe akarea	MVA_UVA.36.Ascorbic acid.LOG_Peakarea	MVA_UVA acid
7.41	8.04	8.14	10.26	8.33	7.80	9.20	8.63	7.65	9.36	9.20	6.90			7.55	9.00	7.64	7.79	
7.04	8.00	7.84	9.86	8.19	7.41	8.97	8.41	7.36	8.84	8.82	6.61	10.70	11.05	7.82	9.10	7.63	7.49	
7.38	8.16	8.22	10.39	8.65	7.92	9.25	8.89	7.62	9.36	9.22	6.62		7.56	7.74	9.15	7.93	8.43	
6.79	7.81	7.81	9.89	8.14	7.48	8.82	8.38	7.17	9.00	8.71	6.65	10.45	10.73	7.79	9.11	7.54	7.49	
7.40	8.24	7.98	9.96	8.13	7.73	8.84	8.31	7.04	8.88	8.58	6.48	5.93	7.77	7.61	9.03	7.58	8.80	
7.80	8.67	8.64	10.45	8.20	8.51	9.36	8.46	8.03	9.48	9.43	6.55	6.07	7.96	7.42	9.02	8.27	7.48	
7.21	8.11	8.09	9.88	7.73	7.75	8.78	7.86	7.47	8.92	8.76	6.62	10.75	10.90	6.98	8.78	7.41	7.23	
7.45	8.18	8.24	10.07	7.91	8.14	9.02	8.12	7.79	9.13	9.00	6.20	6.30	7.81	7.26	8.72	7.81	7.82	
7.59	8.76	8.45	10.18	8.05	8.19	9.05	8.11	7.71	9.09	9.13	6.18	10.71	11.02	7.59	8.94	7.27	7.58	
7.73	8.53	8.45	10.28	8.02	8.29	9.20	8.10	7.78	9.01	8.93	5.85	5.69	7.86	7.03	8.80	7.60	7.80	
7.40	8.50	8.28	9.95	7.77	7.97	8.88	7.89	7.62	8.94	8.96	6.24	10.69	10.89	7.61	8.79	6.39	7.36	
6.97	7.92	7.89	9.91	7.95	7.55	8.90	8.30	7.41	9.02	8.77	6.67	6.14	7.61	7.67	9.06	7.97	7.52	
6.83	7.67	7.64	9.66	7.91	7.26	8.74	8.19	6.96	8.75	8.47	6.77	10.71	10.98	7.73	9.06	7.66	7.17	
7.10	7.87	7.75	9.76	7.94	7.62	8.69	8.22	7.02	8.83	8.62	6.46		7.67	7.63	8.90	8.10	7.43	
6.31	7.39	7.39	9.47	7.88	6.87	8.46	8.04	6.59	8.50	8.26	6.44	10.47	10.72	7.63	8.83	7.30	6.78	
7.38	8.33	8.19	10.27	8.41	7.95	9.13	8.57	7.44	8.99	8.81	6.66		7.74	7.66	9.11	7.75	7.72	
6.64	7.27	7.18	9.42	7.51	6.93	8.28	7.64	6.51	8.29	7.96	6.33		6.69	7.61	8.88	7.79	7.91	
7.61	8.34	8.19	10.03	7.90	8.19	8.87	8.07	7.25	9.17	9.13	6.41	7.06	8.51	7.43	9.09	8.07	7.36	
7.38	8.43	8.27	9.99	7.93	8.02	8.92	8.05	7.54	9.02	9.10	6.69	10.87	11.08	7.75	9.08	7.20	7.18	
7.62	8.66	8.41	10.17	8.00	8.30	8.90	8.24	7.21	9.16	9.27	6.21	6.47	8.08	7.52	9.10	7.68	7.45	
7.46	8.41	8.21	10.03	8.00	7.92	8.83	8.07	7.21	8.98	9.04	6.57	10.84	11.10	7.60	9.00	7.35	8.35	
7.62	8.40	8.28	10.16	7.95	8.15	8.93	8.15	7.42	9.19	9.08	6.25	6.28	8.19	7.23	8.92	7.64	7.10	
7.52	8.12	7.60	9.28	7.70	7.61	8.28	7.94	7.17	8.68	8.20		6.49	8.33	6.72	8.74	6.06	8.41	
7.59	8.16	7.43	8.93	7.38	7.48	7.98	7.57	6.91	8.19	7.69			8.07	7.20	8.81	5.73	8.43	
7.45	8.04	7.51	9.13	7.43	7.51	8.18	7.72	7.04	8.40	7.92	5.15	6.79	8.55	6.87	8.74	5.49	8.40	
7.55	8.25	7.58	9.13	7.43	7.66	8.19	7.66	7.02	8.36	7.80	5.37	7.20	8.58	7.10	8.72	4.70	8.41	
7.55	8.14	7.50	9.04	7.47	7.60	8.11	7.72	7.05	8.41	7.91		6.74	8.46	7.18	8.83	5.74	8.39	
7.64	8.32	7.80	9.37	7.74	7.77	8.45	7.98	7.27	8.61	8.10	5.70	5.94	8.49	7.16	8.80	5.97	8.36	
7.48	7.98	7.44	9.03	7.41	7.51	8.10	7.63	6.93	8.36	7.84	5.66	6.67	8.41	6.97	8.86	5.93	8.55	
7.49	8.04	7.31	8.98	7.30	7.43	8.02	7.49	7.08	8.21	7.71	5.60	5.50	7.99	6.89	8.76	5.61	8.39	
7.52	8.07	7.47	9.03	7.40	7.60	8.10	7.71	7.03	8.44	7.93			7.68	6.75	8.68	5.60	8.44	
7.38	8.00	7.28	8.84	7.23	7.34	7.91	7.49	6.84	8.19	7.72			8.35	6.64	8.73		8.42	

.38.Aspartic LOG_Peakarea	MVA_UVA.46.Caprylic acid.LOG_Peakarea	MVA_UVA.47.Carnitine.LOG_Pe akarea	MVA_UVA.48.Carnosine.LOG_P eakarea	MVA_UVA.5.2-Ketobutyric acid.LOG_Peakarea	MVA_UVA.55.Citrulline.LOG_Pe akarea	MVA_UVA.58.Corticosterone.L OG_Peakarea	MVA_UVA.60.Creatine.LOG_Pe akarea	MVA_UVA.61.Creatinine.LOG_P eakarea	MVA_UVA.63.Cytidine.LOG_Pea karea	MVA_UVA.65.Cytosine.LOG_Pe akarea	MVA_UVA.74.Deoxyuridine.LO G_Peakarea	MVA_UVA.79.Eicosapentanoic acid.LOG_Peakarea	MVA_UVA.82.Fumaric acid.LOG_Peakarea	MVA_UVA.85.Gluconic acid.LOG_Peakarea	MVA_UVA.89.Glutamic acid.LOG_Peakarea	MVA_UVA.9.3-methyl-2- oxovaleric acid.LOG_Peakarea	MVA_UVA.90.Glutamine.L eakarea	MVA_UVA pho
7.46	9.29	6.68	7.77	7.69	7.45	9.11	9.41	8.70	8.38	7.90	8.19	7.75	8.58	8.45	8.82	9.12	7.59
7.12	9.38	6.70	7.87	7.82	6.87	9.46	9.48	8.63	8.32	7.64	7.97	8.03	8.72	8.12	8.84	9.16	7.59
7.44	9.36	6.50	7.74	7.69		9.21	9.47	8.75	8.51	7.82	8.15	7.90	8.52	8.49	8.76	9.17	7.79
7.25	9.36	6.56	7.68	7.80	6.82	9.41	9.42	8.75	8.48	7.61	7.81	7.81	8.56	8.11	8.81	9.13	7.32
7.38	9.46	6.40	7.77	7.70	6.35	9.02	9.56	8.80	8.51	7.86	7.51	7.91	8.78	8.40	8.60	9.17	7.63
7.71	9.39	6.46	7.11	7.87	7.63	9.21	9.63	8.69	8.41	7.84	7.99	7.62	8.63	8.40	9.15	9.15	7.80
7.59	9.14	6.66	7.47	7.71	7.56	9.21	9.49	8.47	8.39	7.72	7.52	7.68	8.66	7.82	9.15	9.05	7.07
7.47	9.30	5.89	7.15	7.61	7.53	9.01	9.34	8.27	8.04	7.53	7.70	7.32	8.25	7.81	8.87	8.90	7.40
7.69	9.06	6.36	7.61	7.83	7.59	9.37	9.66	8.55	8.50	7.65	7.96	7.65	8.62	7.87	9.32	9.25	6.89
7.64	9.34	5.69	7.30	7.47	7.35	9.00	9.34	8.51	8.34	7.57	7.45	7.37	8.31	7.88	9.05	8.93	7.22
7.40	9.07	6.28	7.57	7.62	7.57	9.32	9.52	8.54	8.50	7.53	7.91	7.69	8.45	7.82	9.05	9.15	6.80
7.34	9.31	6.39	7.85	7.68	7.58	9.18	9.32	8.75	8.36	7.60	7.86	7.89	8.57	8.24	8.64	9.09	7.49
7.27	9.27	6.57	7.71	7.81	6.92	9.24	9.34	8.52	8.34	7.46	7.69	7.82	8.41	7.82	8.97	9.14	7.23
6.97	9.16	6.27	7.51	7.60	6.71	9.01	9.17	8.33	8.05	7.41	7.69	7.50	8.04	8.03	8.54	8.96	7.37
7.28	9.10	6.40	7.38	7.55	6.66	9.11	9.06	8.14	8.01	7.19	7.44	7.66	8.08	7.68	8.79	8.84	7.00
7.42	9.47	6.60	7.84	7.78	5.82	9.21	9.43	8.75	8.46	7.64	7.82	7.91	8.81	8.38	8.57	9.27	7.71
7.15	9.25	6.25	7.16	7.49	5.05	9.17	8.98	8.09	7.86	7.10	6.86	7.46	8.18	7.98	8.33	8.90	7.27
7.48	9.67	6.48	7.65	8.00	8.00	9.30	9.72	8.68	8.56	8.08	7.56	7.57	8.65	8.17	9.08	9.25	7.56
7.75	9.30	6.68	7.76	7.67	7.56	9.43	9.65	8.70	8.50	7.75	7.86	8.01	8.82	8.16	9.23	9.19	7.39
7.32	9.33	6.28	7.66	7.66	7.73	9.27	9.51	8.61	8.49	7.71	7.72	7.64	8.38	8.15	8.98	9.22	7.44
7.61	9.40	6.61	7.79	7.67	7.71	9.41	9.59	8.71	8.57	7.89	7.60	7.94	8.69	7.87	9.28	9.22	7.17
7.52	9.50	6.26	7.65	7.72	7.79	9.22	9.46	8.57	8.47	7.72	7.58	7.45	8.31	8.01	9.05	9.04	7.22
7.21	8.41		7.80	7.49	6.32	8.45	9.29	8.46	8.12	7.34	7.18	7.67	7.78	7.59	8.19	8.51	7.09
7.52	8.69	5.54	7.75	7.65	5.88	8.59	9.44	8.61	8.26	7.45	6.90	7.84	8.07	7.97	8.61	8.82	7.21
7.22	8.48		7.77	7.47	6.73	8.56	9.35	8.47	8.16	7.35	7.08	7.66	7.78	7.87	8.17	8.58	7.40
7.27	8.32	5.41	7.76	7.44	5.54	8.60	9.33	8.54	8.15	7.39	7.07	7.70	7.89	7.60	8.40	8.66	7.00
7.26	8.51		7.66	7.46	4.90	8.65	9.27	8.47	8.12	7.35	7.01	7.67	7.73	7.74	8.33	8.64	6.98
7.30	8.65	5.25	7.59	7.52	6.30	8.70	9.39	8.56	8.24	7.45	7.21	7.55	7.75	8.00	8.46	8.87	7.02
6.67	8.55	5.44	7.81	7.69		8.49	9.43	8.43	8.05	7.34	6.97	7.61	7.97	7.62	8.37	8.77	6.99
7.23	8.64		7.63	7.46	5.69	8.53	9.37	8.58	8.21	7.67	6.99	7.55	7.71	7.68	8.45	8.68	6.99
7.42	8.35	5.17	7.66	7.29	5.75	8.58	9.35	8.55	8.20	7.55	7.06	7.61	7.80	7.43	8.29	8.31	7.14
7.14	8.45		7.63	7.22		8.43	9.23	8.52	8.13	7.49	6.94	7.42	7.68	7.69	8.20	8.26	6.84

.95.Glyceryl sphate.LOG_Peakarea	MVA_UVA.96.Glycine.LOG_Pea karea	UVA.116.Hydroxybutyric acid.LOG_Peakarea	UVA.124.Lactic acid.LOG_Peakarea	UVA.141.N-Acetylputrescine.LOG_Peakarea	UVA.155.Nicotinic acid.LOG_Peakarea	UVA.198.Suberic acid.LOG_Peakarea	UVA.213.Trehalose.LOG_Peakar ea	UVA.218.Uracil.LOG_Peakarea	UVA.224.Valeric acid.LOG_Peakarea	UVA.252.PE 36:2.LOG_Peakarea	UVA.272.LPC 20:5.LOG_Peakarea	UVA.277.SM 36:1.LOG_Peakarea	UVA.278.SM 36:2.LOG_Peakarea	UVA.281.SM 40:1.LOG_Peakarea	UVA.282.SM 40:2.LOG_Peakarea	UVA.283.SM 42:1.LOG_Peakarea	UVA.284.SM 42:2.LOG_Peakarea	UVA.6.2.Oxovaleric acid.LOG_Peakarea	UVA.88.Glucuronic acid.LOG_Peakarea	UVA.93.Glyceric acid.LOG_Pea	UVA
7.60	7.32	10.09	6.21	6.70	5.85	6.67	9.12	6.56	7.85	8.90	7.51	6.44	8.53	7.99	8.32	8.63	8.28	7.35	7.80	8.07	
7.35	7.32	10.02	7.02	6.47	5.56	6.76	9.27		7.95	8.67	7.09	6.17	8.23	7.64	7.93	8.41	7.83	7.87	7.91	8.00	
7.47	7.38	10.08	6.32	6.73	6.09	6.72	9.40	6.54	7.85	8.58	7.21	6.47	8.25	7.82	8.00	8.49	8.26	7.41	8.25	8.27	
7.42	7.27	9.81	6.95	6.77	5.42	6.94	9.16	6.51	7.77	8.39	7.16	6.15	8.06	7.64	7.75	8.40	8.26	7.29	7.78	8.09	
7.54	7.50	9.94	5.95	6.90	6.29	6.82	9.38	6.80	7.91	8.57	7.02	6.26	8.08	7.72	7.75	8.30	8.00	7.58	8.38	8.29	
7.79	6.97	9.84	6.47	6.50	5.66		9.30	5.74	7.82	8.59	7.83	6.94	8.14	7.54	7.96	8.57	8.35	7.40	7.73	8.20	
7.57	6.93	9.61	7.58	6.79	5.78	5.43	8.88	6.01	7.71	8.64	7.44	6.79	7.99	7.36	7.82	8.41	8.07	8.10	7.60	7.91	
7.57	6.85	9.74	6.06	6.51	5.73	5.29	8.74	6.40	7.65	8.63	7.61	6.95	7.89	7.53	7.64	8.39	8.29	7.19	7.80	8.06	
7.76	6.94	9.51	7.01	6.84	5.61	6.37	9.03	6.81	8.06	8.44	7.57	6.53	8.37	7.62	7.96	8.33	8.53	7.63	7.85	8.27	
7.44	6.90	9.80	5.83	6.60	5.97	5.47	8.92	6.72	7.83	8.64	7.70	6.96	7.98	7.52	7.85	8.53	8.43	7.17	7.86	8.19	
7.73	6.78	9.35	6.24	6.80	5.72	6.36	8.98	6.45	7.89	7.96	7.52	6.67	8.23	7.54	7.89	8.34	8.25	7.48	7.88	8.25	
7.37	7.31	10.01	6.16	6.55	5.67	6.71	9.07	6.31	7.87	8.61	7.03	6.27	8.23	7.70	7.90	8.32	8.12	7.29	7.73	7.92	
7.44	7.17	9.74	6.90	6.61	5.39	6.82	8.91	6.11	7.69	8.62	6.97	6.30	7.95	7.59	7.87	8.31	7.05	7.56	7.58	7.92	
7.29	7.21	9.96	6.29	6.54	5.12	6.36	8.97	6.33	7.61	8.49	7.09	6.35	7.91	7.67	7.68	8.31	8.10	7.12	7.40	7.86	
7.26	7.06	9.54	6.73	6.49	5.21	6.49	8.65		7.71	8.58	6.84	5.64	7.73	7.61	7.44	8.18	8.30	7.37	7.15	7.74	
7.43	7.33	10.16	6.03	6.91	5.26	6.87	9.38	6.68	8.00	8.85	7.10	6.35	8.25	7.87	7.95	8.42	8.14	7.42	8.10	8.28	
7.06	7.12	9.83	6.13	6.37	5.74	6.24	8.82		7.80	8.32	6.99	6.52	7.63	7.41	7.22	7.97	7.88	7.17	7.57	7.51	
7.67	6.94	9.91	6.99	6.95	6.21	6.16	9.23	6.31	7.57	8.47	7.55	6.81	7.99	7.50	6.76	8.50	8.46	7.36	8.14	8.05	
7.86	6.90	9.80	7.43	6.74	6.26	6.21	9.48	6.56	7.58	8.69	7.14	6.46	8.11	7.39	7.89	8.28	7.52	7.68	7.87	8.27	
7.67	7.03	9.88	6.54	6.75	5.90	6.56	9.42	6.24	7.74	8.68	7.19	6.56	7.97	7.42	7.83	8.31	8.30	7.08	7.78	8.25	
7.62	6.90	9.79	7.56	6.94	6.14	6.71	9.31	6.74	7.73	8.49	7.39	6.25	8.13	7.53	7.97	8.45	8.56	7.71	8.07	8.29	
7.71	6.93	9.79	6.60	6.86	6.04	6.54	9.02	6.67	7.87	8.77	7.56	6.73	8.05	7.65	7.94	8.52	8.25	7.07	7.70	8.29	
5.71	7.36	9.86	5.85			6.40	8.97	6.09	7.65	8.61	7.46	6.76	7.90	7.80	7.26	8.17	7.37	6.98	6.67	8.12	
6.71	7.33	9.75		4.96		6.97	9.02	6.16	7.45	8.53	7.09	6.36	7.92	7.56	7.05	7.97	7.66	7.18	7.40	8.18	
6.15	7.45	9.77	6.22			7.04	8.90	5.94	7.54	8.61	7.17	6.54	7.99	7.71	7.30	7.99	7.77	6.96	6.84	8.20	
6.44	7.42	9.62				6.80	8.97	6.39	7.27	8.64	7.00	6.45	7.88	7.59	7.14	7.86	7.87	6.99	6.96	8.31	
6.41	7.18	9.75	5.49	5.13	5.24	6.66	8.97	6.35	7.47	8.67	6.81	6.13	7.94	7.68	7.25	8.04	7.72	6.91	7.11	8.36	
6.90	7.43	9.59	5.60	5.44		6.97	8.89	6.48	7.45	8.66	7.04	6.64	7.97	7.78	7.42	8.13	7.53	7.02	7.42	8.36	
6.70	7.41	9.75			5.07	6.20	8.97	5.72	7.42	8.60	7.26	6.51	7.98	7.69	7.23	8.04	7.49	7.21	7.33	8.06	
6.59	7.41	9.49	6.04		5.27	6.88	8.88		7.38	8.48	7.29	6.79	8.03	7.71	7.23	7.96	7.87	6.98	7.01	8.14	
6.45	7.32	9.67	4.97			6.61	8.85	6.23	7.32	8.41	7.26	6.50	7.88	7.74	7.10	8.09	7.87	7.12	7.13	8.15	
6.13	7.23	9.62				6.72	8.85	6.43	7.35	8.49	7.05	6.51	7.98	7.70	7.22	7.93	7.57	6.94	6.87	8.13	

Adipocyte glucocorticoid receptor deficiency disrupts the feeding-fasting transition but protects from obesity-induced metabolic disorders

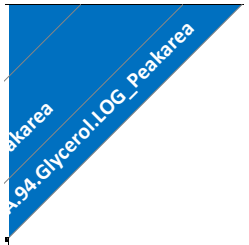

PeakScout_ID	Statistics	Metabolite_Name	Metabolite_Class	sample_name	LOG_Peakarea	Seq_Pos	group	mouse_ID	Genotype	Feeding	BW_terminal_g	storage_yr	age_wee
332	MVA_UVA	Alanine	Amino acids, peptides and metabolites	01_M1_pE_Bl		1	Bl						
332	MVA_UVA	Alanine	Amino acids, peptides and metabolites	02_M1_pE_pool_QC	7.29	2	QC						
332	MVA_UVA	Alanine	Amino acids, peptides and metabolites	03_M1_pE_5552_Cfed	7.55	3	Cfed	5552	CTRL	fed	30.63	1.5	8
332	MVA_UVA	Alanine	Amino acids, peptides and metabolites	04_M1_pE_5553_GRfed	7.67	4	GRfed	5553	GR KO	fed	31.02	1.5	8
332	MVA_UVA	Alanine	Amino acids, peptides and metabolites	05_M1_pE_5558_C48	7.42	5	C48	5558	CTRL	48h fast	22.26	1.5	8
332	MVA_UVA	Alanine	Amino acids, peptides and metabolites	06_M1_pE_Bl		6	Bl						
332	MVA_UVA	Alanine	Amino acids, peptides and metabolites	07_M1_pE_pool_QC	7.37	7	QC						
332	MVA_UVA	Alanine	Amino acids, peptides and metabolites	08_M1_pE_5564_GR48	7.43	8	GR48	5564	GR KO	48h fast	20.08	1.5	8
332	MVA_UVA	Alanine	Amino acids, peptides and metabolites	09_M1_pE_1_CHFD	6.72	9	CHFD	1	CTRL	HFD	21.18	0	6
332	MVA_UVA	Alanine	Amino acids, peptides and metabolites	10_M1_pE_7_GRHFD	6.97	10	GRHFD	7	GR KO	HFD	23.63	0	6
332	MVA_UVA	Alanine	Amino acids, peptides and metabolites	11_M1_pE_Bl	5.84	11	Bl						
332	MVA_UVA	Alanine	Amino acids, peptides and metabolites	12_M1_pE_pool_QC	7.32	12	QC						
332	MVA_UVA	Alanine	Amino acids, peptides and metabolites	13_M1_pE_3186_C48	6.98	13	C48	3186	CTRL	48h fast	25.30	0	8
332	MVA_UVA	Alanine	Amino acids, peptides and metabolites	14_M1_pE_9618_Cfed	7.82	14	Cfed	9618	CTRL	fed	29.03	0	8
332	MVA_UVA	Alanine	Amino acids, peptides and metabolites	15_M1_pE_3189_GRfed	7.73	15	GRfed	3189	GR KO	fed	30.30	0	8
332	MVA_UVA	Alanine	Amino acids, peptides and metabolites	16_M1_pE_Bl	5.23	16	Bl						
332	MVA_UVA	Alanine	Amino acids, peptides and metabolites	17_M1_pE_pool_QC	7.48	17	QC						
332	MVA_UVA	Alanine	Amino acids, peptides and metabolites	18_M1_pE_12_GRHFD	6.75	18	GRHFD	12	GR KO	HFD	18.23	0	6
332	MVA_UVA	Alanine	Amino acids, peptides and metabolites	19_M1_pE_3185_GR48	7.75	19	GR48	3185	GR KO	48h fast	25.50	0	8
332	MVA_UVA	Alanine	Amino acids, peptides and metabolites	20_M1_pE_6_CHFD	7.20	20	CHFD	6	CTRL	HFD	21.03	0	6
332	MVA_UVA	Alanine	Amino acids, peptides and metabolites	21_M1_pE_Bl	5.30	21	Bl						
332	MVA_UVA	Alanine	Amino acids, peptides and metabolites	22_M1_pE_pool_QC	7.35	22	QC						
332	MVA_UVA	Alanine	Amino acids, peptides and metabolites	23_M1_pE_5559_C48	7.26	23	C48	5559	CTRL	48h fast	24.26	1.5	8
332	MVA_UVA	Alanine	Amino acids, peptides and metabolites	24_M1_pE_5579_GRfed	7.63	24	GRfed	5579	GR KO	fed	26.52	1	8
332	MVA_UVA	Alanine	Amino acids, peptides and metabolites	25_M1_pE_5583_Cfed	7.74	25	Cfed	5583	CTRL	fed	24.58	1	8
332	MVA_UVA	Alanine	Amino acids, peptides and metabolites	26_M1_pE_Bl		26	Bl						
332	MVA_UVA	Alanine	Amino acids, peptides and metabolites	27_M1_pE_pool_QC	7.46	27	QC						
332	MVA_UVA	Alanine	Amino acids, peptides and metabolites	28_M1_pE_2_CHFD	6.87	28	CHFD	2	CTRL	HFD	26.03	0	6
332	MVA_UVA	Alanine	Amino acids, peptides and metabolites	29_M1_pE_5589_GR48	7.52	29	GR48	5589	GR KO	48h fast	19.53	1	8
332	MVA_UVA	Alanine	Amino acids, peptides and metabolites	30_M1_pE_8_GRHFD	6.89	30	GRHFD	8	GR KO	HFD	20.94	0	6
332	MVA_UVA	Alanine	Amino acids, peptides and metabolites	31_M1_pE_Bl		31	Bl						
332	MVA_UVA	Alanine	Amino acids, peptides and metabolites	32_M1_pE_pool_QC	7.47	32	QC						
332	MVA_UVA	Alanine	Amino acids, peptides and metabolites	33_M1_pE_3187_GRfed	7.63	33	GRfed	3187	GR KO	fed	33.30	0	8
332	MVA_UVA	Alanine	Amino acids, peptides and metabolites	34_M1_pE_3188_Cfed	7.79	34	Cfed	3188	CTRL	fed	28.80	0	8
332	MVA_UVA	Alanine	Amino acids, peptides and metabolites	35_M1_pE_9114_C48	7.59	35	C48	9114	CTRL	48h fast	25.80	0	8
332	MVA_UVA	Alanine	Amino acids, peptides and metabolites	36_M1_pE_Bl	5.03	36	Bl						

332	MVA_UVA	Alanine	Amino acids, peptides and metabolites	37_M1_pE_pool_QC	7.36	37	QC					
332	MVA_UVA	Alanine	Amino acids, peptides and metabolites	38_M1_pE_3184_GR48	7.60	38	GR48	3184	GR KO	48h fast	22.48	0	8
332	MVA_UVA	Alanine	Amino acids, peptides and metabolites	39_M1_pE_11_GRHFD	6.75	39	GRHFD	11	GR KO	HFD	21.42	0	6
332	MVA_UVA	Alanine	Amino acids, peptides and metabolites	40_M1_pE_5_CHFD	7.10	40	CHFD	5	CTRL	HFD	20.80	0	6
332	MVA_UVA	Alanine	Amino acids, peptides and metabolites	41_M1_pE_Bl	5.84	41	Bl						
332	MVA_UVA	Alanine	Amino acids, peptides and metabolites	42_M1_pE_pool_QC	7.41	42	QC						
332	MVA_UVA	Alanine	Amino acids, peptides and metabolites	43_M1_pE_5584_GRfed	7.66	43	GRfed	5584	GR KO	fed	26.76	1	8
332	MVA_UVA	Alanine	Amino acids, peptides and metabolites	44_M1_pE_5563_C48	7.03	44	C48	5563	CTRL	48h fast	21.48	1.5	8
332	MVA_UVA	Alanine	Amino acids, peptides and metabolites	45_M1_pE_5587_Cfed	7.61	45	Cfed	5587	CTRL	fed	28.32	1	8
332	MVA_UVA	Alanine	Amino acids, peptides and metabolites	46_M1_pE_Bl	5.93	46	Bl						
332	MVA_UVA	Alanine	Amino acids, peptides and metabolites	47_M1_pE_pool_QC	7.49	47	QC						
332	MVA_UVA	Alanine	Amino acids, peptides and metabolites	48_M1_pE_9_GRHFD	6.64	48	GRHFD	9	GR KO	HFD	23.75	0	6
332	MVA_UVA	Alanine	Amino acids, peptides and metabolites	49_M1_pE_3_CHFD	7.18	49	CHFD	3	CTRL	HFD	27.36	0	6
332	MVA_UVA	Alanine	Amino acids, peptides and metabolites	50_M1_pE_5591_GR48	7.23	50	GR48	5591	GR KO	48h fast	20.93	1	8
332	MVA_UVA	Alanine	Amino acids, peptides and metabolites	51_M1_pE_Bl		51	Bl						
332	MVA_UVA	Alanine	Amino acids, peptides and metabolites	52_M1_pE_pool_QC	7.41	52	QC						
332	MVA_UVA	Alanine	Amino acids, peptides and metabolites	53_M1_pE_5588_Cfed	7.69	53	Cfed	5588	CTRL	fed	26.18	1	8
332	MVA_UVA	Alanine	Amino acids, peptides and metabolites	54_M1_pE_9112_C48	7.69	54	C48	9112	CTRL	48h fast	22.66	0	8
332	MVA_UVA	Alanine	Amino acids, peptides and metabolites	55_M1_pE_5586_GRfed	7.61	55	GRfed	5586	GR KO	fed	24.76	1	8
332	MVA_UVA	Alanine	Amino acids, peptides and metabolites	56_M1_pE_Bl	6.01	56	Bl						
332	MVA_UVA	Alanine	Amino acids, peptides and metabolites	57_M1_pE_pool_QC	7.37	57	QC						
332	MVA_UVA	Alanine	Amino acids, peptides and metabolites	58_M1_pE_4_CHFD	7.16	58	CHFD	4	CTRL	HFD	21.75	0	6
332	MVA_UVA	Alanine	Amino acids, peptides and metabolites	59_M1_pE_10_GRHFD	6.87	59	GRHFD	10	GR KO	HFD	21.75	0	6
332	MVA_UVA	Alanine	Amino acids, peptides and metabolites	60_M1_pE_3183_GR48	7.71	60	GR48	3183	GR KO	48h fast	22.70	0	8
332	MVA_UVA	Alanine	Amino acids, peptides and metabolites	61_M1_pE_Bl		61	Bl						
332	MVA_UVA	Alanine	Amino acids, peptides and metabolites	62_M1_pE_pool_QC	7.38	62	QC						
332	MVA_UVA	Alanine	Amino acids, peptides and metabolites	63_M1_pE_HepBlank_HepBlnk	5.81	63	HepBlnk						
332	MVA_UVA	Alanine	Amino acids, peptides and metabolites	64_M1_pE_9110_C48	7.61	64	C48	9110	CTRL	48h fast	22.50	0	8
332	MVA_UVA	Alanine	Amino acids, peptides and metabolites	65_M1_pE_5585_GRfed	7.61	65	GRfed	5585	GR KO	fed	27.68	1	8
332	MVA_UVA	Alanine	Amino acids, peptides and metabolites	66_M1_pE_Bl	5.60	66	Bl						
332	MVA_UVA	Alanine	Amino acids, peptides and metabolites	67_M1_pE_pool_QC	7.36	67	QC						

Please find the full version of the table at <Link will be provided after publication acceptance> or <Link will be provided after publication acceptance>.

ks	sex	outlier	HMDB_ID	HMDB_mapping	Alternative_identity	Scan_polarity	RT_standard	precursor_mass_mz	Peakarea	intra-group_RSD
			HMDB00161	most likley		0	11.04	90.054958		66.4%
			HMDB00161	most likley		0	11.04	90.054958	19706169.35	14.1%
male			HMDB00161	most likley		0	11.04	90.054958	35085034.09	23.2%
male			HMDB00161	most likley		0	11.04	90.054958	46834123.34	9.7%
male			HMDB00161	most likley		0	11.04	90.054958	26214026.33	56.6%
			HMDB00161	most likley		0	11.04	90.054958		66.4%
			HMDB00161	most likley		0	11.04	90.054958	23566930.77	14.1%
male			HMDB00161	most likley		0	11.04	90.054958	26634803.77	40.0%
male			HMDB00161	most likley		0	11.04	90.054958	5195062.009	37.6%
male			HMDB00161	most likley		0	11.04	90.054958	9301224.457	26.9%
			HMDB00161	most likley		0	11.04	90.054958	690072.0893	66.4%
			HMDB00161	most likley		0	11.04	90.054958	20872182.4	14.1%
male			HMDB00161	most likley		0	11.04	90.054958	9514588.188	56.6%
male			HMDB00161	most likley		0	11.04	90.054958	65869747.9	23.2%
male			HMDB00161	most likley		0	11.04	90.054958	53166869.47	9.7%
			HMDB00161	most likley		0	11.04	90.054958	171475.5569	66.4%
			HMDB00161	most likley		0	11.04	90.054958	30174584.77	14.1%
male	outlier		HMDB00161	most likley		0	11.04	90.054958	5658926.452	26.9%
male			HMDB00161	most likley		0	11.04	90.054958	56500260.65	40.0%
male			HMDB00161	most likley		0	11.04	90.054958	15742481.35	37.6%
			HMDB00161	most likley		0	11.04	90.054958	200986.1728	66.4%
			HMDB00161	most likley		0	11.04	90.054958	22370537.79	14.1%
male			HMDB00161	most likley		0	11.04	90.054958	18133235.08	56.6%
male			HMDB00161	most likley		0	11.04	90.054958	43006926.49	9.7%
male			HMDB00161	most likley		0	11.04	90.054958	54462035.39	23.2%
			HMDB00161	most likley		0	11.04	90.054958		66.4%
			HMDB00161	most likley		0	11.04	90.054958	28958241.94	14.1%
male			HMDB00161	most likley		0	11.04	90.054958	7333033.863	37.6%
male			HMDB00161	most likley		0	11.04	90.054958	32771372.7	40.0%
male			HMDB00161	most likley		0	11.04	90.054958	7782850.555	26.9%
			HMDB00161	most likley		0	11.04	90.054958		66.4%
			HMDB00161	most likley		0	11.04	90.054958	29258465.31	14.1%
male			HMDB00161	most likley		0	11.04	90.054958	42442963.78	9.7%
male			HMDB00161	most likley		0	11.04	90.054958	61638375.79	23.2%
male			HMDB00161	most likley		0	11.04	90.054958	39245819.79	56.6%
			HMDB00161	most likley		0	11.04	90.054958	107689.223	66.4%

		HMDB00161	most likley		0	11.04	90.054958	22758058.02	14.1%
male		HMDB00161	most likley		0	11.04	90.054958	40089336.86	40.0%
male		HMDB00161	most likley		0	11.04	90.054958	5681640.558	26.9%
male		HMDB00161	most likley		0	11.04	90.054958	12471778.08	37.6%
		HMDB00161	most likley		0	11.04	90.054958	699690.3284	66.4%
		HMDB00161	most likley		0	11.04	90.054958	25516300.94	14.1%
male		HMDB00161	most likley		0	11.04	90.054958	45925986.52	9.7%
male		HMDB00161	most likley		0	11.04	90.054958	10687335.73	56.6%
male		HMDB00161	most likley		0	11.04	90.054958	40772235.1	23.2%
		HMDB00161	most likley		0	11.04	90.054958	845010.8392	66.4%
		HMDB00161	most likley		0	11.04	90.054958	30813165.02	14.1%
male		HMDB00161	most likley		0	11.04	90.054958	4330426.463	26.9%
male		HMDB00161	most likley		0	11.04	90.054958	14984920.64	37.6%
male		HMDB00161	most likley		0	11.04	90.054958	17021806.01	40.0%
		HMDB00161	most likley		0	11.04	90.054958		66.4%
		HMDB00161	most likley		0	11.04	90.054958	25860681.31	14.1%
male	outlier	HMDB00161	most likley		0	11.04	90.054958	49419184.79	23.2%
male	outlier	HMDB00161	most likley		0	11.04	90.054958	48807139.48	56.6%
male	outlier	HMDB00161	most likley		0	11.04	90.054958	41145291.89	9.7%
		HMDB00161	most likley		0	11.04	90.054958	1020866.463	66.4%
		HMDB00161	most likley		0	11.04	90.054958	23291366.92	14.1%
male		HMDB00161	most likley		0	11.04	90.054958	14516762.72	37.6%
male	outlier	HMDB00161	most likley		0	11.04	90.054958	7374727.135	26.9%
male	outlier	HMDB00161	most likley		0	11.04	90.054958	51291842.74	40.0%
		HMDB00161	most likley		0	11.04	90.054958		66.4%
		HMDB00161	most likley		0	11.04	90.054958	23871595.04	14.1%
		HMDB00161	most likley		0	11.04	90.054958	649835.591	
male		HMDB00161	most likley		0	11.04	90.054958	40903312.07	56.6%
male		HMDB00161	most likley		0	11.04	90.054958	40743232.66	9.7%
		HMDB00161	most likley		0	11.04	90.054958	399651.0696	66.4%
		HMDB00161	most likley		0	11.04	90.054958	23044543.41	14.1%

table_name	content_structure
long_sample-metabolite	The "long" table is structured with one row per metabolite AND sample (incl. blanks, QCs). This table is most suitable for data explorations and single metabolite scatter or box plots. The table also contains selected metabolite information and the most important sample information.
per-sample	The " wide" table contains the same values as the long data set, but is structured with one row per sample and one colum per metabolite (LOG_Peakarea). This table is best suitable for metabolite versus metabolite plots, correlation calculations and plotting of sample specific multivariate statistical results (i.e. PCA scores). Blanks, QCs and Outlier Samples have been removed for the sake of clarity. The metabolite column names are a point seperated concatination of the columns statistics.PeakScout_ID.Metabolite_name.values type.
per-metabolite	The table is structured with one row per metabolite, not containing unaggregated measurement values anymore. This metabolite data set is best suitable for adding and plotting statistical results from multivariate (i.e. PCA loadings) and univariate (i.e. ANOVA) analysis. All available metabolie information are contained.

column_name	content_description	data_type	part of table		
			long_sample-metabolite	per-sample	per-metabolite
Statistics	quality of the metabolite categorized as suitable for MVA_UVA (best) or suitable for UVA only (plot metabolite before interpretation)	string	yes	in metabolite column name	yes
Metabolite_name	name of the measured and identified metabolite	string	yes	in metabolite column name	yes
Metabolite_Class	The metabolite classes serve as a first orientation and were choosen by experience+literature.	string	yes	no	yes
Sample_Name	sample specific, unique name	string	yes	yes	no
Seq_Pos	Sequence in which samples were measured	integer	yes	yes	no
mouse_ID	number identifying a specific mouse	integer	yes	yes	no
group	biological group of the sample, bl = blank, QC = pooled quality control, C = control mice, GR = Adipocyte-specific GR-deficient mice, 48 = 48h fasted, fed = fed ad libitum with standard chow, HFD = high fat diet	string	yes	yes	no
PeakScout_ID	unique identifier of metabolite	string	yes	in metabolite column name	yes
LOG_Peakarea	Log10 of Peakarea (log10 improves values distribution towards normal distrbution, necessary because metabolite values are often right skewed), USE THIS FOR ANY CALCULATIONS&ANALYSIS!	real	yes	as metabolite columns	no
HMDB_ID	identifier connecting to the Human Metabolome Database (HMDB , http://www.hmdb.ca/) assigned manually, non-validated	string	yes	no	yes
HMDB_mapping	mapping type of HMDB_ID: "most likley" the ID was selcted by biological liklehood to occur in the sample type, "exemplaric" in cases with too many matches an exemplaric one was selected	string	yes	no	yes

Adipocyte glucocorticoid receptor deficiency disrupts the feeding-fasting transition but protects from obesity-induced metabolic disorders

Peakarea	integrated area under an identified peak, i.e. the measurement value	real	yes	no	no
intra-group_RSD	relative standard deviation of the metabolite within the relative group (according to entries in column group)	real	yes	no	no